The Kinetic Characterisation of *Rhodotorula graminis* L-mandelate dehydrogenase

Rhona Sinclair

THESIS PRESENTED FOR THE DEGREE OF DOCTOR OF PHILOSOPHY UNIVERSITY OF EDINBURGH JANUARY 1998

To Graham
and in memory of my grandfather, William Armstrong.

Declaration

The work presented in this thesis is the original work of the author, except where specific reference is made to other sources.

R. Sinclair, Jan 1998.

Acknowledgements

I would like to thank my first and second supervisors, Dr. Graeme Reid and Prof. Stephen Chapman for all their help and encouragement throughout my PhD. Special thanks also to Drs. Euan Gordon and Simon Daff and to all members of the Reid and Chapman groups for their friendship, guidance, and countless cups of tea.

Many thanks finally to the Bean family and to my own family, in particular my parents, for their love and support.

Abstract

The L-mandelate dehydrogenase (L-mdh) from *Rhodotorula graminis* is homologous to *Saccharomyces cerevisiae* flavocytochrome b_2, which acts as an L-lactate dehydrogenase (L-ldh). L-ldh can utilise a wide variety of 2-hydroxy acids as substrates but is most effective with L-lactate (k_{cat} = 400 ± 10 s^{-1}). When mandelate is used as a substrate however, the turnover rate is dramatically lower (k_{cat} = 0.02 ± 0.01 s^{-1}).

The crystal structure of L-ldh has been determined to 2.4 Å resolution allowing the active site to be identified. Several hydrophobic residues, for example, Ala198, Leu230 and Ile326 have been identified in the locality of the methyl group of the substrate. The roles of these residues have been investigated by examining the turnover of various mutant enzymes using L-mandelate as substrate. Comparison of the amino acid sequences of L-mdh and L-ldh show that at the position corresponding to Leu230 in L-ldh leucine is replaced by a smaller glycine residue. The Leu230-Gly mutation has been constructed and resulted in a 40-fold increase in turnover with L-mandelate compared to wild type L-ldh (0.02 ± 0.01 s^{-1} to 0.8 ± 0.2 s^{-1}). The *R.graminis* L-mdh also has a glycine residue at the position corresponding to Ala198. The most dramatic increase in turnover was seen with the double mutant A198G.L230A, with a 450 fold increase in k_{cat}, from 0.02 ± 0.01 s^{-1} to 8.5 ± 0.5 s^{-1}.

The recombinant form of the *R.graminis* L-mdh has been overexpressed in *E.coli* to levels around 14% of the total cell protein. The enzyme was purified to homogeneity after several ion-exchange and gel filtration columns. The steady state turnover of the enzyme was measured with the artificial electron acceptor, potassium ferricyanide (550 ± 25 s^{-1}) and with its physiological electron acceptor, cytochrome *c* (225 ± 15 s^{-1}). In both cases the k_{cat} values were similar to those previously obtained with L-ldh with L-lactate as substrate. The individual electron transfer steps in the catalytic cycle of L-mdh were also measured using stopped-flow spectrophotometry.

The flavin reduction rate (280 ± 20 s^{-1}) appeared to be half that observed for the flavin reduction value obtained with L-ldh (604 ± 60s^{-1}). The next step is an intra-molecular electron transfer step between the reduced flavin and oxidised haem, resulting in flavin semiquinone and reduced haem. The rate observed for the haem reduction (605 ± 50 s^{-1}) was similar to that observed with L-ldh (445 ± 50 s^{-1}). This intra-molecular electron-transfer step is thought to occur so rapidly in L-mdh, that full reduction of the flavin groups is not observed until after a disproportionation of the flavin semiquinones, generating 2 fully reduced and 2 oxidised flavins, and further reduction by 2 molecules of mandelate.

Measurement of the flavin and haem midpoint potentials of L-mdh (-120 mV and -10 mV respectively) compared to the values previously obtained for L-ldh (-78 mV and -17mV) confirms that there is a larger driving force between the two prosthetic groups of L-mdh. The third step in the catalytic cycle of L-mdh is the inter-molecular transfer step from the haem group to cytochrome *c*. Stopped-flow studies on the cytochrome *c* reductase activity of L-mdh yielded a second order rate constant of 41.5 ± 2 $\mu M^{-1}s^{-1}$, which represents the rate constant for cytochrome *c* association. The corresponding value with L-ldh is 34.8 ± 0.9 μM^{-1} s^{-1}.

Site directed mutagenesis was used to enable expression of the flavin domain of L-mdh in the absence of the haem containing domain. The flavin domain was purified as the intact enzyme. The steady state turnover of the enzyme with ferricyanide as electron acceptor was measured (500 ± 50 s^{-1}). There was no observed activity with cytochrome *c*. The pre steady-state reduction of the flavin domain was also measured (450 ± 30 s^{-1}).

The kinetic isotope effect (KIE) using DL-[2-^{2}H]mandelate with L-mdh was also measured and compared to the values previously obtained with L-ldh. In the latter enzyme, cleavage of the C(2)-H bond is entirely rate limiting during lactate oxidation, with a KIE value of 8.1 ± 1.4 obtained for the pre-steady-state reduction of flavin. Pre-steady-state flavin reduction of L-mdh has a KIE of 4.9 ± 1.0, suggesting

that C(2)-H bond cleavage by the enzyme is also rate limiting. Kinetic isotope effects were also measured using steady-state methods on the intact and separately expressed flavin domain of L-mdh. In each case the KIE values are similar to those obtained with L-ldh.

Table of contents

List of figures

Figure No.

List of tables

Chapter1:Introduction

Microbial metabolism of aromatic compounds

1.1 Introduction

The citric acid cycle is the central oxidative pathway in respiration, the process by which all metabolic fuels - carbohydrate, lipid and protein are catabolised in aerobic microorganisms. Feeding into this cycle are the secondary catabolic pathways, such as glycolysis, or the ß-ketoadipate pathway. In turn, there are numerous peripheral pathways which convert all the organic compounds on which microorganisms grow into one or another of the substrates for the secondary pathways, or directly, to a citric acid cycle intermediate.

The ability of microorganisms to use aromatic compounds as a source of carbon and energy has attracted a great deal of interest over the years. Plants synthesise large quantities of natural products that contain the chemically stable and inert benzene ring. If the ring could not be cleaved open by certain microbial enzymes, then vast quantities of carbon, locked up in stable rings of six atoms, would be lost from the biosphere when the plants died. In addition to what we may learn about the part played by microbes in the general economy of nature, the investigation of aromatic catabolism is also relevant to problems that arise from the disturbance of natural cycles by the activities of man. Synthetic compounds, such as pesticides and detergents that contain benzene groups are often resistant to microbial attack, leading to long term environmental pollution. Therefore an in depth knowledge of the breakdown of aromatic compounds is vital in order to prevent any lasting damage similar to that incurred by the use of DDT as a pesticide.

1.2 The β-ketoadipate pathway

One of the major microbial pathways used in the breakdown of aromatic compounds is the ß-ketoadipate pathway (Stanier and Ornston, 1973; Harwood and Parales, 1996). This pathway enables bacteria to utilise a wide variety of substrates

including the amino acid tryptophan, phenol, toluene and the 2-hydroxy acid, **mandelic acid** (Gibson, 1968). Before these substrates can enter the ß-ketoadipate pathway, they are converted either to protocatechuate or catechol which then undergo ring fission to form either β-carboxy-cis,cis-muconate (in the case of protocatechuate) or cis,cis-muconate in the case of catechol (Ornston and Stanier, 1966). The two routes eventually converge upon a common metabolite, ß-ketoadipate enol-lactone which is converted to ß-ketoadipate. Through these reactions, the six carbon atoms of the aromatic nucleus have been converted to those of an aliphatic acid (ß-ketoadipate), which is in turn cleaved to form acetyl-CoA and succinate, both of which are components of the citric acid cycle (Ornston and Stanier, 1964). See fig 1.1.

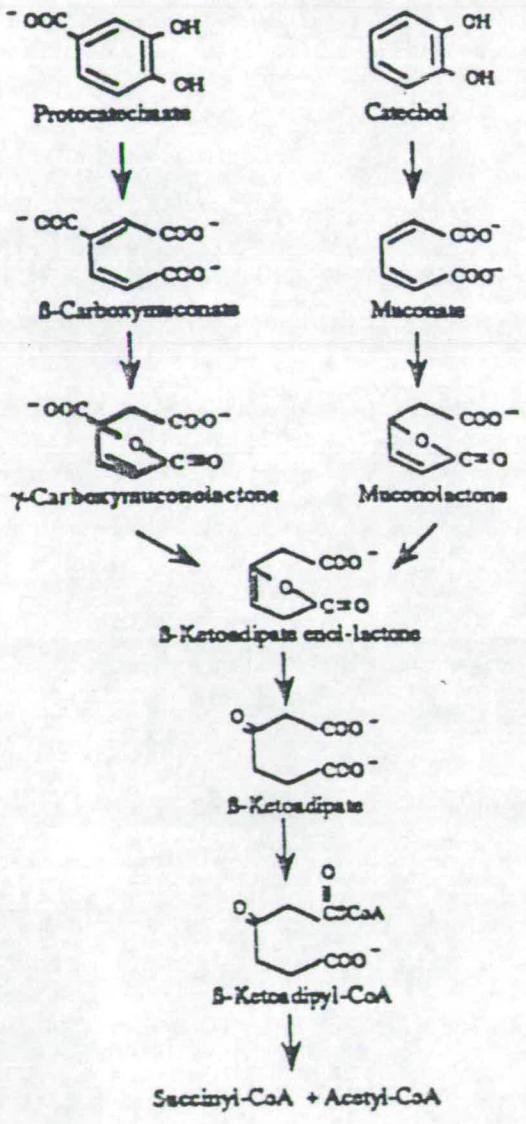

Figure 1.1 Prokaryotic catabolism of aromatic compounds (Harwood and Parales, 1996)

In eukaryotic organisms which contain this pathway, that is, fungi and yeasts, there are certain steps which differ to those found in prokaryotic organisms. For example, the protocatechuate branch in eukaryotes differs in that ß-carboxy-cis,cis muconate is converted to ß-carboxymuconolactone, whereas in prokaryotes the product is γ-carboxymuconolactone (Harwood and Parales, 1996). Another difference is that the two branches of the eukaryotic ß-ketoadipate pathway converge at ß-ketoadipate rather than ß-ketoadipate enol-lactone.

1.3 Mandelate as a source of carbon and energy

There are hundreds of aromatic compounds which are converted into the key substrates described above via a number of peripheral catabolic pathways. In the following section the mandelate pathway is described as an example of these peripheral pathways.

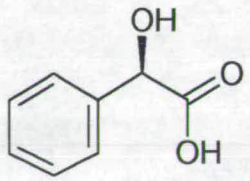

D-mandelate

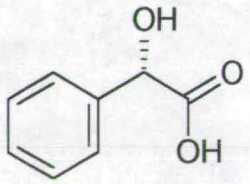

L-mandelate

Figure 1.2 The two enantiomeric forms of mandelate

Mandelate (2-hydroxy-2-phenylacetate) is an aromatic 2-hydroxy acid which occurs naturally in the tissues of plants, for example, in wheat leaves and in grapes (Cologrande, 1959). Much of the mandelate found in nature is a product of the degradation of other compounds found in animal urine, for example, after exposure to styrene (Chakrabarti, 1979) or after ingestion of various pharmaceutical formulations (Middleton *et al.*, 1983). Also, closely related compounds such as 4-hydroxy-3-methoxymandelate, 3-4 dihydroxymandelate and 4-hydroxymandelate are metabolites

of adrenaline, noradrenaline and octopamine, and substantial amounts are continuously being excreted into the environment (Goodhal and Alton, 1969).

Despite mandelate being a relatively uncommon compound in nature, the ability to metabolise either one or both enantiomers of the molecule is found in a wide variety of Gram-negative and Gram-positive bacteria, as well as in filamentous fungi and yeast (Fewson, 1988). For example, mandelate-utilising strains of various species of *Pseudomonas, Arthrobacter, Azotobacter, Bacillus, Nocardia, Rhizobium,* and *Rhodopseudomonas* have all been reported (Fewson, 1988; Chen *et al.*, 1989). In addition, a substantial number of strains of *Acinetobacter calcoaceticus, Arthrobacter* spp. *Pseudomonas fluorescens, P. multiovrans* and *P. putida* which cannot utilise either enantiomer of mandelate can grow on phenylglyoxalate, which is only one metabolic step from mandelate (Fewson, 1988). Among the eukaryotes, several yeasts, including *Aspergillus flavus, Neurospora crassa* and *Rhodotorula graminis,* grow well on both enantiomers of mandelate (Iyayi and Dart, 1980, Durham *et al.*, 1984). Some organisms can also metabolise a wide range of mandelate analogues. For example, *Acinetobacter calcoaceticus, Pseudomonas putida* and *Aspergillus niger* can all convert one or both enantiomers of 4-hydroxymandelate into protocatechuate (Kennedy and Fewson, 1968).

In addition to using mandelate and related compounds as sources of carbon and energy, certain organisms can carry out interconversions of compounds structurally related to mandelate. For example, the fungus *Polyporus tumulosus* can synthesise 4-hydroxymandelate, 2,5-dihydroxymandelate and 3,4-dihydroxymandelate from shikimate. Other examples include *Polyporus hispidus, Penicillium chrysogenum* and *Aspergillus niger* which can convert L-phenylalanine, phenyl acetate and L-tyrosine into mandelate or 4-hydroxymandelate (Hockenhall *et al.*, 1952; Kishore *et al.*, 1974).

1.4 The mandelate pathway

The initial attack on mandelate can be by racemization, ring hydroxylation or stereospecific dehydrogenation. *P. putida* can grow on both enantiomers of mandelate by utilising a mandelate racemase which converts D-mandelate to L-mandelate (Stanier *et al.*, 1966). L-Mandelate dehydrogenase oxidises L-mandelate to form phenylglyoxalate which is in turn converted to benzaldehyde by phenylglyoxalate decarboxylase. There are then two isofunctional benzaldehyde dehydrogenases, one specific for NAD and one for NADP which form benzoate. Benzoate is converted into catechol by the action of benzoate oxygenase and 3,5-cyclohexadiene-1,2-diol-1-carboxylate dehydrogenase. Catechol is subject to ortho cleavage by catechol 1-2-dioxygenase and enters the ß-ketoadipate pathway (Stanier and Ornston, 1973). *P. convexa* can also grow on both enantiomers of mandelate but instead of a dehydrogenation step after racemization, L-mandelate is converted to 4-hydroxymandelate. This product is oxidatively decarboxylated directly to 4-hydroxybenzaldehyde. The substrate for ring cleavage is protocatechuate rather than catechol as in most bacteria (Bhat *et al*, 1973; Bhat and Vaidyanathan, 1976).

Filamentous fungi *Aspergillus niger* (Jamaluddin *et al.*, 1970) and *Neurospora crassa* (Ramakrishna and Vaidyanathan, 1977) and the yeast *Rhodotorula graminis* (Durham *et al.*, 1984) can metabolise both enantiomers of mandelate. In these cases, there are two stereospecific dehydrogenases to form phenylglyoxalate and this is then converted to benzoate. Again, as in *P.convexa,* these organisms metabolise mandelate via the protocatechuate branch of the ß-ketoadipate pathway. (See figure 1.3).

1.4.1 Mandelate racemase

The enzyme, which so far has been found only in strains of *Pseudomonas putida,* is a octamer with an overall molecular weight of 320000 and requires either Mg^{2+} or Mn^{2+} for activity (Hageman *et al.,* 1970). The mechanism of the reaction

catalysed by mandelate racemase involves two proton transfer reactions. The C2 proton of the substrate enantiomer is abstracted by an active site base and the C2 proton of the product enantiomer is derived from the solvent via an active site acid. It has further been suggested that an additional acidic residue, Glu 317, protonates the carbonyl oxygen of the substrate to aid proton abstraction and that the metal ion (the physiological metal ion is Mg^{2+} rather than Mn^{2+}) also serves to increase the acidity of the carbon acid. This enzyme has a high degree of sequence similarity (30%) with an enzyme of the ß-ketoadipate pathway, muconate lactonizing enzyme, indicating that the two proteins share a common ancestor (Tsou *et al.*, 1990).

Figure 1.3 The mandelate pathway of *P. putida*, *P. convexa*, *Rhizobium leguminosarum*, *Aspergillus niger*, *Neurospora crassa* and *R.graminis* a, mandelate racemase; b' L-mandelate dehydrogenase; b'', D-mandelate dehydrogenase; c, phenylglyoxalate decarboxylase; d, benzaldehyde dehydrogenase; e, L-mandelate 4-hydroxylase; f, L-4-hydroxymandelate dehydrogenase; g, L-4-hydroxymandelate oxidase; h, benzoate 4-hydroxylase; h, benzoate 4-hydroxylase; i, benzoate 1,2-oxygenase, j, 3,5-cyclohexadiene-1-2-1-carboxylate dehydrogenase; k, 4-hydroxybenzoate 3-hydrolase (From Fewson, 1988)

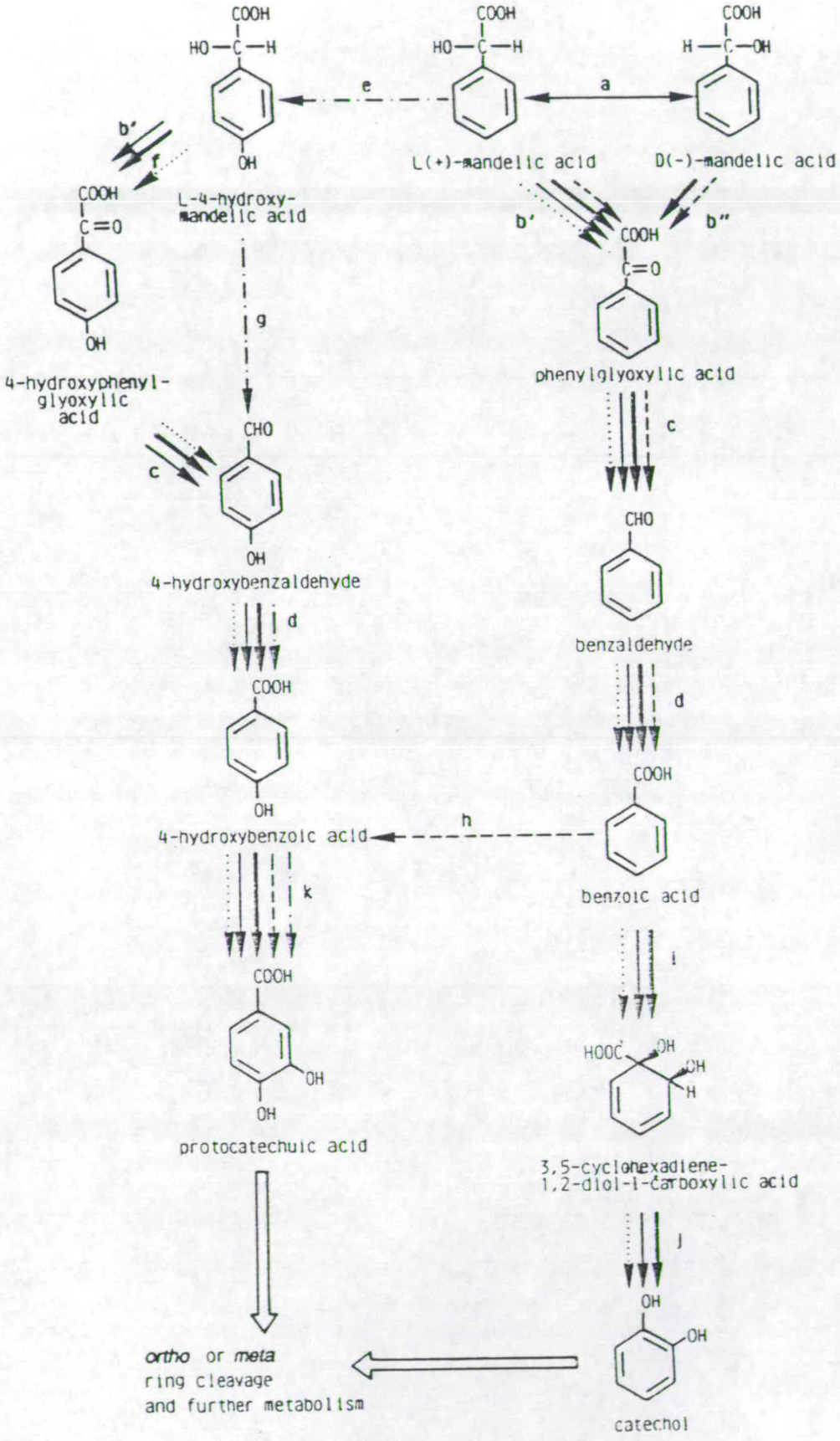
L(+)-mandelic acid
D(-)-mandelic acid
L-4-hydroxy-mandelic acid
4-hydroxyphenyl-glyoxylic acid
phenylglyoxylic acid
4-hydroxybenzaldehyde
benzaldehyde
4-hydroxybenzoic acid
benzoic acid
protocatechuic acid
3,5-cyclohexadiene-1,2-diol-1-carboxylic acid
catechol
ortho or meta ring cleavage and further metabolism
a
b'
b''
c
d
e
f
g
h
i
j
k

1.4.2 Mandelate dehydrogenases

All known mandelate dehydrogenases are stereospecific and they can be divided into two classes: the NAD(P)-independent enzymes and the NAD(P)-dependent enzymes.

The NAD(P) independent mandelate dehydrogenases may be further subdivided into those which contain a flavin molecule in the flavin mononucleotide form, for example, the L-mandelate dehydrogenases of *Acinetobacter calcoaceticus,* (Allison *et al.,* 1985) *Pseudomonas putida* (Tsou *et al.,* 1990) and *Rhododorula graminis* (Yasin and Fewson, 1993) and those which contain a flavin cofactor in the flavin adenine dinucleotide form, for example, the D-mandelate dehydrogenase of *A. calcoaceticus* (Allison *et al.*, 1985b). The FMN containing enzymes have regions of sequence similarity to FMN containing enzymes such as spinach glycolate oxidase (Lindqvist *et al.*, 1991), the FMN domain of *Saccharomyces cerevisiae* L-lactate dehydrogenase (flavocytochrome $b_{2,}$ Chapman *et al.*, 1991) and also the L-lactate dehyrogenases found in *A. calcoaceticus* (Allison and Fewson, 1980) and *Escherichia coli* (Hoey *et al.*, 1987). However, the FAD containing D-mandelate dehydrogenase from *A.calcoaceticus* is similar to the D-lactate dehydrogenase from the same organsim and also the D-lactate dehydrogenase from *E.coli* (Futai, 1973). All the bacterial NAD independent D-and L-mandelate and lactate dehydrogenases are membrane bound.

The second group of mandelate dehydrogenases are the soluble NAD(P) linked enzymes. Examples include the D-mandelate dehydrogenases of *R.graminis* (Baker and Fewson, 1989) and *Lactobacillus curvatus* (Hummel *et al.*, 1988). These enzymes have some similarities to the NAD(P)-dependent D-hydroxyisocaproate dehydrogenase of *Streptococcus faecalis* (Yamazaki and Maeda, 1986) and D-glycerate dehydrogenase from *Hyphomicrobium methylovorum* (Goldberg *et al.,* 1994)

The evidence summarised table 1.1 indicates that the two groups of mandelate dehydrogenases display sufficient difference with regard to their properties that they are unlikely to be homologous with each other. The existence of these two very different categories of mandelate dehydrogenases is similar to the situation with regard to microbial lactate dehydrogenases. Lactate, a 2-hydroxy acid, which has a methyl side group instead of a benzene ring, is also stereospecifically interconverted both by flavoproteins and by NAD(P) linked soluble enzymes. For example, as previously mentioned, *A. calcoaceticus* has membrane bound D- and L-lactate dehydrogenases as well as D- and L-mandelate dehydrogenases. There are striking similarities between the L-specific enzymes and between the D-specific enzymes. For example, the subunit M_r values of the two L- specific dehydrogenases are very similar (44000) and both contain FMN, likewise the subunit M_r values of the two D-specific enzymes are also very similar (60000) and these enzymes contain FAD (Fewson *et al.*, 1993). Comparison of the properties of the four dehydrogenases has led to the conclusion that the two enzymes specific for the D-enantiomers strongly resemble each other, as do the the two enzymes specific for the L-enantiomers, and so each of these pairs of enzymes may have had a common evolutionary origin, and subsequently diverged to act on different 2-hydroxyacid substrates.

The L-mandelate dehydrogenase from the yeast *R. graminis* appears similar to the equivalent enzymes found in *A. calcoaceticus and P. putida* but has some significant differences. The enzyme is a soluble component of the intermembrane space of the yeast mitochondria, rather than being membrane bound (Yasin and Fewson, 1993). Furthermore, the enzyme not only contains FMN but also a haem prosthetic group in each subunit. A similar situation is found in the L-lactate dehydrogenase from the yeasts *Saccharomyces cerevisiae* and *Hansenula anomala.*

The NAD(P) dependent D-mandelate dehydrogenases, from *R. graminis* and *L. curvatus* are dimers with native M_r values which are similar to those of the NAD(P) linked D-lactate dehydrogenases of lactic acid bacteria and staphylococci. The low redox potential of the NAD^+/NADH couple (-320mV) means that this strong

reductant will drive the mandelate/phenylglyoxalate equilibrium in the opposite direction to the FMN-linked L-mandelate dehydrogenase (Fewson, 1992). The equilibrium constant when mandelate dehydrogenation is linked to NAD reduction ($1.6x10^{-11}$ M at pH 9.2) is so unfavourable that the enzyme might be better described as a "phenylglyoxalate reductase". Presumably, during growth on mandelate the reaction is driven in the forward direction by the decarboxylation of phenylglyoxalate and by the oxidation of NADH.

To conclude, mandelate dehydrogenases have almost certainly arisen by recruitment of dehydrogenases from other metabolic pathways. As mentioned earlier, there are scores of peripheral metabolic pathways containing enzymes which may be suitable candidates for gene duplication.

1.4.3 Phenylglyoxalate decarboxylase

The next enzyme in the mandelate pathway is phenylglyoxalate decarboxylase (Fewson, 1988 and 1992). The enzyme, purified from prokaryotic and eukaryotic sources, uses thiamin pyrophosphate (TPP) to remove CO_2 producing benzaldehyde. An entire family of TPP-dependent decarboxylases, for example pyruvate decarboxylase, one of the central enzymes in metabolism, resemble the phenylglyoxalate decarboxylase enzyme with respect to sequence similarity, choice of cofactor and subunit M_r values (Hegeman, 1970).

1.4.4 Benzaldehyde dehydrogenases

The final enzyme in the part of the mandelate pathway which appears to be common to both prokaryotic and eukaryotic organisms is benzaldehyde dehydrogenase, which catalyses the NAD(P) dependent oxidation of benzaldehyde to benzoate. There are pairs of isofunctional benzaldehyde dehydrogenases in the mandelate pathway of both *P. putida* (Tsou *et al.*, 1990) and *A. niger* (Jamaluddin *et*

1. NAD-independent
(a) FMN-dependent
(I) FMN, non-haem, M_r = approx. 44000
L-mandelate dehydrogenase of *A. calcoaceticus*
L-mandelate dehydrogenase of *P. putida*
L-lactate dehydrogenase of *A. calcoaceticus*
L-lactate dehydrogenase of *E.coli*
(II) FMN, haem M_r = approx. 59000
L-mandelate dehydrogenase of *R. graminis*
L-lactate dehydrogenase of *S. cerevisiae*
L-lactate dehydrogenase of *H. anomala*
(b) FAD-dependent, Mr = approx. 60000
D-mandelate dehydrogenase of *A. calcoaceticus*
D-lactate dehydrogenase of *A. calcoaceticus*
D-lactate dehydrogenase of *E. coli*
2. NAD-dependent
D-mandelate dehydrogenase of *R. graminis*
D-mandelate dehydrogenase of *L. curvatus*
D-hydroxyisocaproate dehydrogenase of *S. faecalis*
D-hydroxyisocaproate dehydrogenase of *L. casei*

Table 1.1 The relationship between mandelate and lactate dehydrogenases (Fewson *et al.*, 1993)

al., 1970) but in each case it is unclear whether the separate enzymes have separate functions. The NADP specific enzyme from *P. putida* has an M_r of 200000 and is activated by K^+ ions. The NAD specific enzyme isolated from *A. calcoaceticus* has a similar molecular weight and is also activated by K^+ ions (Chalmers *et al.*, 1991).

Broadly speaking, the mandelate pathway in eukaryotes deviates completely from the bacterial pathway at the benzoate level. In fungi, benzoate is metabolised via the protocatechuate pathway, whereas in bacteria catechol is the terminal aromatic compound derived from mandelate.

1.5 L-Mandelate dehdrogenase from *Rhodotorula graminis*

L-Mandelate dehydrogenase from the yeast *R. graminis* (**L-mdh**) may be described as a flavocytochrome b_2, since it contains a flavin mononucleotide molecule and a *b*-type haem as cofactors in each of its subunits (Yasin and Fewson, 1993). Other flavocytochromes b_2 are the L-lactate dehydrogenases found in the yeasts *Saccharomyces cerevisiae* (**L-ldh,** Jacq and Lederer, 1972) *and Hansenula anomala* (Laberyrie and Baudras, 1972). As mentioned previously, there are numerous similarities between the three enzymes, including a high degree of amino acid sequence identity, M_r values, substrate specificities (both enzymes catalyse the oxidation of a 2-hydroxy acid with subsequent electron transfer to cytochrome *c*) and location of the enzymes in the yeast cell (both enzymes are soluble components of the mitochondrial intermembrane space).

S. cerevisiae flavocytochrome b_2 has been extensively studied over the years and is a paradigm for investigating both inter- and intra- protein electron transfer. The gene encoding the enzyme has been cloned and sequenced (Guiard 1985, Black *et al.*, 1989a) allowing site-directed mutants to be constructed (Reid *et al.*, 1988) and the protein has been overexpressed in *E. coli* (Black *et al.*, 1989b). Furthermore, the crystal structure of the native (Xia and Mathews, 1990) and recombinant (Tegoni and Cambillau, 1994) wild type protein are known to high resolution.

What follows is a summary of the work carried out on *S. cerevisiae* flavocytochrome b_2 as an introduction to the work of this project, which is mainly on

the enzyme homologous to the L-lactate dehydrogenase, namely *R. graminis* L-mandelate dehydrogenase.

1.6 Flavocytochromes

Most biological electron transfer reactions occur between redox centres located in proteins. The redox centres can be organic molecules, such as flavin mononucleotide and nicotinamide adenine dinucleotide; metal ions coordinated to protein side chains, such as iron-sulphur clusters and copper, or coordinated to organic molecules such as protoporphyin. Redox proteins can either be membrane spanning, as is the case for the photosynthetic and respiratory complexes or they can be soluble as is the case for the more simple redox proteins such as the cytochromes *c* and blue copper proteins.

Flavocytochromes are found in both prokaryotic and eukaryotic cells and carry out a vast array of redox reactions. Usually there is little or no functional or physical similarity between these enzymes apart from the fact that they contain a flavin molecule in either the FMN or FAD form and also one or more haems as prosthetic groups.

Flavocytochromes may be best described as 'molecular transformers' as they generally mediate electron transfer between an organic substrate, (a 2 electron donor/acceptor) to a one electron acceptor/donor. This ability arises because the flavin can exist in 3 oxidation states: oxidised, semiquinone and reduced and hence can pass electrons one at a time to the electron acceptor via the haem. (See figure 1.4)

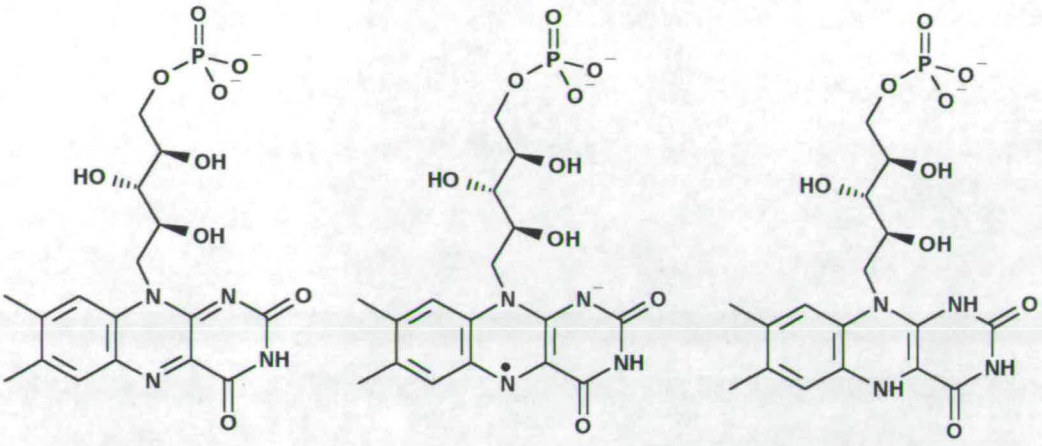

oxidised (ox) **semiquinone (sq)** **hydroquinone (reduced)**
yellow **red** **colourless**

Figure 1.4 The three oxidation states of a flavin mononucleotide molecule

1.7 Flavocytochrome b_2 (L-ldh)

1.7.1 Isolation and Purification of the Native Enzyme

L-Lactate dehydrogenase activity in yeast was first reported in 1928 (Bernheim). It was also noted that this 'lactic acid dehydrase' could also reduce cytochrome *c*. In 1942 Bach *et al.* isolated a soluble cytochrome in yeast extract which was thought to be responsible for the L-lactate dehydrogenase activity reported earlier. The enzyme was purified by crystallisation in 1954 by Appleby and Morton who found that the enzyme contained a flavin mononucletide prosthetic group in stoichiometric ratio with protohaem IX.

Initially, the enzyme was purified from yeast cells. However, this procedure would yield only around 50 mg of pure protein per kg of dried yeast (Labeyrie *et al*, 1978). In order to increase the levels of expressed L-ldh, the enzyme has been overproduced in the bacterium *Escherichia coli* (Black *et al.*, 1989). The enzyme

expressed in *E. coli* contains the same amount of cofactors as the native enzyme, and has a subunit M_r value of 57500. However, recombinant L-ldh is missing the first five residues of its amino acid sequence, though this appears to have no effect on the kinetic properties of the enzyme, which are identical to the native yeast enzyme. It is likely that the nucleotides which encode the first five amino acids are part of the translational initiation site in *E.coli* (Reid *et al.*, 1988). The yield of L-ldh from *E. coli* cells is estimated to be between 500-1000 fold more than from a simiar wet weight of yeast.

1.7.2 The structure of L-ldh

The high resolution (2.4 Å, Xia and Mathews, 1990) crystal structure of the native enzyme, reveals that the enzyme exists as a homotetramer with a four fold axis of symmetry and that each subunit is composed of two distinct domains. The smaller N-terminal domain, termed the haem domain, comprises amino acids 1-100 and has a bis-histidine co-ordinated protohaem IX prosthetic group. The larger domain, the flavin containing domain, consists of amino acids 101 to 487, with the flavin mononucleotide prosthetic group non covalently bound at the enzyme active site. However two crystallographic distinguishable subunits were observed in the asymmetric unit. In subunit one, the structure of the haem domain is resolved and no electron density attributed to either substrate or product (pyruvate) is apparent and the flavin is in the reduced state; in subunit two a molecule of product is bound in close proximity to the flavin, which is in the semiquinone state. In this subunit the entire haem binding domain is unresolved. This anomaly, along with the unusually sharp NMR lines observed for the haem resonances (Labeyrie *et al.*, 1988) was used as evidence that the haem binding domain possesses intrinsic mobility with respect to the FMN binding domain. The haem domain is connected by a single strand of polypeptide to the flavin domain and this region is referred to as the interdomain hinge.

In addition to the the disorder observed in alternate haem domains, a length of polypeptide within the flavin domain was unresolved in the crystal structure. Early preparations of the native (yeast expressed) enzyme had often contained enzyme which had been modified by site specific protelytic cleavage, resulting in two polypeptide chains of 36 and 21 kDa. The position (293 to 314) of this disordered loop suggests that it contains the site for proteolytic cleavage. Therefore this length of protein is often referred to as the proteolytically sensitive loop (Lederer and Simon, 1970). Residues 488 to 511 comprise the C-terminal tail, which winds around the four fold axis of symmetry making contact with the three other subunits and maintaining the tetrameric nature of the enzyme. (See figure 1.5).

1.7.3 The Haem Domain of L-ldh

The haem domain of L-ldh was found to have extensive structural similarity to microsomal cytochrome b_5 (Cristiano and Steggles, 1989) The haem is bound in a hydrophobic crevice consisting of two α-helices, (these contain the co-ordinating histidine residues), and are connected by mixed β-pleated sheet. The family of b_5-like cytochromes also includes mitochondrial and erythrocyte cytochrome b_5 (Lederer, 1994) as well as the haem binding domains of sulfite oxidase (a molybdohaemoprotein, Guiard and Lederer, 1977) and of assimilatory nitrate reductase (a flavomolybdohaemoprotein, Crawford *et al.*, 1988). The existance of a common fold for the haem binding domain of *R. graminis* L-mandelate dehydrogenase was predicted after sequence comparison of its haem binding domain with those of L-ldh and other b_5 like cytochromes (R. Illias, 1997).

The haem domain of L-ldh has been individually expressed in *E.coli* (Brunt *et al.*, 1992). No reduction of the b_2 'core' protein was observed under pre-steady state conditions, when excess reduced flavin domain was mixed with oxidised b_2 core, suggesting that the two domains need to be covalently linked by the hinge region in

order for there to be efficient interdomain communication. The reduced flavin domain could also not efficiently transfer electrons to the physiological redox partner of L-ldh, cytochrome *c*, despite such a transfer being thermodynamically feasible (Brunt *et al.*, 1992). It therefore seems likely that the haem acts as a mediator between the *two*-electron reduction of the FMN by the organic substrate, and the *one*-electron reduction of cytochrome *c*.

Figure 1.5a A single subunit of the *S.cerevisiae* L-ldh tetramer based on the X-ray crytstal structure (Xia and Mathews, 1990)

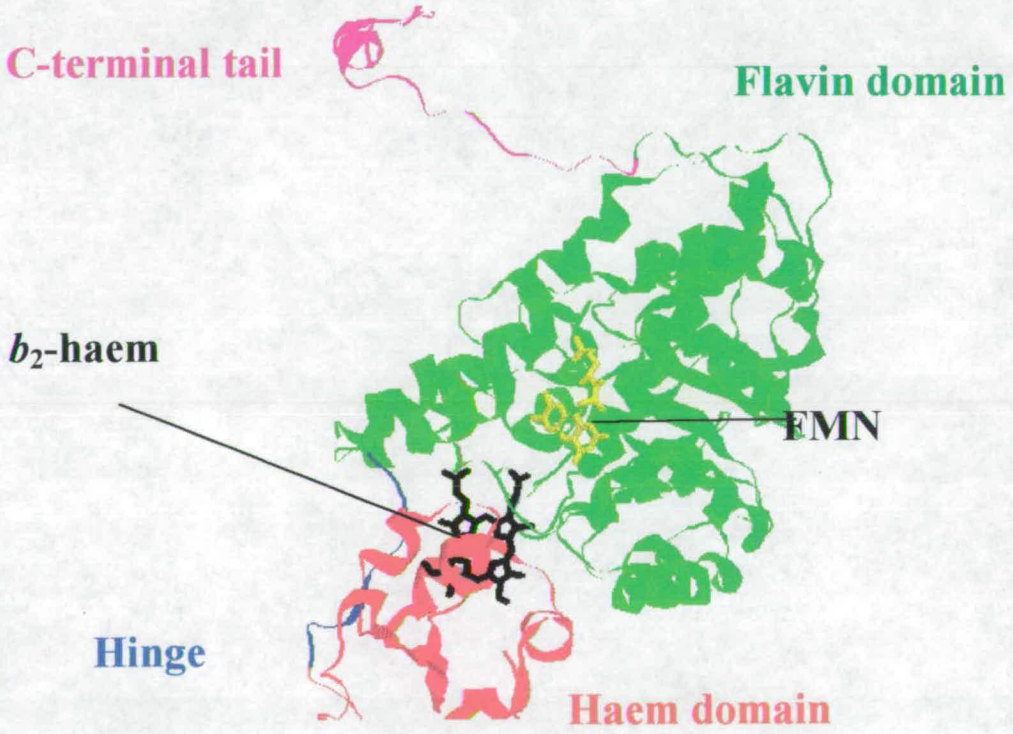

Figure 1.5b The tetrameric structure of L-ldh shown in spacefill representation

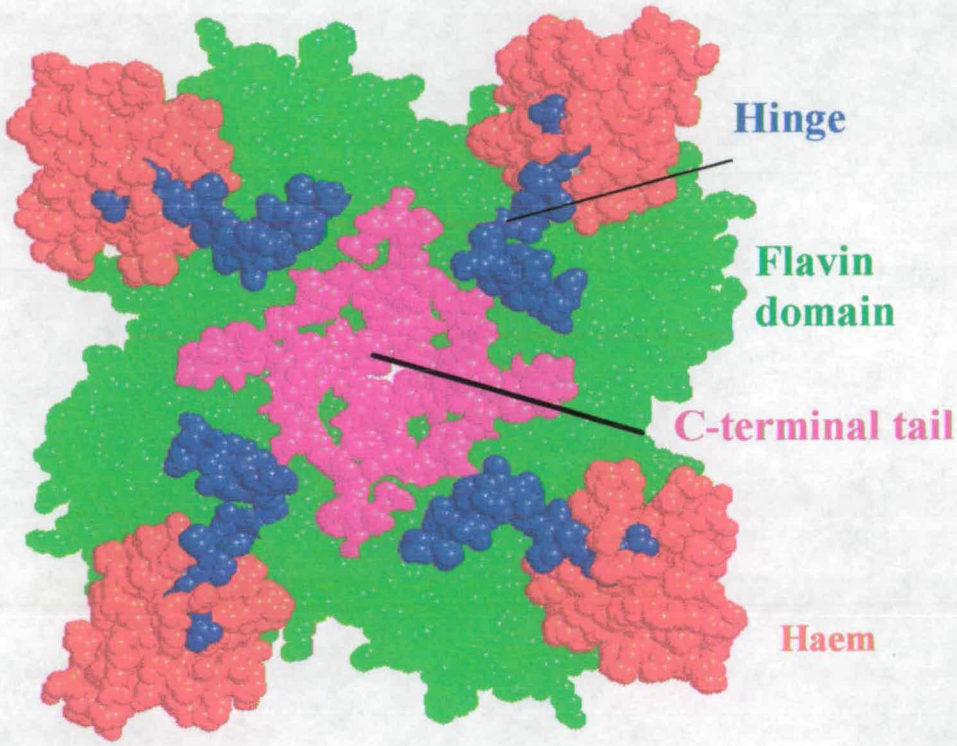

1.7.4 The family of 2-hydroxy acid-oxidising FMN containing enzymes

The flavin domain of L-ldh has an $\alpha_8\beta_8$ TIM barrel structure (Banner *et al.*, 1975), The same folding motif is found in a number of flavoenzymes including spinach glycolate oxidase (Linqvist and Branden, 1989), which also catalyses the oxidation of a 2-hydroxy acid (glycolate) to its corresponding ketoacid (glyoxalate). Figure 1.6 aligns the L-ldh flavin binding domain sequence (Scb_2) with those from *H.*

anomala flavocytochrome b_2 (Hab$_2$) *Mycobacterium smegmatis* L-lactate monooxygenase (Mslox), *E.coli* L-lactate dehydrogenase, *P. putida* L-mandelate dehydrogenase (PpMdh), spinach glycolate oxidase (SpGox) and rat kidney hydroxy acid dehydrogenase (Haox). There is a high degree of sequence similarity between members of this enzyme family, including *R. graminis* L-mandelate dehydrogenase (see section 4.12), suggesting that this enzyme has a similar 3D arrangement, and active site architecture as the other 2-hydroxyacid dehydrogenases/ oxidases.

```
                          hinge
Scb2  KLGPLQGSMP-PELVCPPYAP-GETKEDIARK EQLKSLLPPL DNIINLYDFE YLASQTLTKQ AWAYYSSGAN DEVTHRENHN  159
Hab2  HLGPLVGEFE QE......EE ELSDEEIDRL ERIER.KPPL SQMINLHDFE TIARQILPPP ALAYYCSAAD DEVTLRENHN  151
b5    IIGELHPDDR SKI(87)
MsLox                       SNWGDYENEI YGQGLVGVAP TLPMSYADWE AHAQQALPPG VLSYVAGGSG DEHTQRANVE   60
EcLdh                                 MII SAA...SDYR AAAQRILPPF LFHYMDGGAY SEYTLRRNVE   40
PpMdh                                  MS QNLFNVEDYR KLRQKRLPKM VYDYLEGGAE DEYGVKHNRD   42
SpGox                                    MEITNVNEYE AIAKQKLPKM VYDYYASGAE DQWTLAENRN   40
Haox                                      PLVCLADFK AHAQKQLSKT SWDFIEGEAD DGITYSENIA   39

                                                                                  230
Scb2  AYHRIFFKPK ILVDVRKVDI STDMLGSHVD VPFYVSATAL CKLGNPLEGE KDVARGCGQG VTKVPQMIST LASCSPEEII  239
Hab2  AYHRIFFNPK ILIDVKDVDI STEFFGEKTS APFYISATAL AKLGHP.EGE VAIAKGAGRE ..DVVQMIST LASCSFDEIA  228
MsLox AFKHWGLMPR MLMAATERDL SVELWGKTWA APMFFAPIGV IALC.AQDGH GDAASAQASA RTGVPYITST LAVSSLEDIR  139
EcLdh DLSEVALRQR ILKNMSDLSL ETTLFNEKLS MPVALAPVGL CGMYAR.RGE VQAAKAADAH ..GIPFTLST VSVCPIEEVA  117
PpMdh VFQQWRFKPK RLVDVSRRSL QAEVLGKRQS MPLLIGPTGL NGALWP.KGD LALARAATKA ..GIPFVLST ASNMSIEDLA  119
SpGox AFSRILFRPR ILIDVTNIDM TTTILGFKIS MPIMIAPTAM QKMAHP.EGE YATARAASAA ..GTIMTLSS WATSSVEEVA  117
Haox  AFKRIRLRPR YLRDMSKVDT RTTIQGQEIS APICISPTAF HSIAWP.DGE KSTARAAQEA ..NICYVISS YASYSLEDIV  116

                                                                        loop
Scb2  EAAPSDKQIQ WYQLYVNSDR KITDDLVKNV EKLGVKALFV TVDAPSLGQR EKDMK...LK FSNTKAGP-- ..........  304
Hab2  DARIPGQQ.Q WYQLYVNADR SITEKAVRHA EERGMKGLFI TVDAPSLGRR EKDMK...MK FEADSDVQ.. ..........  292
MsLox KHA..GDTPA YFQLYYPEDR DLAESFIRRA EEAGYDGLVI TLDTWIFGWR PRDLTISNFP FLRGLCLTNY VTDPVFQK..  215
EcLdh PAIKR.P..M WFQLYVLRDR GFMRNALERA KAAGCSTLVF TVDMPTPGAR YRDAH.SGMS GPNA.AMRRY LQAVTHPQWA  192
PpMdh RQC.DGD..L WFQLYVIH.R EIAQGMVLKA LHTGYTTLVL TTDVAVNGYR ERDLH.NRFK IPMSYSAKVV LDGCLHPRWS  194
SpGox STGP.G..IR FFQLYVYKDR NVVAQLVRRA ERAGFKAIAL TVDTPRLGRR EADIK.NRFV LPPFLTLK.. ..........  181
Haox  AAAPEG..FR WFQLYMKSDW DFNKQMVQRA EALGFKALVI TIDTPVLGNR RRDKR.NQLN LEANILLK.. ..........  181

                                  326
Scb2  .......... KAMKKTNVEE SQGASRALSK F....IDPSL TWKDIEELKK KTKLPIVIKG VQRTEDVIKA AEIGVSGVVL  370
Hab2  .......... G..DDEDIDR SQGASRALSS F....IDPSL SWKDIAFIKS ITKMPIVIKG VQRKEDVLLA AEHGLQGVVL  356
MsLox ........KF KAHSGVEAEG LRDNPRLAAD FWHGLFGHSV TWEDIDWVRS ITKMPVILKG IQHPDDARRA VDSGVDGIYC  287
EcLdh WDVGLNGRPH DLGNISAYLG KPTGLEDYIG WLGNNFDPSI SWKDLEWIRD FWDGPMVIKG ILDPEDARDA VRFGADGIVV  272
PpMdh LDFVRHGMP. QLANFV..SS QTSSLEMQAA LMSRQMDASF NWEALRWLRD LWPHKLLVKG LLSAEDADRC IAEGADGVIL  271
SpGox .......... NFEGIDLGKM DKANDSGLSS YVAGQIDRSL SWKDVAWLQT ITSLPILVKG VITAEDARLA VQHGAAGIIV  251
Haox  .......... DLRAL...KE EKPTQSVPVS FPKA....SF CWNDLSLLQS ITRLPIILKG ILTKEDAELA MKHNVQGIVV  244

      373 376
Scb2  SNHGGRQLDF SRAPIEVLAE TMPILEQRNL KDKLEVFVDG GVRRGTDVLK ALCLGAKGVG LGRPFLYANS CYGRNGVEKA  450
Hab2  SNHGGRQLDY TRAPVEVLAE VMPILKERGL DQKIDIFVDG GVRRGTDVLK ALCLGAKGVG LGRPFLYAMS SYGDKGVTKA  436
MsLox SNHGGRQANG GLPALDCLPE VVK......A SGDTPVLFDS GIRTGADVVK ALAMGASAVG IGRPYAWGAA LGGSKGIEHV  361
EcLdh SNHGGRQLDG VLSSARALPA I.....ADAV KGDIAILADS GIRNGLDVVR MIALGADTVL LGRAFLYALA TAGQAGVANL  347
PpMdh SNHGGRQLDC AISPMEVLA. ......QSVA KTGKPVLIDS GFRRGSDIVK ALALGAEAVL LGRATLYGLA ARGETGVDEV  344
SpGox SNHGARQLDY VPATIMALEE VVK.....AA QGRIPVFLDG GVRRGTDVFK ALALGAAGVF IGRPVVFSLA AEGEAGVKKV  326
Haox  SNHGGRQLDE VSASIDALRE VVA.....AV KGKIEVYMDG GVRTGTDVLK ALALGARCIF LGRPILWGLA CKGEDGVKEV  319

                                                    Tail
Scb2  IEILRDEIEM SMRLLGVTSI AELKPDLLDL STLKARTVGV PNDVLYNEVY EGPTLTEEED A      511
Hab2  IQLLKDEIEM NMRLLGVNKI EELTPELLDT RSIHNRAVPV AKDYLYEQNY QRMSGAEFRP GIED  500
MsLox ARSLLAEADL IMAVDGYRNL KELTIDALRP TR                                     393
EcLdh LNLIEKEMKV AMTLTGAKSI SEITQDSL.. VQGLGKELPA ALAPMAKGNA A               396
PpMdh LTLLKADIDR TLAQIGCPDI TSLSPDY... LQNEGVTNTA PVDHLIGKGT HA              393
SpGox LQMMRDEFEL TMALSGCRSL KEISRSHIAA DWDGPSSRAV ARL                        369
Haox  LDILTAELHR CMTLSGCQSV AEISPDLIQF SRL                                    352
```

Figure 1.6 The flavin binding domain sequence of L -ldh and other 2-hydroxyacid oxidising FMN containing enzymes See 1.7.4 for abbreviations. Amino acids which are catalytically important are marked with arrows. The regions marked with a line are the inter-domain hinge, the proteolytically sensitive loop and the C-terminal tail.

1.7.5 The evolutionary formation of L-ldh

Since both domains of the L-ldh subunit have such different ancestries, it is likely that the enzyme arose during evolution as the result of the fusion beween a gene coding for a *b*-type cytochrome and another one coding for an FMN binding oxidase. A family tree has been proposed (figure 1.7, Lederer, 1991, 1994). The haem branch of the family tree initially separates because of the presence of an N-terminal presequence in both the flavocytochrome b_2 and sulphite oxidase (Guiard and Lederer, 1977), which is necessary for their translocation to the mitochondrial intermembrane space. Furthermore, the cytochromes b_5 contain a hydrophobic tail at the C-terminus of the protein which is not found in either L-ldh or sulphite oxidase. Since *R. graminis* L-mandelate dehydrogenase also contains a b_5-like cytochrome and an FMN binding oxidase, the position of L-ldh in the family tree could be replaced by this enzyme. It seems likely that gene encoding one of these flavocytochromes b_2 evolved directly from the other after various mutations.

1.7.6 The physiological role of L-ldh

The reaction catalysed by L-ldh is the oxidation of L-lactate to pyruvate with subsequent electron transfer to cytochrome *c*. The citric acid cycle, which is the central oxidative pathway in metabolism, requires a constant source of acetyl CoA. This activated acetyl unit can be formed by the oxidative decarboxylation of a pyruvate molecule (Baldwin and Krebs, 1981). As well as providing pyruvate for the citric acid cycle, an additional role of L-ldh is to direct the energy generated by L-lactate dehydrogenation (in the form of electrons) ultimately to oxygen. In this

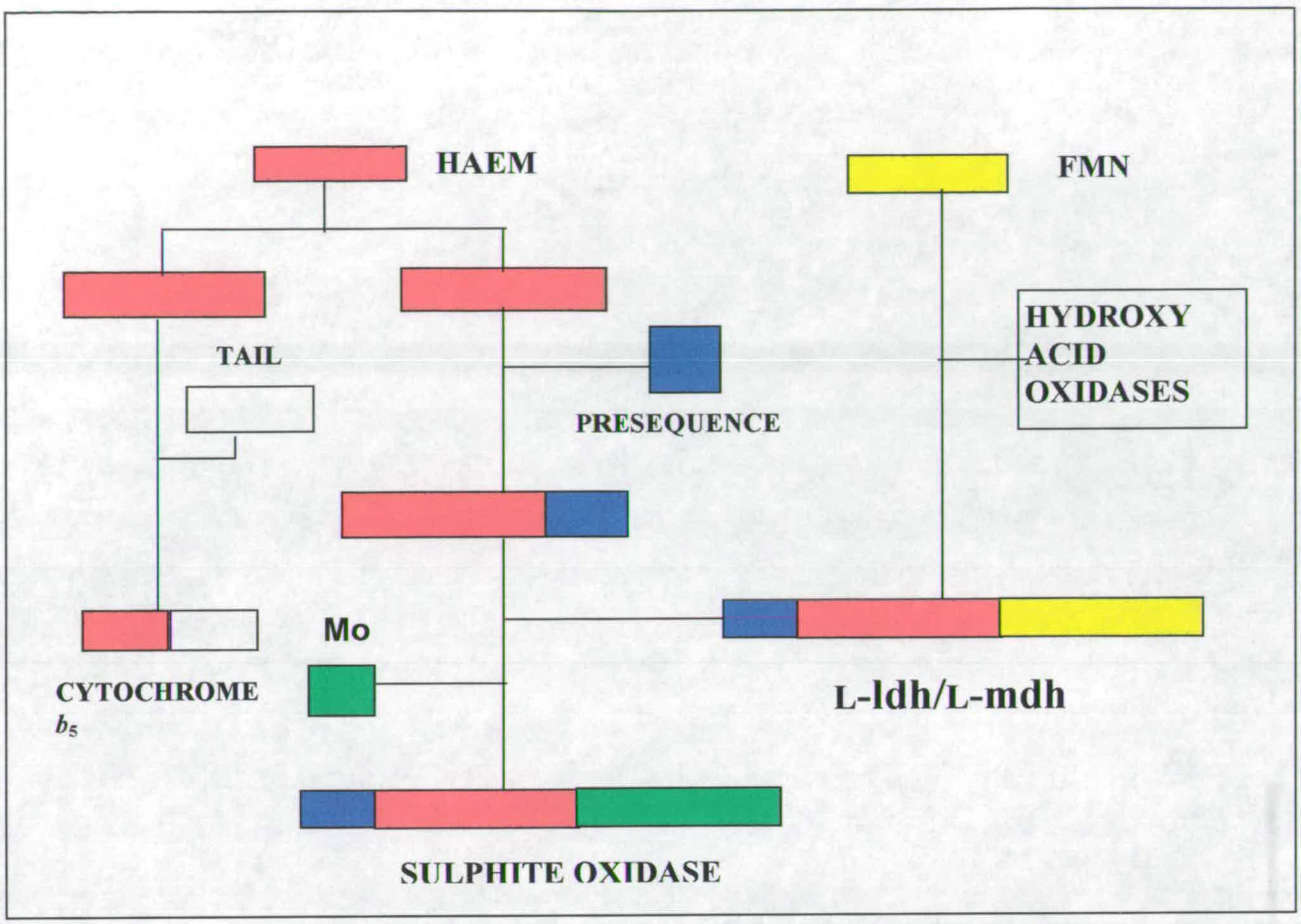

Fig 1.7 The family tree of L-ldh/L-mdh

shorter respiratory chain L-ldh acts as a cytochrome *c* reductase and bypasses the citric acid cycle. The normal degradation of pyruvate via the citric acid cycle yields 15 equivalents of ATP. Even when the normal respiratory chain is inhibited, for example, after addition of the antibiotic antimycin which blocks electron transfer at the level of complex III (ubiquinol: cytochrome *c* reductase), the yeast is still able to survive by utilising the shorter respiratory chain which yields one equivalent of ATP (Pajot and Claisse, 1974). It seems likely that an additional role for the L-mandelate dehydrogenase in *R.graminis* is to provide electrons for a similar, shortened electron transport chain.

1.7.7 Residues involved in cofactor and substrate binding

A. Haem binding

As mentioned previously, the haem group is bound by the haem domain of L-ldh via axial co-ordination to the imidazoles of His43 and His66. The importance of these co-ordinating histidines was examined by replacing His43 with methionine (Miles *et al.*, 1993). The H43M mutant results in a colour change from red in wild type L-ldh to green in the mutant. The mutant enzyme has an electronic absorption spectrum associated with high-spin (five co-ordinate) ferric haem proteins, suggesting that methionine does not act as an axial ligand. This mutation also has a dramatic effect on the cytochrome *c* reductase activity of the enzyme (~750 fold lower than the value observed for wild type enzyme).

B FMN binding.

Close inpection of the crystal structure of L-ldh reveals that a number of ionic and hydrogen bond contacts are formed between FMN and amino acid side chain and backbone atoms of the flavin domain (Lederer, 1991). It is thought that the ionic interaction between the N1 of the flavin pyrimidine ring with Lys349 is of particular importance in flavin reactivity. The corresponding lysine has been mutated to a methionine in *M. Smegmatis* L-lactate monooxygenase (Muh *et al*, 1994a). The effect of this mutation was to destabilise the reduced form of the enzyme, with the midpoint potential of the mutant being more than 100mV more negative than the wild type enzyme. Furthermore, flavoproteins which contain this lysine residue all form red anionic semiquinones (Capeillere-Blandin *et al.*, 1975) in preference to the blue neutral semiquinones found in high potential flavodoxins (Mayhew and Ludwig, 1975). The anionic semiquinone formation of these flavins was thought to be

facilitated by the stabilising influence of the positively charged residue in the vicinity of the flavin N1.

The stereochemistry of flavin reduction is clearly established by the three dimensional structure of the enzyme. The flavin isoalloxazine nucleus *re* face is anchored to the protein by a number of interactions, in particular those between the ribityl O_2 and Ala196 carbonyl, and between the FMN N5 and Ala198 backbone amide. The substrate molecule occupies the *si* face of the cofactor. A comparison of the structures of L-ldh with spinach glycolate oxidase (Lindqvist *et al.*, 1991), shows that not only do both enzymes share the same structural motif ($\alpha_8\beta_8$ barrel), but FMN is also bound in a similar fashion. However, detailed analysis of their active sites shows that the orientation of the glycolate oxidase isoalloxazine ring is tilted relative to the ring system found in L-ldh (see figure 1.8). This creates a pocket on the *re* side of the FMN ring where a water molecule is bound. It is thought that this subtle difference between the two enzyme structures could account for the differences in the enzymes' catalytic properties. Glycolate oxidase, like L-ldh, catalyses the oxidation of a 2-hydroxy acid, but reacts directly with oxygen as its redox partner, rather than cytochrome *c* via a haem molecule. In the flavin oxidative half reaction of glycolate oxidase, the oxygen is reduced to form hydrogen peroxide. It has been proposed that the pocket, occupied by a water molecule in the crystal structure is where the hydroperoxide moiety of a FMN-4a-hydroperoxide intermediate is accommodated. Subtle differences between the *reductive* half reactions of the flavins in each of the two enzymes are explored further in chapter 3.

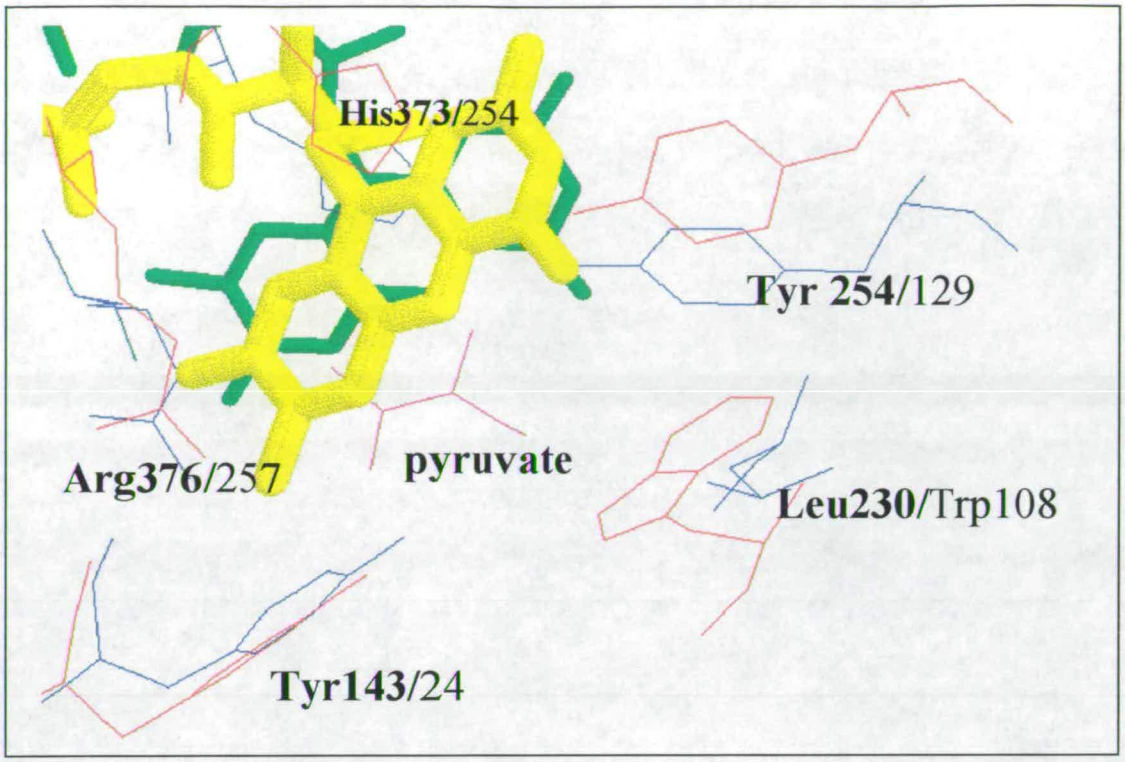

Figure 1.8 The superimposed active sites of L-ldh and spinach glycolate oxidase The active site residues of L-ldh are shown in blue and in bold type and the FMN molecule is shown in green. The corresponding residues in spinach glycolate oxidase are shown in red and normal type. (Lindqvist and Branden., 1991)

C Substrate binding

In the crystal structure of L-ldh, electron density not belonging to the protein was observed close to the isoalloxazine ring of FMN. It corresponded in size to a three carbon ligand and was ascribed to the product of L-lactate oxidation, pyruvate. Its presence in the active site might seem surprising since the crystals were grown in the presence of lactate only. However the crystals were not kept under anaerobic conditions and the enzyme is known to be slightly auto-oxidizable which results in the formation of pyruvate (Chapman *et al.*, 1991).

The carboxylate end of pyruvate forms a salt bridge with the guanido Nε of Arg376. The mutant R376K has a K_m value 100-fold higher than the wild type

enzyme (Miles, 1992), indicating a decrease in the substrate binding affinity of this mutant compared to wild type. This residue is found in the active sites of all FMN binding 2-hydroxy acid dehydrogenases, which highlights the importance of this amino acid in controlling the group-specific nature of L-ldh .

Another conserved active site residue is Tyr143. The hydroxyl group of the amino acid's side chain hydrogen bonds to the carboxylate end of the substrate. This was demonstrated by replacing tyrosine with phenylalanine using site directed mutagenesis (Miles *et al.*, 1992). The Y143F mutant not only had a larger K_m value than the wild type enzyme, attributed to destabilsation of the Michaelis complex but the most drastic effect of this mutation was the reduction in the rate of electron transfer from FMN to the b_2 haem (the rate constant for haem reduction fell 20 fold from $445s^{-1}$ to $21s^{-1}$). The implication of this is that Tyr143, an active site residue which lies between the flavin and haem domains of L-ldh, plays a key role in facilitating electron transfer between FMN and haem groups.

1.7.8 The path of electron flow

The path of electron flow catalysed by L-ldh is the following:

L-lactate → FMN → haem → cytochrome *c*

The L-lactate dehydrogenase activity of the flavin was first assigned by Appleby and Morton after it was noted that there was a correlation between the loss of haem reducibility by lactate and flavin loss upon aging of the protein. The electron transfer functionality was assigned to the b_2 haem since no cytochrome *c* reductase activity was observed in denatured enzyme which had been reconstituted with flavin only (Baudras, 1962).

The catalytic cycle for L-ldh is illustrated (figure 1.9) in terms of its component electron transfer processes. L-ldh catalyses L-lactate dehydrogenation and cytochrome *c* reduction at a rate of 207 s^{-1} per electron transferred (Miles *et al.*,

1992). Since two equivalents of cytochrome *c* are reduced for every revolution of the cycle, the turnover rate is approximately $100s^{-1}$. However this only applies when the concentrations of both cytochrome *c* and L-lactate are at saturation. The K_m values for the former was determined to be 10μM and for the latter to be 0.49 mM.

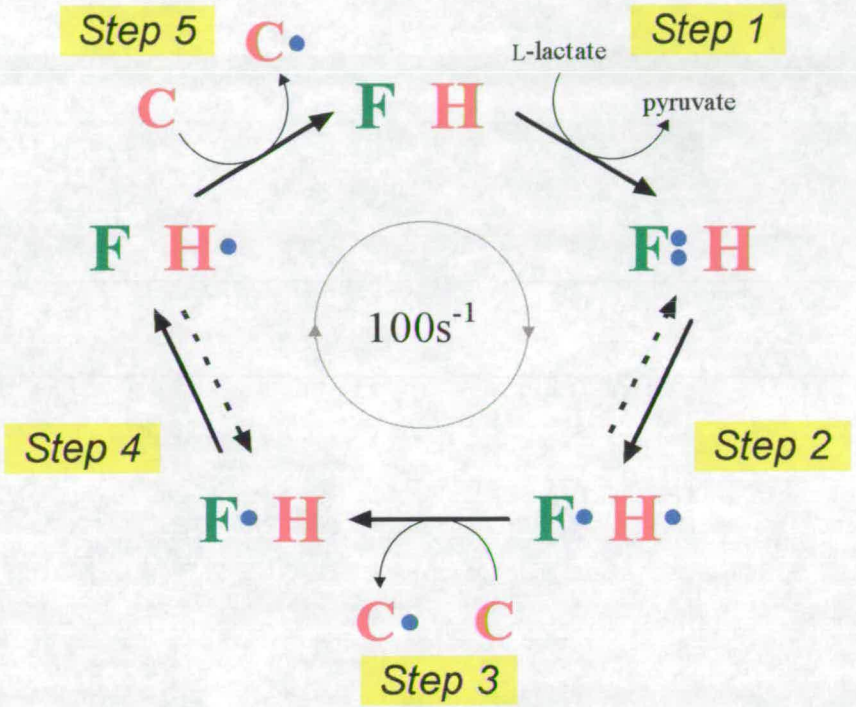

Figure 1.9 The catalytic cycle of L-ldh

The five sequential steps of the catalytic cycle result in an overall turnover rate of $100s^{-1}$. **F H** represents a single subunit of L-ldh, with **F** = FMN and **H** = haem. **C** = cytochrome *c*, and • = a reducing equivalent of electrons. (From Daff *et al.*, 1996).

1.7.9 L-Lactate dehydrogenation/FMN reduction

The first event after substrate binding is proton abstraction by His373, which acts as a general active site base. This reaction is facilitated by electrostatic stabilisation of the imidazolium ion by the carboxylate of Asp282. The role of His373 is central to the catalyic mechanism though so far it has been impossible to

unambigously prove that the proton abstracted by His373 is from the hydroxyl or the α-carbon (C2) of L-lactate. The former leads to the so called 'hydride' mechanism and the latter to the 'carbanion' mechanism.

The hydride mechanism involves the transfer of the C2 hydrogen as a hydride ion to N5 of FMN, while the hydroxyl group is being deprotonated by His373. The carbanion mechanism involves the formation of a carbanion intermediate as His 373 removes the C2 hydrogen as a proton. The carbanion then forms a transient covalent intermediate with N5, before the bond is cleaved resulting in pyruvate and reduced FMN. A large amount of evidence accumulated over the years has been used to suggest that the initial step in catalysis is the formation of a carbanion intermediate.

However, there is some rationale for discriminating against a carbanion in favour of a hydride mechanism. The main factor is that for a carbanion mechanism to operate the active site base responsible for the H abstraction from C2 of L-lactate would have to have a pK_a shift to 25-30 (Williams and Bruice, 1976). Also the pK_a of flavin N5 would have to be in the same region. These pK_a values represent extreme shifts even for a protein environment to impose. Substitution of FMN by 5-deaza-FMN in L-ldh has also been carried out (Pompon and Lederer, 1979) in order to determine the role of FMN N5 in catalysis. 5-Deaza-FMN has the N5 replaced by CH, so if a covalent intermediate is formed along the pathway, then a covalent bond with 5-deaza-FMN should be unable to undergo cleavage to yield products. However, it was found that 5-deaza-FMN L-ldh is reducible by lactate and oxidizable by pyruvate. Furthermore, using tritiated lactate [2-^{3}H] as substrate, tritium is incorporated onto the flavin analogue, a result that would be consistent with hydride transfer.

Finally, by examining the crystal structure of L-ldh it is apparent that the most favourable orientation of the substrate molecule is one that positions the molecule optimally for hydride transfer, rather than for the formation of a carbanion intermediate. The carbanion mechanism relies on the direct interaction of His373

with the C2 hydrogen. However this results in the other two side groups of C2 (-OH and $-CH_3$) being placed in less favourable environments. The methyl group would be placed close to the flavin N5, and the hydroxyl group would be in close contact with the hydrophobic side chain of Leu230. There is however, Tyr254 which may interact by hydrogen bonding to the hydroxyl group. To probe the role of this amino acid, Tyr254 was mutated to phenylalanine (Miles, 1992). The Y254F mutant had no effect on the K_m, suggesting that this residue is not involved in the stabilisation of the Michaelis complex. It has been proposed that the putative role of Tyr254 would be to hydrogen bond to His373 prior to substrate binding and to hydrogen bond to the hydroxyl/carbonyl of the substrate in the transition state (Daff, 1996). In the hydride mechanism the hydroxyl group would hydrogen bond to His373 and the methyl group would interact with the side chains of Leu230 and Leu286 (see chapter 3). The C2 hydrogen would then be in a prime position to interact with the flavin N5.

The rate determining step in flavin reduction has been shown to be the abstraction of the hydrogen from the C2 of L-lactate. A deuterium kinetic isotope effect (KIE) measured by pre-steady-state reduction of FMN of 8 was determined, (Miles *et al.*, 1992, see section 4.5.2). Both mechanisms described above are compatible with this. The reduction of FMN by L-lactate has been studied using stopped flow spectrophotometry, and the rate constant reported to be $604s^{-1}$. This is much larger than the rate determined for the overall turnover of the enzyme ($\sim 100s^{-1}$) and therefore this step should not be rate limiting to the enzyme turnover.

Figure 1.10 The mechanism of L-lactate dehydrogenation . Two possible mechanisms for the abstraction of the αH at C2 of the substrate. A: carbanion transfer B: hydride transfer

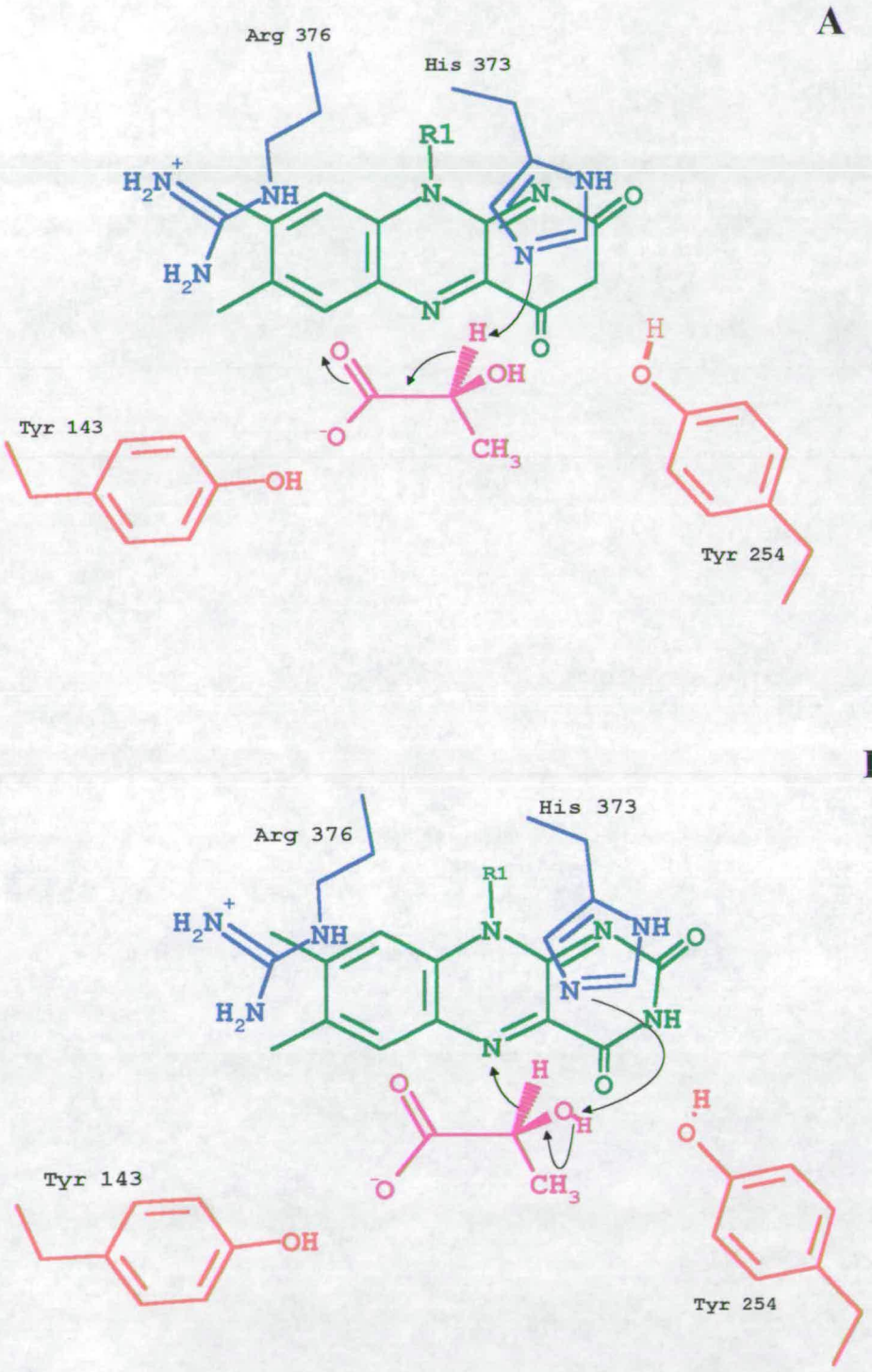

1.7.10 Interdomain electron transfer

As illustrated in steps 2 and 4 of the catalytic cycle of L-ldh, there are two interdomain electron transfer steps: electron transfer from fully reduced flavin to haem and electron transfer from semiquinone to haem.

A. Fully reduced FMN to haem electron transfer

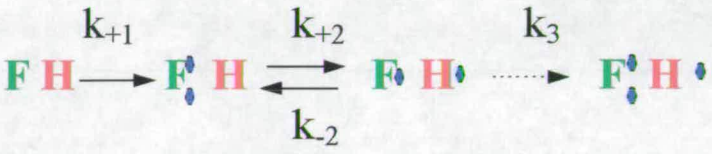

Figure 1.11The individual electron transfer steps which result in the reduction of L-ldh (see figure 1.9 for legend)

Under pre-steady-state conditions, in the absence of any external electron acceptors, the full reduction of the enzyme proceeds as illustrated in figure 1.11. The first two steps relate directly to the catalytic cycle, but a slow phase is always observed in the kinetic traces generated during both FMN and haem reduction. This is due to the entry of a third electron per subunit, (corresponding to four electrons from two L-lactate molecules entering the tetramer), which is made possible by intersubunit electron transfer. The slow phase is catalytically irrelevant during turnover of the enzyme under physiological condtions. The biphasic fit for the haem absorbance has a rapid rate constant of $445s^{-1}$ (Miles *et al.*, 1992), though this is only a poor approximation of the actual rate of haem reduction, as the rate constant will have contributions from all three steps in the scheme above. However, as step 3 only contributes around 15% of the total absorbance change and is much slower than the preceding steps, the contribution of step 3 over the initial 80% of the absorbance change is small. The proportion of reduced haem in this fast phase of the curve can be described by the function:

$$A(1 + k_b e^{-kat} - k_a e^{-kbt}/k_a - k_b) \qquad \textbf{Equation 1.1}$$

This function describes the accumulation of C in an A → B → C consecutive process with step B-C being in equilibrium. if k_a is the value of k_1 in scheme 1 ($600s^{-1}$, Miles *et al.*, 1992) and A is the amplitude of the trace over the fast phase of the haem reduction curve, then a value for k_b of $1800\ s^{-1}$ is obtained (Chapman *et al.*, 1994). From the redox potentials of flavin and haem couples (Walker and Tollin, 1991), step 2 is calculated as lying 85% in favour of the reduced haem, which gives limiting values of $k_{+2} = 1500s^{-1}$ and $k_{-2} = 270s^{-1}$. Hence the rate of electron transfer from fully reduced flavin to oxidised haem proceeds at a rate of at least $1500s^{-1}$. Since this rate is significantly larger than the overall turnover value this step should contribute little towards limiting the rate of turnover.

B. Semiquinone FMN to haem electron transfer

Flavin *oxidation* rates were recently measured (Daff *et al.*, 1996) in an attempt to determine the rate constant for this second, intraprotein electron transfer step. Using a poor substrate of L-ldh (which dramatically slows down the overall turnover rate at step 1 of the catalytic cycle) enables step 4, flavin oxidation, to be monitored as a pre-steady state process (figure 1.12).

Glycolate, which L-ldh turns over at a rate of $7s^{-1}$ compared to $400s^{-1}$ with L-lactate, was used to prereduce a solution of enzyme. The reduced enzyme was then mixed with an excess of cytochrome *c*, which immediately oxidised the b_2-haem. Since the initial FMN-haem electron transfer step (step 2) and subsequent cytochrome *c* reduction step (step 3) occur too quickly to be detected by stopped flow methods, the fast phase of the flavin absorbance trace is only due to the conversion of the flavin semiquinone to oxidised flavin. The rate constant for the flavin oxidation process was

determined to be $120s^{-1}$ by fitting the fast phase to a single exponential function. Therefore this step appears to rate limit the overall catalytic cycle to $100s^{-1}$. Confirmation of this comes (Daff *et al.*, 1996) from quenched-flow EPR experiments which show that during steady state turnover, around 75% of the enxyme is in the FMN semiquinone form.

C. Inter-protein electron transfer

It has been shown that the separately expressed flavin domain of L-ldh can only transfer electrons to cytochrome *c* very slowly ($0.02s^{-1}$ compared to $207s^{-1}$ for the intact enzyme) therefore the role of the haem group is to facilitate electron transfer between reduced flavin and oxidised cytochrome *c*. The interaction between the b_2-haem and cytochrome *c* has been studied extensively as a model system for inter-protein electron transfer. The most recent work investigating this interaction, described below, has been carried out by S. Daff and D. Short.

Figure 1.12 The oxidation of L-ldh flavin An excess of cytochrome *c* is used initially to oxidise L-ldh. Using glycolate as a substrate enables the enzyme to be fully reduced initially, but then slows down the overall turnover rate at step 1, which allows step 4, the semiquinone-haem electron transfer step, to be monitored as a pre-steady-state process. (From Daff *et al.*, 1996).

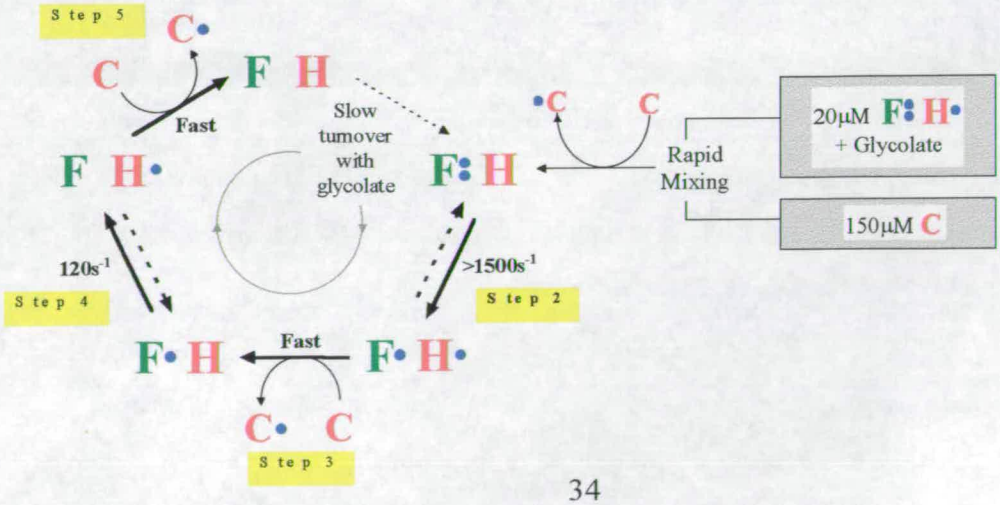

The pre-steady-state reduction of cytochrome *c* was measured by stopped-flow spectrophotometry. Each of the traces generated fitted to a single exponential function indicating that the process is controlled by a single rate determining step. Either the L-ldh-cytochrome *c* complex formation is rapid and reversible and electron transfer within the complex is slow, or the L-ldh-cytochrome *c* binding is slow and electron transfer is faster than both binding and dissociation (Daff *et al.*, 1996). The stopped flow kinetic data has been fitted to a straight line at enzyme concentrations less than 10 μM. If the complex formation was fast and the inter-protein electron transfer slow, the K_d of the Michaelis-Menten curve fitted to all the data points (figure 1.13) would have to be much greater than the enzyme concentrations in the linear region (*i.e*) at concentrations much greater than 10 μM. This is obviously not the case, since a value for the dissociation constant of 8 μM was obtained by studying the inhibition of cytochrome *c* reduction by ferro- and Zinc- cytochrome *c* (Daff *et al.*, 1996). The curvature shown in the graph below may in fact be due to a decrease in accuracy of the rates obtained, since an increasing amount of the reaction will occur in the dead time of the instrument as the concentration of enzyme is increased. We can therefore assume that complex formation is not rapid and that the second order rate constant obtained over the linear part of the graph (<10 μM L-ldh) represents the on-rate constant for cytochrome *c*: L-ldh (35 ± 1 $\mu M^{-1} s^{-1}$) and the rate constant for cytochrome *c* reduction occurs at rates beyond the reliable range of the stopped flow apparatus (>1000 s^{-1}). The dissociation constant derived from inhibition studies (K_d = 8 μM) can be used to estimate the rate of cytochrome *c* dissociation (280s^{-1}). This relatively slow rate of dissociation does not affect the overall rate of turnover, since there appear to be alternative binding sites for cytochrome *c* so that at high cytochrome *c* concentration the turnover rate is unaffected. This has been demonstrated by the inhibition of cytochrome *c* reduction by Zn-cytochrome *c*. Even at saturating concentrations of inhibitor a significant rate constant (around 20 % of the maximum value) can still be measured. This evidence, combined with the similar rate constants determined for the reduction of non-physiological redox partners such

as azurin and stellacyanin, suggests that the interaction between L-ldh and cytochrome *c* is fairly non specific, the major determinant being a favourable driving force for electron transfer.

Figure 1.13 Derivation of the second-order rate constant for cytochrome *c* reduction k_{obs} = pseudo-first order rate constant . Data points < 10 μ M were fitted to a straight line, gradient 35 μMs^{-1} . Points also fitted to Michaelis Menten equation, Km = 42 μM, k_{cat} = 1585 s^{-1}. (From Daff *et al.*, 1996).

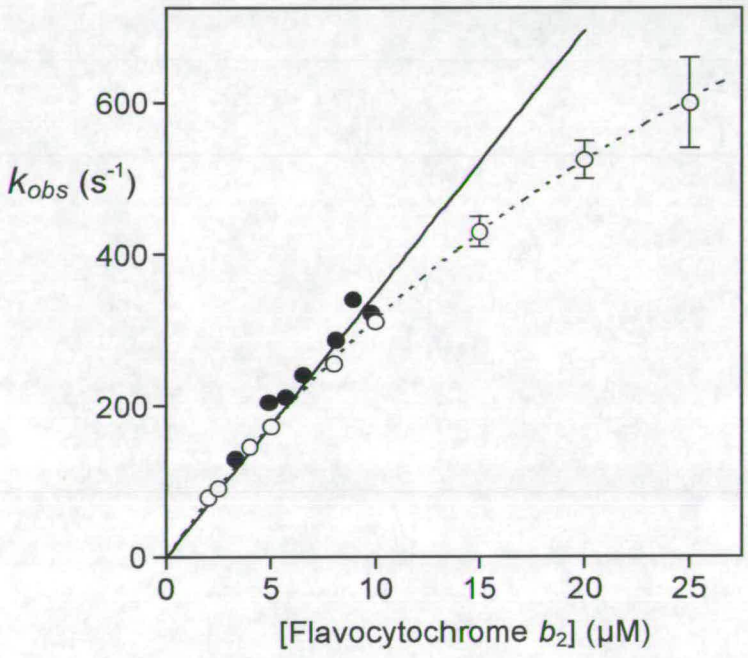

Attempts to co-crystallise L-ldh and cytochrome *c* have so far been unsuccessful. However, Tegoni *et al.* (1983), have proposed a hypothetical complex for the interaction of the two proteins. The model binding site consists of a number of electrostatic interactions between Arg13, Arg38, Lys 54 and Lys79 of cytochrome *c* and Glu91, Glu105, Glu110 and Asp510 of L-ldh. A possible electron transfer pathway has also been suggested based on this model from the L-ldh haem to cytochrome *c*. The electron was predicted to proceed from the haem through residues Ile50-Lys51 and emerge on the protein surface at the side chain of Phe52. However, the actual distance between Phe52 and the porphyrin ring of cytochrome *c* is at least

10Å, an extremely long distance for the electron to pass through space. To test this model, several point mutations were constructed. E91K reverses the charge of a residue thought to bind electrostatically to a cytochrome *c* residue and F52A removes a phenyl ring thought to be part of the electron transfer pathway between the two haems. The second order rate constants for the reduction of cytochrome *c* by the mutants E91K and F52A were measured and found to be within error the same as wild type, suggesting that neither of these residues were critically involved in cytochrome *c* binding or in the electron transfer pathway(Chapman *et al.*, 1996; Daff *et al.*, 1996). However, with the aid of molecular graphics a new model has been proposed. The individual mutations of glutamate 63 and aspartate 72 to lysine residues led to a decrease in the second order rate constant from 34.8 $\mu M^{-1} s^{-1}$, to 13.0 $\mu M^{-1} s^{-1}$ and 24.3 $\mu M^{-1} s^{-1}$ respectively. The construction of the double mutant led to a decrease in the second order rate constant to 6 $\mu M^{-1} s^{-1}$, suggesting that these residues form part of the major cytochrome *c* binding site in L-ldh (Short *et al.*, 1996). The model predicts that a third residue glutamate 237, located in the flavin domain, is also involved in the formation of the complex. An electron transfer pathway has also been proposed: the pathway extends from histidine 66, the axial ligand to the L-ldh haem, through the backbone of alanine 67 and onto proline 68. There is then a 3Å through-space jump to the cytochrome *c* haem. Four cytochromes *c* can be accommodated on the tetramer, each cytochrome *c* binds to one subunit.

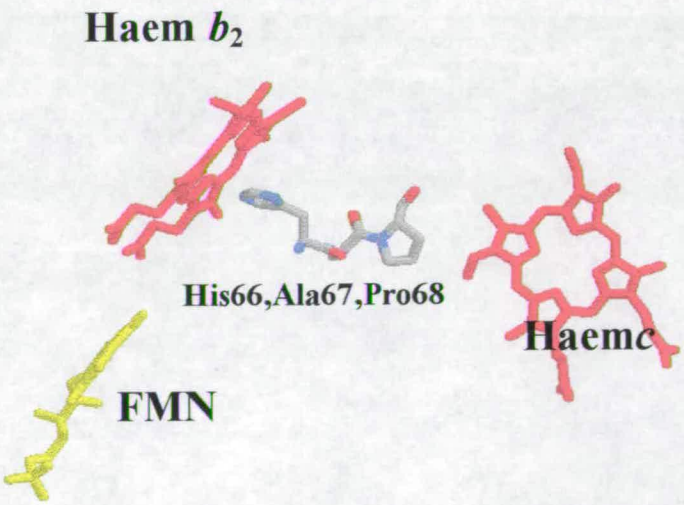

Figure 1.14 The proposed electron transfer pathway from L-ldh haem to cytochrome *c* follows the covalently linked route through the side chain of His66, the backbone of residue 67, and the side chain of Pro68. There is then a through-space jump to the cytochrome *c* haem.

1.8 Previous work on *R. graminis* L-mandelate dehydrogenase

The main aim of this project is to compare the flavocytochrome b_2 from *Saccharomyces cerevisiae*, which acts as an L-lactate dehydrogenase, with the flavocytochrome b_2 from *Rhodotorula graminis*, which acts as an L-mandelate dehydrogenase. What follows is an introduction to the work previously done on the L-mandelate dehydrogenase.

R. graminis is an imperfect yeast (*i.e*, reproduces asexually) that can grow well on mandelate as a sole source of carbon and energy. Baker *et al.* (1989) purified and characterised the D-mandelate dehydrogenase from *R. graminis* and found that unlike the equivalent bacterial D-mandelate dehydrogenases the enzyme was soluble and NAD-dependent. The L-mandelate dehydrogenase was more recently chcarcterised by Yasin *et al.* (1993) and was found to represent a new type of microbial mandelate dehydrogenase in that it was a flavocytochrome b_2.

1.8.1 Purification of L-mdh from *R. graminis* (Yasin and Fewson, 1993)

Approximately 1mg of pure protein was isolated from 80 g wet weight of yeast. The enzyme was then purified to homogeneity by a combination of ammonium sulphate precipitation, ion exchange, hydrophobic interaction and gel filtration chromatography. The N-terminal sequence of the enzyme was determined and found to have around 50% sequence similarity to the N-terminal (haem containing) domain of L-ldh. The relative molecular mass of the L-mdh was determined by gel filtration and the apparent native M_r was 239900. The subunit M_r was determined by SDS/PAGE to be 59100, which suggested that the enzyme was tetrameric.

The L-mdh had broad absorption peaks at 560 and 530 nm and a sharp peak at 413 nm and after reduction with substrate there were absortion peaks at 557, 528 and

423 nm. This absorption pattern is characterisitc of a *b* type cytochrome. The amount of haem present was calculated to be one haem group per subunit. The absorption spectra of trichloroacetic acid extracts of the enzyme were very similar to those of standard FAD and FMN solutions and the addition of *Naja Naja* snake venom resulted in a 9 fold increase in the fluoresence of a standard solution of FAD at 523 nm but had no effect on the fluoresence spectra of either FMN or the extract. These results suggest the presence of FMN as a non covalently bound prosthetic group. The amount of FMN present was calculated to be 1 mole per mole of subunit.

1.8.2 Initial kinetic characterisation of L-mdh (Smekal *et al.*, 1993)

L-mdh is able to use the same electron acceptors as L-ldh (2-6 dichloroindophenol, cytochrome *c* and potassium ferricyanide) and the steady state kinetic properties of the two enzymes were first compared by Smekal *et* al (table 1.2). The most striking result was that L-mandelate dehydrogenase appeared to be unable to oxidise L-lactate and L-ldh was unable to oxidise L-mandelate. Moreover, L-lactate was a competitive inhibitor of L-mdh and L-mandelate a competitive inhibitor of L-ldh.

substrate/ inhibitor	enzyme	k_{cat} (s^{-1})	K_m (mM)	K_i (mM)
L-mandelate	L-mdh	109 ± 3	0.27 ± 0.03	-
	L-ldh	-	-	0.26 ± 0.08
L-lactate	L-mdh	-	-	0.40 ± 0.04
	L-ldh	400 ± 10	0.49 ± 0.05	-
L-phenyllactate	L-mdh	-	-	1.90 ± 0.40
	L-ldh	16 ± 1	0.18 ± 0.04	-

Table 1.2 The kinetic parameters for L-ldh and L-mdh with L-lactate and L-mandelate (from Smekal *et al.*, 1993)

In L-ldh, the major rate determining step in lactate oxidation is hydrogen abstraction at the C2 of L-lactate. This has previously been demonstrated by measuring the kinetic isotope effect (KIE) using deuterated substrate. With ferricyanide as electron acceptor and using lactate deuterated at the C2 position a KIE of 5 was obtained. Steady state experiments were also carried on L-mdh using deuterated mandelate. The KIE value obtained (1.1, Smekal *et al.*, 1993) showed that there was no significant deuterium isotope effect and that the rate limiting step in L-mdh was different to that in L-ldh. This meant that the transition steps of the two enzymes must also be different. The oxidation of mono substituted mandelates by L-mdh was also carried out to evaluate the role of the substrate in the catalytic mechanism (Smekal *et al.*, 1994). Values of K_m and k_{cat} were determined for mandelate and 8 substrate analogues which varied in the position (meta and para) and electron withdrawing/donating power of the ring substituent. Values of the activation parameters ΔH and ΔS were determined over the range 5-37°C in order to determine the free energy of formation of the transition state. This was calculated to be approximately 60kJmol^{-1}.

The oxidation of various substituted mandelates by L-mdh was analysed using a Hammett type approach. The Hammett equation correlates the effect of a meta or para ring substituent on the rate of reaction. (See equation 1.2)

$$\log(k_{cat})_R = \log(k_{cat})_H + \sigma\rho \qquad \textbf{(Equation 1.2)}$$

Where $(k_{cat})_R = k_{cat}$ for substituted mandelate and $(k_{cat})_H = k_{cat}$ for mandelate. σ values are numbers which sum up the total electronic effects (resonance plus inductive) of a group R attached to the ring; and ρ is the reaction constant. Reactions with a positive ρ are helped by electron withdrawing groups and reactions with a negative ρ are helped by electron donating groups. All fits resulted in a fairly small ρ value (between 0.25 and 0.5) indicating that the ring substituents had only a small demand on the electron density at the C2 of the transition state. This was consistent

with a fairly electron rich C2 in the transition state. To gain further insight into the separate contributions of inductive and resonance effects the data were analysed in terms of dual substituent parameters. Using Taft's dual substituent parameters equation, (See equation 1.3),

$$\log(k_{cat})_R = \log(k_{cat})_H + \rho(\sigma_I + \lambda\sigma_R^+) \quad \textbf{(Equation 1.3)}$$

where σ_I is the value for the inductive effect and σ_R+ is the value for the resonance effect. The value of λ gives an estimate of the resonance demand on the C2 carbon of mandelate by the aromatic ring. The best fit value of λ was found to be 0.64 which suggested that the relative importance of the resonance effect is only around two thirds that of the inductive effect. The reason for this was explained in terms of the transition state structure of L-mdh. If the transition state involved the formation of a carbanion type species at the C2 position then maximum resonance stabilisation would be achieved if the C1-C2 bond were coplanar with the ring of the mandelate. If however, the C2-C3 bond were to twist such that the transition state lost planarity then the resonance contribution would fall. This loss of planarity would have no effect on the inductive effect contribution. It was proposed, based on these results that the oxidation of mandelate by L-mdh proceeded as follows. The enzyme-substrate Michaelis complex is formed and the enzyme imposes considerable strain on the substrate distorting the geometry at the C2 position and polarising the C2 carbon. This represents the rate limiting step in mandelate oxidation. The C2 hydrogen is lost as a proton generating a carbanion intermediate, and electron transfer from carbanion to flavin then occurs generating reduced flavin and phenylglyoxalate, the oxidised product. As shown from the different KIE effects of the two flavocytochromes, the L-mdh catalysed reaction proceeds via a different transition state from that in L-ldh.

The pre-steady-state reduction of recombinant L-mdh (flavin domain) by substituted mandelates have also been measured recently (D. Robertson, unpublished results). However, experiments have tended to show that rates of flavin reduction are

increased using substituted mandelates which have electron *donating* groups, such as 4-hydroxy mandelate. These results are explained in terms of the kinetic isotope values measured on the recombinant enzyme (Section 4.5.2).

1.8.3 Cloning, sequencing and expression of L-mdh (R. Illias, 1997)

Based on the N-terminal sequence of the *R. graminis* L-mdh (Yasin *et al*, 1993) two degenerate oligonucleotide primers for PCR were designed. Single stranded cDNA made by reverse transcription of total RNA from *R. graminis* was used as a template in the PCR, which amplified a fragment of 81 base pairs. Chromosomal DNA from *R. graminis* was isolated and digested with different restriction enzymes and Southern blot analysis was carried out on the digested chromosomal DNA. This was then probed with the ^{32}P labelled 81bp fragment. A 5.5 kb fragment containing the entire L-mdh gene was cloned and primers designed for sequencing. About 2788 bp were sequenced from the 5.5 kb insert with the coding sequence ending at position 2603. However, there are numerous introns in the L-mdh genomic sequence and in order to determine the coding sequence of L-mdh in the absence of introns, single stranded cDNA was used as a template in the PCR reaction. Two primers were designed based on the the known N-terminal sequence of the enzyme and the C-terminal sequence predicted from the genomic DNA. A fragment of 1.5 kb was amplified and the primers that were used to sequence the genomic DNA of L-mdh were used to sequence the cDNA.

1					E	P	K	L	D	M	N	K	Q	K	I	S	P	A	E	V	A	K	H	N
2	D	A	Q	L	P	V	K	Q	R	G	R	A	R	S	I	S	A	A	E	V	A	K	H	N
3									S	K	A	V	K	Y	Y	T	L	E	Q	I	E	K	H	N

Figure 1.15 Comparison of the N-terminal amino-acid sequences of 1. L-ldh, 2. L-mdh and 3. microsomal cytochrome b_5 of beef

The amino acid sequence based on the 1479 bp sequence of the amplified L-mdh cDNA is 492 amino acids long. A computer search of the Swissprot protein sequence data bank demonstrated that the *R. graminis* L-mdh exhibits 26-42% identity to each of: L-ldh, *H. anomala* L-lactate dehydrogenase, glycolate oxidase from spinach, L-lactate dehydrogenase from *E. coli* and L-mandelate dehydrogenase from *P. putida*.. All these enzymes are members of the family of FMN dependent 2-hydroxy acid oxidising enzymes. Comparisons of the sequences of the haem domains of L-mdh and L-ldh shows there are 22 invariant residues conserved in this region. These include the two histidine ligands to the haem iron (His47 and His70 in L-mdh) and the tyrosine residue which hydrogen bonds to a haem propionate in L-ldh is also conserved (Tyr141). The flavin binding domain of L-mdh contains almost all of the catalytically important residues found in the L-ldh active site, including Asp282 (Asp380), His373 (His377) and Lys349 (Lys353). Most of the residues thought to be involved in controlling substrate specificity are conserved between the two enzymes. However, the residues corresponding to Ala198 and Leu230, which are thought to interact with the methyl side group are not. In L-mdh these are both replaced by smaller glycine residues. The possible importance of these residues in determining the substrate *side-chain* specificity of of the two enzymes is investigated in chapter 3.

Two methods were used to express L-mdh: the *L-mdh* gene was inserted into the expression vector pKK223-3 and transformed into *E.coli* JM105 cells, the gene was also inserted into pRC23 and transformed into *E. coli* NF1 cells. A single strong band with size at around 59 kDa was detected on a Western blot, using the latter expression system. Preliminary kinetic data on partially purified enzyme indicated k_{cat} and K_m values similar to those calculated for the native enzyme.

1.9 Project aims

(1) To investigate the reasons for the different substrate specificities of L-ldh and L-mdh by 'engineering in' mandelate dehydrogenase activity into the L-lactate dehydrogenase enzyme.

(2) To increase the expression levels of the recombinant form of L-mdh in *E.coli* and to purify the enzyme to homogeneity.

(3) To compare the kinetic properties of this enzyme with the recombinant form of L-ldh.

(4) To clone, express and purify the flavin domain of L-mdh (L-mdh fdh), in the absence of the haem domain.

(5) To compare the kinetic properties of L-mdh fdh with intact L-mdh and also the isolated flavin domain of L-ldh (L-ldh fdh).

Chapter 2: Materials and Methods

2.1 Growth and maintenance of strains

Bacterial stocks		
Name	**Genotype**	**Reference**
E. coli TG1	*sup E, hsdΔ5, thi, Δ(lac-proAB), F' [traΔ36, proAB$^+$, lac I^q, lacZΔM15]*	Gibson, 1984
E. coli AR120	*λN99 (F$^-$, galK2, LAM$^-$,rpsL200* derivative *(lacI, Δ-gal, nad A::Tn10)*	Gottesman & Yarmolinsky, 1968
E. coli BW313	*dut, ung, thi-1, relA, spoT1/F' lysA*	Kunkel, 1985
E. coli JM109	*rec A1, supE44, end A1, hsdR17, gyrA96, rel A1, thi (Δlac-proAB)*	Lab Stock
E. coli NF1	*K12ΔH1, Δtrp , lacZ, λNam 7, Nam 53, cI857, ΔH1*	Stanley &Luzio, 1983

2.1.1 Growth media

Luria Broth	**Per litre**		**Terrific broth**	**Per litre**
Tryptone (Difco Bacto)	10 g		Tryptone	12 g
Yeast extract (Difco Bacto)	5 g		Yeast extract	24 g
NaCl	5 g		Glycerol	4 ml
$MgSO_4$	6 g		K_2HPO_4	12.54 g
			KH_2PO_4	2.31 g

2.1.2 Maintenance and storage of cultures

Bacterial colonies were stored at 4°C for up to 4 weeks on agar plates containing 100 $\mu g ml^{-1}$ ampicillin (Sigma). For long term storage, 20 % (v/v) glycerol was added to 1ml aliquots of bacterial culture and stored in a sterile microcentrifuge tube at -80°C.

2.1.3 Preparation of ultra competent cells

200ml of Luria Broth was innoculated with 1ml of an overnight culture and shaken at 18-23°C until an $O.D_{600nm}$ of 0.6 was reached. Cells were placed on ice for 10 minutes to arrest growth, then pelleted by centrifugation at 2500***g*** for 10 minutes in a Sorvall RC-5B centrifuge using a SS34 head. The pellets were gently resuspended in 80 ml of ice cold TB solution. After another 15 minutes on ice, the cells were pelleted as before. The pellets were resuspended in 20ml of TB solution and DMSO was added to a final concentration of 7%. The cells were left on ice for another 10 minutes, divided into 1ml aliquots and snap frozen in an ethanol/ dry ice bath .

TB solution	
PIPES	10mM
$CaCl_2$	15mM
KCl	250mM
pH to 6.7 then add	
$MnCl_2$	55mM

2.1.4 Transformation of *E. coli*

Supercoiled plasmid DNA was added to 200 µl of ultracompetent *E.coli* cells and left on ice for 30 minutes. The cells were then heat shocked at 42°C for 30 seconds. SOC media (800µl) was added to the cells, which were incubated at 37°C (or 30°C in the case of NF1 cells) for 1 hour. The cells were then pelleted in a microcentrifuge and resuspended in 50µl of SOC media. The resuspended cells were spread onto agar plates containing 100µgml^{-1} ampicillin. The plates were incubated at 37°C (30°C for NF1 cells) overnight.

SOC media	
Tryptone	2 %
Yeast extract	0.5 %
NaCl	10 mM
KCl	2.5 mM
$MgSO_4$	10 mM
$MgCl_2$	10 mM
Glucose	20 mM

2.2 DNA Manipulation

TE buffer	
Tris.HCl pH 8.0	10 mM
EDTA	1 mM
TEG/lysozyme	
Tris.HCl pH 8.0	25 mM
EDTA	10 mM
glucose	50 mM
add 20 mg lysozyme (Sigma) per 10 ml buffer	

Solution B	
sodium acetate	0.1 M
EDTA	1 mM
Tris. HCl pH 8.0	40 mM
SDS (Sigma)	0.1%

2.2.1 Plasmid DNA

Plasmid DNA was isolated from *E. coli* using the alkaline lysis method (Birnboim and Doly,1979). Luria broth (50ml), containing 100μgml^{-1} ampicillin was inoculated with a single colony of the plasmid-bearing strain and grown at 37°C overnight with shaking. The culture was pelleted by centrifugation (a Sorvall SS-34 head was used throughout) and resuspended in 2ml of TEG/lysozyme. Lysis buffer (4ml of 0.2M NaOH, 1% SDS) was added and placed on ice for 5 minutes. Following lysis, 3ml of 3M sodium acetate (pH 5.0) was added to precipitate chromosomal DNA, SDS and proteins.

After a further incubation on ice for 15 minutes the precipitate was removed by centrifugation for 10 minutes (10000***g***). Ethanol (16 ml) was added to the supernatant, which had been transferred to a sterile Corex tube, mixed, incubated at -20°C for 15 minutes and then centrifuged for 10 minutes at 8000***g***. The pellet was resuspended in 2 ml of Solution B and 2ml of phenol/ chloroform added. The corex tube was spun at 4000***g*** for approximately 5 minutes and the aqueous phase transferred to a fresh corex tube. 8 ml of ethanol was added which precipitated DNA and the mixture left on ice for another 15 minutes.

The DNA was pelleted by spinning the tube at 8000g for 10 minutes. The pellet was resuspended in 0.4ml TE buffer, transferred to a microcentrifuge tube and 20μl boiled RNaseA (Sigma) was added and incubated at 37°C for 1 hour. 20μL 4M NaCl was added and the aqueous phases extracted twice with equal volumes of phenol/chloroform. 1ml of ethanol was added to the final aqueous phase and the tube left for 10 minutes on ice. The microcentrifuge tube was spun for 5 minutes (12000***g***)

and the pellet of plasmid DNA was then dried under vacuum and resuspended in 200µl H_2O. Plasmid DNA was stored at 4°C.

2.2.2 Single stranded DNA

Single stranded DNA from plasmids with the F1 origin of replication (phagemids) were prepared from E. coli using M13KO7 helper phage (Vieira and Messing, 1987). A single colony of E. coli host containing the phagemid was grown in 2ml of Luria broth with 100 μgml^{-1} ampicillin, at 37°C to mid-log phase (OD_{600nm} = 0.5). M13KO7 helper phage was added to a multiplicity of infection of 10 and the culture was shaken vigorously. After 1 hour, 400µl of infected cells were mixed with 10ml of Luria broth (+100μgml^{-1} ampicillin), to which kanamycin was added at a final concentration of 70μgml^{-1}, to select for the phage. The culture was grown overnight at 37°C, with shaking.

Cells were removed from the culture supernatant by centrifuging 1.5ml of the overnight culture at 12000***g*** for 5 minutes. To precipitate the phage, 1.2ml of the supernatant was added to 0.3 ml of NaCl/PEG solution (2.5M NaCl, 20% polyethylene glycol 6000) and left at room temperature for 15 minutes. The phage were pelleted at 12000g for 5 minutes. After removing all the NaCl/ PEG solution, the phage were resuspended in 100µl TE. Phenol (50µl) was added and the suspension vortexed and centrifuged for 1 minute. DNA, which was located in the aqueous layer, was removed to another tube and 0.5 ml chlorofom added. The mixture was vortexed, spun and the chloroform layer removed. 10µl 3M sodium acetate (pH 5.5) and 250µl ethanol were added and left for 1 hour at -20°C, then spun for 5 minutes at 4°C. The supernatant was removed and the pellet of single stranded DNA was dried and resuspended in 50µl of TE.

2.2.3 Gel electrophoresis of DNA

Agarose gel electrophoresis of DNA

10 X TBE	
Tris base	108g
Boric acid	55 g
0.5 M EDTA	40 ml
dH_2O	made up to 1 litre

DNA was separated in 0.8% (w/v) agarose BRL electrophoresis grade with 0.5μgml^{-1} ethidium bromide in 1 X TBE. Prior to loading, DNA samples were mixed with 0.1 x volume of loading buffer (20% glycerol; 20mM EDTA; 0.1% bromophenol blue). Electrophoresis was carried out horizontally across a potential difference of 1-10Vcm^{-1}. Bacteriophage λcI857 DNA restricted with *Hind*III was used as size markers. DNA was visualised by UV illumination and photographed.

Recovery of DNA from agarose gels

DNA was electrophoresed through an agarose gel until there was a clear separation of DNA fragments. The desired fragment was visualised by UV illumination, cut out, and extracted from the agarose using Geneclean (Bio 101 Inc). The agarose was weighed and 0.5 volume of TBE modifier (part of the Geneclean kit) and 4.5 volumes of 6M NaI solution were added (the approximate volume of the gel was determined by 1g ≈ 1 ml). The agarose was dissolved by heating to 55°C for 5 minutes with occasional mixing, and then cooled on ice for 5 minutes. The molten agarose was treated with 5 μl of 'glass milk' (a silica matrix suspended in water) and left for 5 minutes on ice with occasional mixing to allow the DNA to bind to the silica matrix. The glass milk was pelleted by centrifugation at 15000***g*** for 1 minute. The supernatant was discarded and the pellet washed three times with 500μl of NEW

wash (NaCl/ ethanol/ water mix). After a final spin all the NEW wash was discarded and the DNA was eluted from the glass milk in 20µl of TE buffer at 55°C. The mixture was spun again, and the supernatant containing the DNA, transferred to a fresh microfuge tube and stored at 4°C.

2.3 Site directed mutagenesis (SDM)

5 x phosphorylation buffer	
Tris. HCl pH 7.5	250 mM
$MgCl_2$	50 mM
DTT	25 mM
Spermidine	0.5 mM
ATP	5 mM
10 x annealing buffer	
Tris.HCl pH 7.5	250mM
$MgCl_2$	100mM
NaCl	500mM
5 x synthesis buffer	
Tris.HCl pH 7.5	50 mM
dNTPs	2.5 mM
ATP	5 mM
DTT	10 mM
DNA sequencing gel (6% acrylamide)	
Protogel (30 % acrylamide; 0.8 % bis-acrylamide)	16 ml
Urea	33.6 g
10 x TBE	8 ml
dH_2O	to 80 ml
TEMED (Sigma)	180 µl
10% ammonium persulphate (Sigma)	180 µl

2.3.1. Phosphorylation of oligonucleotide

100 pMol of oligonucleotide

5µl 5 x Phosphorylation buffer

5 units T4 polynucleotide kinase (Gibco-BRL)

sterile dH_2O to 25µl (final oligo conc = 4pMol/µl)

The reaction mix was incubated at 37°C for 45 minutes and then incubated at 68°C for 10 minutes to inactivate the enzyme and stop the reaction. The phosphorylated oligonucleotide was used immediately.

2.3.2 Annealing of oligo to template

0.05 pMol (~250ng) of single stranded uracil template DNA

1.25 pMol of phosphorylated oligonucleotide

2µl 10 x annealing buffer

sterile dH_2O to 20µl

The annealing mix was incubated at 70°C for 5 minutes and then allowed to cool slowly to 4°C over 30 minutes.

2.3.3. Synthesis

6µl 5 x synthesis buffer

1µl T4 DNA polymerase (10U/µl)

1µl T4 DNA ligase (2U/µl)

(Both Gibco-BRL)

sterile dH_2O to 30 µl

This was incubated at room temperature for ~5 minutes and then at 37°C for 90 minutes.

This was performed by the method of non-phenotypic selectrion, as described by Kunkel (1986). The L230G mutation was constructed using the oligonucelotide L230G (5′ GAT ATC TAC TGG TGC TTC ATG ATG T 3′) (Oswel DNA Service). In order to test the efficiency of the extension/ ligation reactions, a 5µl volume of the SDM reaction mix was electrophoresed in a 1% agarose gel along side single stranded and double stranded pGR401 DNA as controls. If the reaction product DNA co-migratedwith the double stranded DNA and not the single stranded DNA control, the reaction was deemed successful and 25µl of the reaction mix was used to transform *E. coli* TG1 cells. As a further test, 25µl of the SDM mix was also transformed into a dut⁻ ung⁻ strain (BW313). All TG1 colonies should be positive since colonies should only arise from the new strand of DNA, the template (u)DNA being destroyed. In comparison, there ought to be twice as many colonies on the BW313 plate as transformants would occur from both the template DNA and the new SDM strand. Potential mutants were screened directly by DNA sequencing of single stranded DNA.

2.3.4 Sequencing of single stranded DNA

Sequencing of DNA was carried out using the Sequenase Version 2.0 kit (United States Biochemicals) which uses the dideoxy chain termination method. The entire L-ldh gene was sequenced using a combination of oligonuctoride primers.

Appropriate sequencing primer (1 µl of 3ngµl^{-1}) was annealed to 7µl of template DNA (approximately 1µg) in 2µl of 5 x reaction buffer (200mM Tris/HCl, pH 7.5; 100mM $MgCl_2$; 250mM NaCl) by heating to 65°C for 2 minutes then cooled slowly to below 37°C. Extension from the annealed primer was done by adding 1µl 0.1M DTT, 2µl dGTP label mix (a 1 in 4 dilution of 7.5µM dGTP, dCTP, dATP and dTTP), 0.5µl α-[^{35}S]-dCTP (400Ci/mmole) (Amersham) and 2µl diluted sequenase (a 1 in 8 dilution of sequenase at 13 EUµl^{-1} in 10mM Tris.HCl, pH 7.5; 5 mM DTT; 0.5mgml^{-1} BSA). The extension mix was left at room temperature for 2 to 5 minutes. Further extension and termination was performed by dispensing 3.5µl of extension

mix into 4 tubes preheated to 37°C containing 2.5µl of one of the for termination mixes:

ddGTP mix - 80µM dNTPs; 8µMddGTP; 50mM NaCl

ddATP mix - 80µM dNTPs; 8µMddATP; 50mM NaCl

ddCTP mix - 80µM dNTPs; 8µMddCTP; 50mM NaCl

ddTTP mix - 80µM dNTPs; 8µMddTTP; 50mM NaCl

The termination reaction was allowed to proceed at 37°C for 5 minutes and the reaction was stopped by the addition of 4µl of stop solution (95% formamide; 20mM EDTA; 0.05% bromophenol blue). Extension products were separated by electrophoresis through a 6 % denaturing polyacrylamide gel. Sequencing reactions were heat denatured at 75°C for 3 minutes, loaded onto the gel and electrophrosed in 1 X TBE at 65 Watts for ~ 90 minutes. The gel was fixed in 10% acetic acid (v/v), washed with water then dried under vacuum at 80°C for 1 to 2 hours. The gel was then autoradiographed, overnight, at room temperature.

After identifying a clone which contained the L230G mutation (GGT replaced TTG),the entire L-ldh gene was sequenced using a combination of oligonucleotide primers to check for any unwanted mutations elsewhere in the sequence.

2.3.5 Oligonucleotide primers

Sequence 5′-3 ′:	Name	Position in L-ldh coding sequence
CTGCACAATATTTCAAGC	102A	primes in ADH
TAGACAACAAGCCGAA	E1K	233-248
CTACCAAATATGCCAGGTGGG	H43M	358-378
GTCATCGACAAGTATAGC	XCla450	448-467
TCCTCCTTTGCTCCTTG	Y97F	522-538

GTGGGCCTCTATTCCT	Y143F	660-676
AATGCGTATCATAGG	b_2 730	715-729
CCAACTATTTGTTAACT	Y254F	993-1009
GTCACTGTGAATGCTCCAAGG	D282N	1075-1094
GGTCCAAAATCGATGAAG	Cla 1155	1147-1164
GGTGGTAAACAATTACAT	R376K	1360-1377
CTTGAAAGCTTTATGTCT	Hind1500	1494-1511
GATATCTACTGGTGCTTCATGT	L230G	918-929

(See chapter 5 for list of oligonucleotide primers used with L-mdh)

2.4 Cloning

Name:	Description:	Reference:
pTZ19R	phagemid cloning vector (used for L-mdh)	Rokeach *et al.*, 1988
pGR401	phagemid cloning vector (used for L-ldh)	Reid *et al.*, 1988
pRC23	expression vector (used for L-mdh)	Crowl *et al.*, 1984
pDS6	expression vector (used for L-ldh)	Black *et al.*, 1989

2.4.1 Cleavage of DNA with restriction enzymes

Plasmid DNA (0.1 to 20μg) was cut usually in a mixture of: 1μl restriction enzyme (either Promega or Amersham); 1μl of 10 x "multicore" buffer (Promega); 1μl boiled RNaseA and dH_20 to make a final volume of 10μl for 2 to 8 hours at 37°C. For the L230G mutation in L-ldh, the entire gene was excised from the phagemid pGR401 on an EcoRI-HindIII fragment and ligated into the expression vector pDS6 to form pDSL230G. The double mutant A198GL230G was constructed by cleavage

of pDSA198G (made by F. Manson, 1994) with and *Psh*AI (found at approximately K222) and *Hin*dIII. The corresponding *Psh*AI-*Hin*dIII fragment from pDSL230G was ligated to the cleaved vector. See chapter 5 for the DNA manipulation techniques carried out on L-mdh.

2.4.2 Ligation of DNA ends

50 to 100 ng of pDS6 vector (cut with the appropriate restriction enzymes) was incubated with an excess of fragment in 1 x ligation buffer (10mM Tris/HCl pH7.2; 1mM EDTA; 10mM $MgCl_2$; 10mM DTT; 1mM ATP) with 10 EU of T4ligase (BRL). The reaction was made up to a final volume of 10µl and incubated overnight at 16°C.

.2.5 SDS PAGE and Protein purification

2.5.1 One dimensional SDS-polyacrylamide gel electrophoresis of proteins

4 x Resolving buffer for SDS-PAGE	
Tris base	181.6 g
SDS	4.0 g
dH_2O	600 ml
conc HCl	10 ml
adjust to pH 8.8	make up to 1 litre
4 x Stacking buffer	
Tris Base	30.28 g
SDS	2.0 g
dH_2O	450 ml
conc HCl	15 ml
adjust to pH 6.8	make up to 500 ml
10 % Resolving gel	
Protogel	10 ml
4 x resolving buffer	7.5 ml

dH_2O	12.3 ml
10 % ammonium persulphate	190 µl
TEMED	50 µl
5% Stacking gel	
Protogel	1.6 ml
4 x stacking buffer	2.5 ml
dH_2O	5.86 ml
10 % ammonium persulphate	30µl
TEMED	10µl
5 x Tris-glycine running buffer	
Tris base	15.1 g
glycine	94 g
10 % SDS	50 ml
dH_2O	to 1 litre
2 x Loading buffer	
1M Tris. HCl pH 6.8	3.31 ml
SDS	2 g
Glycerol	9 ml
2-mercaptoethanol	5 ml
1% bromophenol blue	1ml
dH_20	to 100 ml

This technique was used to separate proteins according to their molecular weight (Laemmli, 1970). The protein samples were prepared as follows: approximately 50µg protein was resuspended in 20µl 2 x SDS-PAGE loading buffer and boiled in a water bath for 5 minutes. 5µl prestained SDS-PAGE standard molecular weight markers (1mg total protein/ml, Biorad) was heated to 40°C for 1 minute to dissolve any solids which may have precipitated after storage at -20°C. The polyacrylamide gel was prepared in two phases, a resolving gel for the separation of the protein samples and a stacking gel for the concentration of the protein samples

before separation. The resolving gel was mixed well, poured between two glass plates and overlaid with water denaturated butanol. It was then left to polymerise for 1 hour. Once the resolving gel had polymerised the water saturated butanol was rinsed off with distilled water and the stacking gel prepared. The stacking gel was poured on top of the resolving gel and a comb inserted into the top of the stacking gel. The gel was clamped into a vertical electrophoresis tank filled with 1 X running buffer, the comb was then carefully removed and the protein samples (10µl) were loaded into the wells. The gel was then run at 10V cm^{-1} (approximately 0.02 Amps) for 4 hours, or until the dye front reached the foot of the gel. The gels were stained with a 1% PAGE Blue Electran in 20% (v/v) methanol, 5% (v/v) acetic acid, to visualise the electrophoresed proteins. To remove excess stain, the gel was destained (25 % methanol, 10 % acetic acid) for several hours and the gel dried to filter paper under vacuum. For the L230G mutation, a single band ~57.5 kDa was observed by comparing the position of the band relative to the bands of the standard molecular weight markers (see diagram 2.1). For the SDS-PAGE for L-mdh and L-mdh fdh, see chapters 4 and 5.

Western Transfer

10 x Transfer buffer	
1 M Tris. HCl pH 8.3	250 ml
Glycine	112.6 g
dH_2O	to 1 litre
Tris-buffered saline (TBS)	
1 M Tris. HCl pH 7.5	10 ml
4 M NaCl	37.5 ml
dH_2O	to 1 litre

An SDS-PAGE gel was run and then soaked in 1 X transfer buffer for two minutes. It was then assembled into a "sandwich" with the gel adjacent to a piece of nylon membrane (Hybond-N) placed between 2 by 2 layers of 3mm filter paper and foam sponge (all soaked in 1 X transfer buffer). The proteins were then transferred onto the membrane, by immersing the sandwich in a tank containing 1 X transfer buffer and passing a current of 1 Amp through it for 1 hour. The membrane was placed nearest the positive electrode. The membrane was then placed in 100 ml of 20 % skimmed milk powder made up in TBS and left shaking gently overnight. The blocked membrane was placed the following day in 20 ml of 5 % milk solution made up in TBS and 30 µl of the L-ldh polyclonal antibody from rabbit was added and the membrane incubated with shaking at room temperature for 3 hours. The milk solution was poured off and the membrane was washed by shaking in TBS for 4 x 5 minutes. The membrane was then placed in fresh 5 % milk solution and 10µl Horse Radish Peroxidase-conjugated anti-rabbit antibody (Scottish Antibody Production Unit). After incubation with the secondary antibody for 2 hours, the membrane was again washed thoroughly with TBS and developed in 10 ml of developing solution.

Developing solution	
Dianisidine (5mgml^{-1}, Sigma)	0.5 ml
Imidazole (0.1M, pH7.4, Sigma)	1 ml
H_2O_2 (30 %)	0.1 ml
H_2O	8.5 ml

Addition of peroxide and dianisidine resulted in the catalytic production of an orange dye identifying the correct protein band. The reaction was stopped by rinsing the membrane in distilled water.

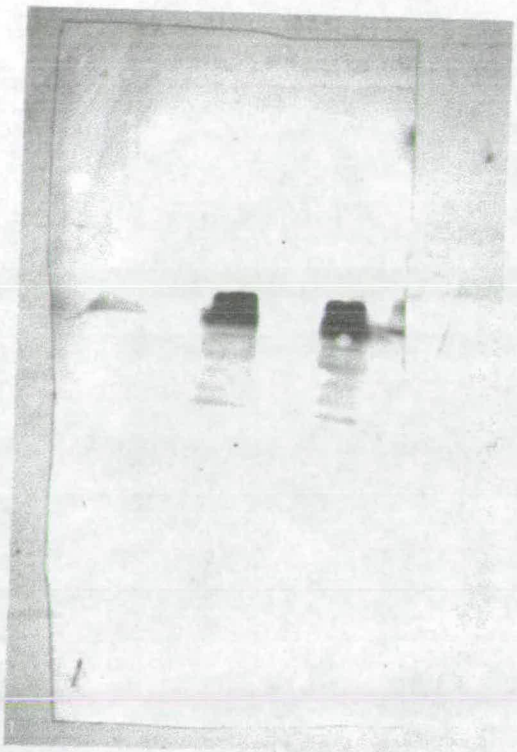

Figure 2.1 Western blot of WT L-ldh (left) and L230G mutant (right) Both from 1 ml of overnight culture (approx 50μg enyme). See section 2.5.1 for details

57kDa

2.5.2 Production of L-ldh protein (for L-mdh, see chapter 4)

Liquid cultures of bacteria were grown in terrific broth by innoculating 500ml of media with a single colony of the plasmid bearing strain using a sterile innoculating loop. The growth media contained 150 $\mu g ml^{-1}$ ampicillin as a selectable marker. The inoculated flask was left to grow at 37°C, with shaking, to stationary phase. The stationary phase cells were harvested in a Sorvall RC5-B centrifuge with a GS3 head run at 5000***g*** for 20 minutes. A typical batch, harvested from 5 litres of culture, yielded 20 g of cells (wet weight).

2.5.3 Cell lysis

0.1M Protein purification buffer	
5mM L-lactate (Li salt, Sigma)	0.96 g
1 mM EDTA	0.74 g

0.2MKH_2PO_4 solution	400 ml
0.2 M K_2HPO_4 solution	600 ml
adjusted to pH 7.0	
dH_2O	to 2 litres

The frozen pellet of cells was snap-frozen in liquid nitrogen to facilitate cell lysis and then resuspended in about 50ml of purification buffer per 5g cells. The EDTA chelated calcium ions released upon cell lysis and the lactate maintained the L-ldh in its more stable reduced form. Lysozyme (grade III, chicken egg white, Sigma) was added to a concentration of approximately 0.2 $mgml^{-1}$ and the mixture stirred for one hour at 4°C (the protein solution was maintained at 4°C throughout the entire purification). After this time, the cell debris and any unlysed cells were removed from suspension by centrifugation at 39000***g*** for 10 minutes. A red/ pink colouration of the supernantant indicated the presence of L-ldh. If necessary the process was repeated to release more enzyme, and the resultant supernatants pooled.

2.5.4Ammonium sulphate fractionation

After lysis the supernatant was fractionated by addition of ammonium sulphate. Initially the solution was adjusted to 40 % ammonium sulphate saturation (243 gl^{-1}) and the precipitated proteins removed by centrifugation at 39000***g*** for 10 minutes. This supernatant was then further adjusted to take the total concentration to 70 % saturation (205 gl^{-1}), which was sufficient to precipitate L-ldh out of solution, and the protein removed by repeating the centrifugation.

2.5.5 Dialysis

The protein pellets were dissolved in a minimum volume of 0.1M phosphate buffer and dialysed overnight against a 10-fold excess of half-strength buffer, under a N_2 atmosphere. The protein was dialysed in order to remove the ammonium sulphate and any other low molecular weight contaminants. Seamless dialysis tubing (Sigma)

with a molecular weight exclusion limit of 12 kDa was used. Following dialysis the enzyme solution was centrifuged at 39000*g* for 10 minutes to remove any aggregated protein.

2.5.6.Column Chromatography

A. DEAE Ion exchange column

The column material consists of diethyl-aminoethyl groups covalently crosslinked to a cellulose matrix. When equilibrated at pH 7, it forms a positively charged binding surface for negatively charged proteins. The material used was Whatman DE-52 which was prepared by preswelling in purification buffer and adjusted to pH7.0 by the addition of HCl. After pouring, the (15cm x 2.5 cm) column was further equilibrated by elution with two column volumes of buffer. The protein solution was loaded onto the column, however L-ldh does not bind to the column, but passes straight through the column. The eluted protein fractions were collected immediately and loaded onto the hydroxylapatite column. At this stage the eluted fractions of L-ldh had a UV/Vis ratio (A_{269}/A_{423nm}) of between 1.5 and 2.0, compared to a ratio of >10 after dialysis. This ratio is a measure of purity; the UV wavelength quantitates total protein and the Vis wavelentgh quantitates L-ldh (Pajot & Groudinsky, 1970). A pure solution of L-ldh has a ratio of 0.5. After use, the column material was regenerated by washing with 5 column volumes of 1M salt and 2 column volumes of 0.1M phosphate buffer.

B. Hydroxylapatite column

Hydroxylapatite (Biorad) is the crystalline form of $Ca_{10}(PO_4)_6OH_2$. Binding is believed to occur via the phosphate groups and bound proteins are eluted by increasing the ionic strength of the eluting buffer. As the column material consists of a majority of negatively charged groups, neutral and positively charged molecules bind well. The eluted protein fractions were loaded onto a 10 x 2.5 cm hydroxylapatite column which had previously been equilibrated with two column volumes of purification buffer. L-Ldh bound at the top of the column and was washed with

several column volumes of purification buffer until there were no more contaminating proteins eluted at this ionic strength (this was determined by monitoring the decrease in A_{269nm} of successive protein fractions). The enzyme was eluted using a 0 to 10% ammonium sulphate gradient, the fractions being collected manually. Each fraction was assayed for the degree of purity as described previously and fractions with a purity ratio of around 0.5 were pooled, adjusted to 70 % ammonium sulphate saturation (472 gl^{-1}) and centrifuged at 39000*g* for 10 minutes. The hydroxylapatite column could also be regenerated after washing with 1M NaCl.

C. Sephadex G25

10mM Tris.HCl buffer, pH 7.5 (I 0.10)	
NaCl	5.265 g
1M HCl	10 ml
dH_2O	to 1 litre
adjusted to pH 7.5 with Tris base	

After centrifugation, the resulting pellets were redissolved in a minimum volume of Tris.HCl buffer and passed down a Sephadex G25 column (15 x 1.5 cm, Sigma). Drops of the L-lactate free, oxidised enzyme were immediately snap frozen in liquid nitrogen and stored at -194°C . Typical yields of purified WT and mutant forms of L-ldh were about 15mg of enzyme per litre of culture media. The column material of this final column consisted of cross-linked dextran and epichlorohydrin and is used to separate molecules according to their size. Very large molecules, such as proteins move quickly through the column material because such large molecules are excluded from the polymeric grains, whereas $(NH_4)_2SO_4$, free FMN, and lactate are all contained within a slow moving band.

2.6 Molecular mass determination of the flavin domain of L-mdh

Gel filtration using Sephacryl S-300 beads (Sigma) was used to determine the approximate molecular weight of the flavin domain. A plot of V_e/V_o versus log

(molecular weight) where V_e is the elution volume (volume at which the most active fraction is eluted) and V_o is the void volume, is linear. V_o can be calculated by passing Blue Dextran (Sigma, average M_r 2 000 000) through the column. The column is then calibrated using molecules of known M_r to plot a graph of V_e/V_o vs. log M_r. The column material was resuspended in Tris. HCl buffer and a 120 x 2.5 cm column poured. The following markers were used in the calibration: L-ldh (approx. M_r 230 000); alcohol dehydrogenase (M_r 150 000); bovine serum albumin (M_r 66 000 and cytochrome *c* (M_r 12 500). (See section 5.6)

2.7 Preparation of DL-[2-^{2}H]mandelate (Achim Neu)

Steady-state and pre-steady-state experiments were carried out using DL-[2-^{1}H] mandelate and DL-[2-^{2}H] mandelate as substrates. Each experiment was carried out under the same conditions described below for enantiomerically pure L-mandelate as substrate. The values for the KIEs were calculated by :

$$\frac{k_{cat}\ \text{DL-[2-}^1\text{H] mandelate}}{k_{cat}\ \text{DL-[2-}^2\text{H] mandelate}}$$

that is, a large decrease in rate for the deuterated substrate suggests that the rate is dependent on the breaking of the C-D bond.

Deuterated mandelate was prepared by A. Neu by boiling DL-mandelic acid with deuterated sodium hydroxide. Because of the enormous amount of heat generated in this reaction, the entire reaction was carried out under a nitrogen atmosphere. The purity of the DL-[2-^{2}H]mandelic acid crystals was determined by ^{1}H and ^{13}C NMR spectroscopy and mass spectrometry.

2.8 Steady-state kinetic analysis

The initial rate, V_0 of an enzyme catalysed reaction tends towards a maximal, limiting value, V_{max}, with increasing substrate concentration. This kinetic behavior can be described by the basic equation governing enzyme kinetics, the Michaelis-Menten equation:

$$V_0 = (V_{max}[S]/ K_m + [S]) \qquad V_{max} = k_{cat}[E_0]$$

where: V_0 = initial velocity

[S] = substrate concentration

$[E_0]$ = total enzyme concentration

k_{cat} = rate constant at substrate saturation

K_m = substrate dissociation constant

The kinetic parameters which can be determined experimentally are; k_{cat}, the catalytic turnover number, which represents the maximum number of substrate molecules converted to product per active site per unit time (s^{-1}), and K_m, the Michaelis constant which in some cases is effectively K_d, the dissociation constant for the enzyme substrate complex (M), so that a low K_m value indicates tight substrate-enzyme binding and a high K_m indicates weak binding.

Both L-ldh and L-mdh catalyse the two electron oxidation of an L-hydroxy acid and can transfer electrons to a wide variety of external electron acceptors. The turnover of the enzyme under steady-state conditions can be monitored by observing the reduction of an external electron acceptor under saturating conditions. Both the physiological electron acceptor of L-ldh and L-mdh, cytochrome *c*, and the artificial electron acceptor, potassium ferricyanide, were used in steady-state experiments.

Experiments were performed using a Shimadzu 2101PC spectrophotometer and all steady-state data was analysed by non-linear least squares regression using the Michaelis-Menten equation. Curve fitting was conducted using the PC based software, Origin (Microcal). All kinetic experiments were carried out at 25°C in 10mM Tris.HCl pH 7.5 (*I* 0.10) and the assays were performed in glass or quatrz cuvettes with either 1 or 0.2 cm path lengths. The kinetic parameters, k_{cat} and K_m for substrate were determined by carrying out assays at varying substrate concentration under saturating conditions of electron acceptor and vice versa to determine the K_m for the electron acceptor. Catalytic amounts (10 -25µl) of enzyme were added via a syringe to a cuvette containing electron acceptor and substrate (total volume = 3ml for 1 cm cuvette, 1 ml for 0.2 cm cuvette). The concentration of the enzyme added was determined by the absorbance of the Soret peak at 423 nm (for reduced

Lmdh/Lldh, ε_{red} = 183000M^{-1} cm^{-1}). To determine the concentration of L-mdh/L-ldh flavodehydrogenase domains, the absorbance peak at 450 nm was measured (ε_{ox} = 11100 M^{-1} cm^{-1}). All substrate solutions were prepared by dissolving an appropriate amount of the acid in Tris.HCl buffer and titrating to pH 7.5 by addition of NaOH. The range of substrate concentrations used in assays was usually between 0-20 mM. Chirally pure L-2-hydroxy (long) chain acids were obtained from Oxford Asymmetry Ltd. L-Lactic acid (Li salt) and L-mandelic acid were obtained from Sigma.

2.8.1 Ferricyanide as the electron acceptor

For intact L-mdh, wild type and mutant forms of L-ldh, assays were performed at saturating concentrations (1mM) of ferricyanide. However, due to the high K_m values of the flavin domains of L-mdh and L-ldh for the electron acceptor, assays were performed at 3.33 and 6mM ferricyanide concentration respectively. This necessitated all the assays for the flavin domain enzymes being performed in 0.2cm path-length cuvettes. Activities were calculated from the absorbance decrease at a wavelength of 420nm, using a difference in extinction coefficient of $\varepsilon_{ox\text{-}red}$ =1010.

2.8.2 Cytochrome c as the acceptor

Horse heart cytochrome *c* (typeVI-Sigma) was used in the assays and was always freshly made up in Tris.HCl buffer before use. Concentrations were determined by measuring the absorbance at 550nm of dithionite reduced cytochrome *c*, using an extinction coefficient ε_{red} = 30900 M^{-1} cm^{-1}. Assays were performed in both 0.2 and 1 cm path length cuvettes. The cytochrome *c* assay concentration used was 35μM. Acitivites were calculated fron the absorbance increase at a wavelentgh of 550nm, using the extinction coefficient $\varepsilon_{ox\text{-}red}$ = 22640.

2.9 Stopped flow kinetic analysis (*L-mdh only*)

The turnover number, k_{cat} for L-mdh with cytochrome c is around 100s^{-1}, which suggests that the slowest step in the enzyme's catalytic cycle is likely to have a

half life of only a few milliseconds. Stopped-flow rapid mixing techniques can be used to monitor the build up and decay of these reaction intermediates over such a time scale. The principle of this technique is that equal volumes of enzyme and substrate are rapidly injected into an observation chamber and the course of the reaction monitored by recording the absorbance of the reacting solution over time. A major limitation of this technique is the time taken to mix enzyme and substrate, as well as the time taken by the spectrophotometer to record the absorbance. These contribute to the so-called 'dead-time' of the instrument and is usually around 1 millisecond.

2.9.1 Pre steady-state oxidation of L-mandelate

All experiments were conducted on an Applied Photophysics SF.17 Micro Volume stopped-flow spectrofluorimeter at 25±0.1°C. Data were collected, displayed in the absorbance mode and were processed using the SF.17 MV software package and Origin (Microcal). Fully oxidised enzyme (prepared by passing through a Sephacryl S-300 column equilibrated in 10mM Tris.HCl buffer pH 7.5, I 0.10) was used when measuring flavin and haem reduction rates. Reduction of the FMN prosthetic group was monitored at 438.3 nm, which is a haem isobestic and haem reduction was monitored at 557 nm. In the flavodehydrogenase domain of L-mdh FMN reduction was measured at 450 nm.

2.9.2 Pre steady-state reduction of cytochrome *c*

The pre-steady state reduction of horse-heart cytochrome *c* by fully pre-reduced L-mdh was also monitored with the stopped-flow apparatus. The reaction was followed at 416.5 nm, which is an isobestic for L-mdh. L-Mdh was fully reduced by the addition of 10 mM L-mandelate. Experiments were performed under aerobic conditions, as auto-oxidation of L-mdh did not occur to any significant extent over the time scale of the experiment (2 to 3 hours).

To ensume that reduction of cytochrome *c* occurred under pseudo-first order conditions, L-mdh was always present in excess. Reduction was carried out over a

wide range of L-mdh concentrations (1.5 - 15 μM) and the cytochrome *c* concentration was 0.75 μM.

2.10 Redox potentiometry

The method described by Dutton (1978) coupled with spectrophotometry was used to measure the haem and flavin mid-point potentials of L-mdh. Measurements were carried out with a calomel electrode, under anaerobic conditions.

2.10.1 Preparation of redox standard solutions

1. Fe (III)/EDTA solution: EDTA was dissolved in 10ml of 0.1M acetate buffer to 10 mM concentration and the pH adjusted to 5.0. Iron (III) sulphate was dissolved in this solution to 0.5 mM concentration.

2. Fe(II) solution: Iron (II) ammonium sulphate was dissolved in 10 ml of degassed dH_2O to 100 mM concentration

3. Dithionite solution: 30 mg of sodium dithionite was dissolved in 5 ml of degassed 0.1 M phosphate buffer, pH 7.0.

4. Ferricyanide solution: 30 mg of potassium ferricyanide was dissolved in 5ml of degassed 0.1 M phosphate buffer

5. Mandelate solution: 300 mg of mandelic acid dissolved in 100 ml of 0.1 M phosphate buffer and the pH increased to 7.0 by the addition of dil NaOH. The solution was then degassed.

6. Phenyl glyoxalate solution : 225 mg of phenylglyoxylic acid was dissolved in 100 ml of 0.1 M phosphate buffer and the pH increased to 7.0 by the addition of dil NaOH. The solution was then degassed

2.10.2 Redox Mediators

The redox centres of L-mdh are shielded from solvent by the surrounding protein framework and this has the effect of hindering effective contact between the redox centres of the enzyme and the electrode surface. To counteract this effect, redox mediators, which act as fluxes between the redox couple and the measuring

electrode were added to the enzyme solution before measurement began. The mediators used had midpoint potentials that covered the range of the redox couples of the L-mdh FMN and haem groups. The mediators used also did not react chemically with either of the redox centres.

The mediators used for the redox potential determination of the haem group are listed below. 10 mM stock solutions were prepared in dH_20 (with 20% ethanol for DAD and HNQ) and were foil wrapped to prevent light induced decomposition.

Mediator:	E_m (MV)
2-hydroxy-1,4-napthaquinone (HNQ)	-140
phenanzine methosulphate (PMS)	+60
phenanzine ethosulphate (PES)	+80
2,3,5,6-tetramethyl-p-phenylenediamine (DAD)	+220
Benzyl viologen	-300

In intact L-mdh, the flavin absorbance is swamped by the much more intense haem absorbances so that it is impossible to monitor the spectroscopic properties of the flavin and therefore the redox midpoint potential of the FMN group without individually expressing the flavin domain. This has been carried out successfully, and the flavin domain of L-mdh has been expressed and purified (see chapter 5).

The midpoint of the flavin domain has also been determined using a similar method to the one used for the haem group of the intact enzyme. Since the midoint potential of the FMN was expected to be much lower than the haem, a slightly different set of mediators was used.

Mediator	E_m (mV)
2-hydroxy-1,4-napthoquinone	-140
Anthraquinone	-220

Benzyl Viologen -300

2.10.3 Calibrating the electrode

The calibration solution used was 10 ml of 0.5 mM Fe (III), 10mM EDTA and 0.1M acetate buffer at pH 5.0. This solution was thoroughly degassed with water saturated nitrogen and kept under anaerobic conditions during calibration. To calibrate, 10µl of Fe (II) solution was injected and the potential was recorded. A firther 40 µl was injected, bringing the solution to a concentration of 0.5mM Fe (II)/0.5M Fe (III) that is, log[ox]/[red] = 0 (see Nernst eqn below), and the potential was recorded.

Figure 2.1 Calibrating the calomel electrode

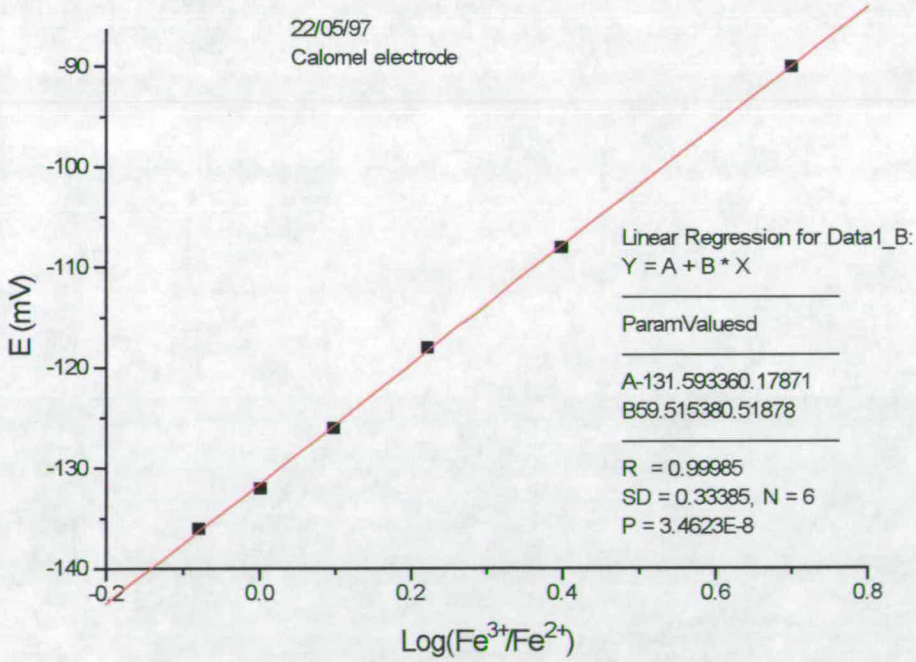

2.10.4 Measurement of the haem/flavin potential

L-mdh (intact or fdh), was passed through a G75 gel filtration column (5 cm x 2.5 cm) and eluted with 0.1M phosphate buffer, pH7.5, under anaerobic conditions. Approximately 30 mg of pure enzyme was used in each experiment in order to give a 50μM enzyme solution in a 10 ml final volume. 10 μl of each meditator was added to the solution (final mediator concentration = 10μM), and the solution stirred by means of a magnetic 'flea'. The enzyme was reduced either by titrating with the anaerobic dithionite or mandelate solutions. Visible absorption spectra were sequentially recorded over the range 400-750 nm, at a scan speed of 2 nms^{-1} and the potentials were noted each time for the haem peak at 557nm (intact enzyme) or for the flavin peak at 450 nm (flavin domain). L-Mdh was reoxidised by titrating with the ferricyanide solution and the potentials noted as before. The semiquinone form of the flavin group was detected by first fully reducing the enzyme with L-mandelate, then adding an excess of phenylglyoxalate (see chapter 5 for details). The semiquinone spectrum of L-mdh has an absorbance peak at 490 nm (see figure 5.10) resulting in a pink coloured solution. This red anionic semiquinone is also found in all members of the 2-hydroxy acid dehydrogenase/oxidase family.

All the potentials were corrected so that they were relative to the standard hydrogen electrode (SHE), $E_h = E + 244$ mV. The data collected was presented as a modified Nernst plot in which the sum of the absorbances on either side of the maximum absorbance peak, for example, 570-540 nm for the haem absorbance peak at 557 nm, was plotted against the corrected electrode potentials. The resultant curve was sigmoidal in shape and the slope of the curve, if the system was in equilibrium should have been 59 ± 10 for a one electron transfer process and 29 ± 5 for a two electron process. The midpoint value of the curve gave the value of the midpoint potential of the group.

Nernst equation: $E = E_h + RT/nF \ln[ox]/[red]$ for the redox couple: ox +ne- = red

Where E is the measured potential (V), E_h is the mid-point potential (V), R is the molar gas constant ($Jmol^{-1}$ K^{-1}), T is the absolute temperature (K), F is the Faraday constant ($Cmol^{-1}$), n is the number of electrons, [ox] is the concentration of the oxidised species, [red] is the concentration of the reduced species.

Chapter 3: Enzyme redesign

The substrate specificity of *S. cerevisiae* L-lactate dehydrogenase

3.1 Introduction

Developments over the last 20 years in recombinant DNA techniques have had a profound effect on the study of enzymes. For example, site-directed mutagenesis has been used extensively to investigate the role of specific amino acid residues, and has been used more recently to modify the substrate/coenzyme specificities of various enzymes. In the following section some of the work previously carried out on this form of enzyme redesign is described: the coenzyme specificity of glutathione reductase; the substrate specificity work on the NAD^+ dependent L-lactate dehydrogenase from *Bacillus stearothermophilius*, and the substrate side chain specificity of the *S. cerevisiae* L-lactate dehydrogenase (L-ldh) . The latter should serve as an introduction to the enzyme redesign work of this project, in which the substrate specificity of L-ldh is further investigated by attempting to modify the enzyme so that its preferred substrate is L-mandelate .

3.2. Coenzyme specificity - engineering the coenzyme binding site of a NADPH dependent enzyme in favour of NADH

The flavoprotein glutathione reductase reduces glutathione at the expense of NADPH and is involved in combating oxidative stress in the cell (Holmgren, 1985). The crystal structure of human glutathione reductase has been solved to high resolution (Pai *et al.*, 1988), and provides important information about the geometry of coenzyme binding. It appears that the nicotinamide ring of NADPH stacks against the middle ring of the enzyme bound FAD prosthetic group and the pyrophosphate moiety is bound at the C-terminal end of a β-sheet in the coenzyme binding domain.

The enzyme can only loosely bind NADH, the most likely explanation for this is that the NADH lacks the coulombic interaction with the positive charges provided by two arginine residues (Arg218 and Arg224) in the 2-phosphate binding site. The corresponding residues in *E. coli* glutathione reductase were mutated to methionine and leucine respectively (Scrutton *et al.*, 1990). This resulted in a decrease in the specficity for NADPH, but there was no corresponding increase in affinity for NADH.

Futher enhancement in NAD+ specificity was obtained by the replacement of Val197, Lys299 and His200 in *E. coli* glutathione reductase by Glu, Phe and Asp respectively. These changes were designed to remove any residual positive charge in the 2-phosphate binding pocket and also to introduce a negatively charged side-chain (V197E) which would hydrogen bond to the hydroxyl group of NADH. Furthermore, in most NADH linked dehydrogenases there is a sequence motif Gly-X-Gly-X-X-Gly-X-X-X-Gly that constitutes a tight turn at the end of the first strand of a β-sheet and marks the beginning of the succeeding α-helix in the NADH binding domain (Wierenga *et al.*, 1985). In glutathione reductase the third and fourth glycine residues are substituted by larger alanine residues. Replacing Ala179 with glycine decreased the K_m for NADH significantly, a 20 fold decrease from 2 mM for wild type to 50μM for A179G. The enzyme which contained all of the above mutations had an increased selectivity for NADH over NADPH by a factor of 18000.

3.3 The NADH-dependent lactate dehydrogenase of *Bacillus stearothermophilus*

The glycolytic lactate dehydrogenase from *B. stearothermophilus* catalyses the interconversion of an oxo-acid (pyruvate) and a 2-hydroxyacid (lactate) using a NADH/NAD pair as a redox cofactor. The reaction, which occurs in the opposite direction to the one catalysed by *S. cerevisiae* L-ldh is achieved by the donation of a hydride ion from NADH to the α-carbon of pyruvate and a proton from the protein to the carbonyl oxygen. (See figure 3.1)

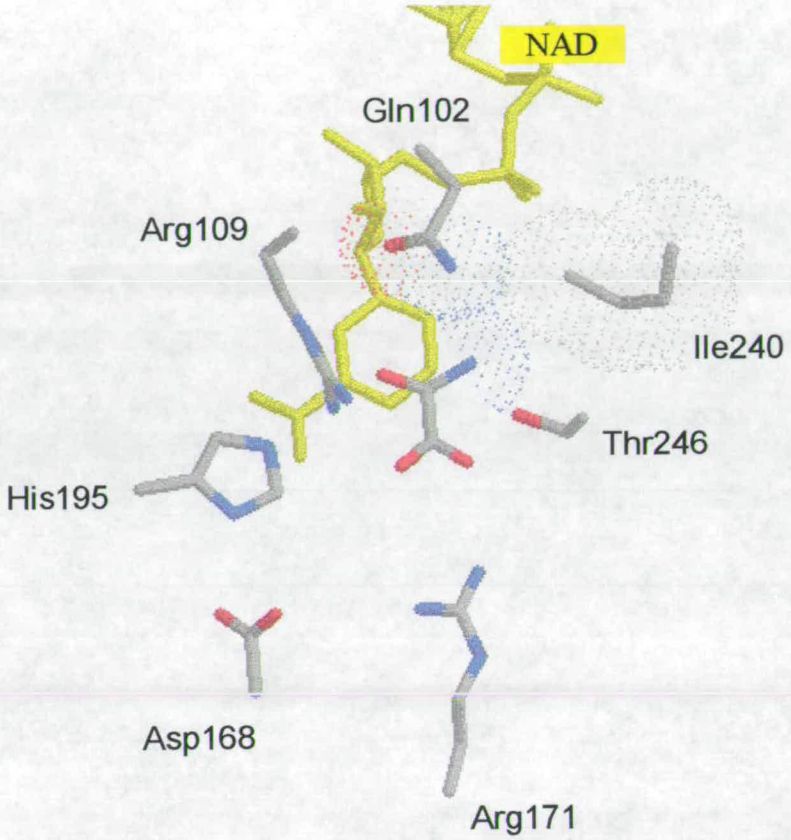

Figure 3.1 The active site of the NADH dependent L-lactate dehydrogenase from *Bacillus stearothermophilus*. Adapted from the X-ray crystal structure (2.5 Å resolution) of Wigley *et al.*, 1992. The substrate analogue, oxamate, is shown in a parallel plane above the nicotinamide ring of NAD cofactor.

The catalytic efficiency of the enzyme is reduced 1000 fold if oxaloacetate is used as a substrate instead of pyruvate (Clarke et al., 1987). This molecule differs from pyruvate only in its side group - it contains a carboxylate group instead of a methyl side chain. By examining the three dimensional structure of the enzyme the residues thought to interact with the substrate side chain were identified (Wilks *et al.*,

1988, 1990, 1991, 1992). Removing bulk from the active site in order to accommodate the larger side chain of oxaloacetate had a dramatic effect in shifting the efficiency of the enzyme towards oxaloacetate. Replacing the active site residue threonine 246 with glycine achieved a shift in specificity of more than a factor of 3000 (Clarke *et al.*, 1989). However the provision of a direct protein counter ion for the substrate side chain proved to be the most effective way of switching the preference of the enzyme. This was achieved by replacing Gln102 with arginine (Wilks *et al.*, 1988) to form an electrostatic interaction and this resulted in an enzyme which was 8400 times more efficient with oxaloacetate than with pyruvate . (See figure 3.2).

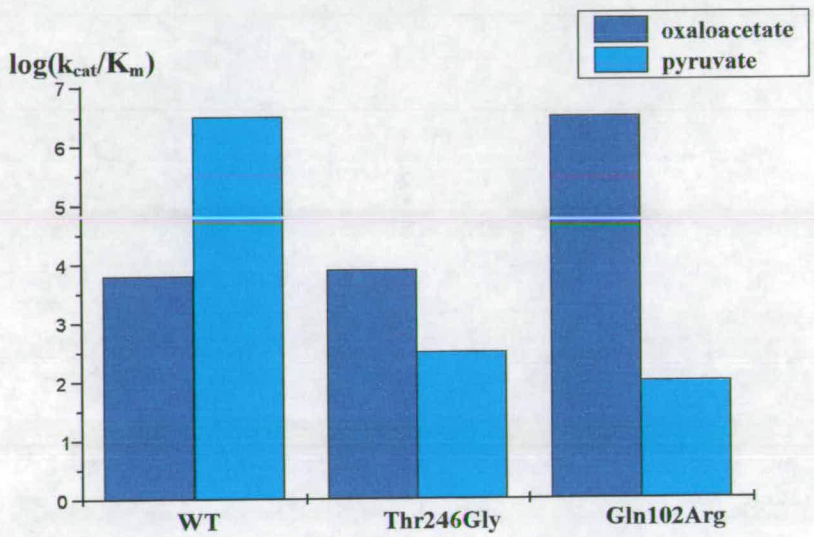

Figure 3.2 The swing in substrate specificity of Q102R (NADH dependent L-lactate dehydrogenase of *B. stearothermophilus*)

Comparison of the crystal structures of free and substrate bound enzyme revealed that there were rearrangements in the protein structure which were induced by binding of the substrate. The most striking difference between the two structures was the encasement of the coenzyme with the substrate molecule by a 13 residue loop of polypeptide which closes over the catalytic site. Therefore the mechanism by which lactate dehydrogenase distinguished different substrates was the ability of the enzyme

to form a fixed size vacuole when the loop closes down onto the protein. This loop closure is only possible over suitably small substrates. This was tested by the introduction of a set of mutations in the loop region (Q102M, K103V, P105S) which increased the hydrophobicity and flexibility of the loop and enabled the enzyme to accommodate bulkier 2-hydroxy acids (Wilks *et al.*, 1990). These mutations, coupled with the A235GA236G mutants on a portion of α-helix which also interacts with substrate gave rise to an broad-specificity enzyme with an increased ability to dehydrogenate larger 2-hydroxyacids. This enzyme provided a useful system for the production of chiral 2-hydroxyacids.

In a separate approach site directed mutagenesis was used to insert restriction sites into the coding sequence for the active site loop. This enabled DNA coding for new loops to be inserted into the gene in order to test how the size of the loop affected the substrate specificity of the enzyme (Wilks *et al.*, 1992). The loop was extended in the 99-109 region by the insertion of 4 residues. It was predicted that this new loop would bulge out to create a more open vacuole which would favour larger substrate side chains. These mutations were made in an enzyme which already had the mutations A235G and A236G in the α-2G helix. This change of two alanines to two glycines had been previously shown to increase space in the vacuole adjacent to the substrate side chain. The k_{cat}/K_m for pyruvate fell from 4.2×10^{3} $mM^{-1}s^{-1}$ for wild type to just 4.7×10^{-3} $mM^{-1}s^{-1}$ in the 'big loop' enzyme. The k_{cat}/K_m for phenylpyruvate was almost unchanged compared to wild type (18 to 8 $mM^{-1}s^{-1}$). In other words, there was a 1700 swing in catalytic efficiency observed for the mutant enzyme towards phenylpyruvate compared to wild type. The ability of this enzyme to turnover phenylpyruvate has clinical applications as a biosensor for determining phenylpyruvate levels in physiological fluids. Inborn errors in the metabolism of amino acids, such as phenylketonuria result in a build up of phenylalanine in the blood and phenylpyruvate is one of several metabolites that are excreted at high concentrations in urine.

3.4. Flavocytochrome b_2 substrate specificity

The substrate specificity of flavocytochrome b_2 has been previously investigated by Daff *et al.* (1994). Flavocytochrome b_2 acts physiologically as a lactate dehydrogenase though it is also able to utilise a wide variety of 2-hydroxy acids. Examination of the crystal structure of the enzyme (see figure 3.6) reveals that Arg376 and Tyr143 are capable of interacting with the carboxylate end of the substrate molecule while His373 and Tyr254 are thought to deprotonate and stabilise respectively the hydroxyl end of L-lactate. These residues are all conserved between members of the 2-hydroxy acid oxidase/dehydrogenase family of enzymes and so are thought to play crucial roles in controlling the group specific nature of the enzyme and also its stereospecificity. However, the methyl side-chain appears to be in a relatively uncrowded region of the active site, and lies in a hydrophobic pocket formed by the side chains of Ala198, Leu230, Leu286 and Ile326, several of which are in van der Waals contact range of the methyl group. None of these residues are well conserved between members of the family and it seems likely that these are the residues reponsible for making flavocytochrome b_2 principally a lactate dehydrogenase.

In order to test the role of these amino acids several point mutations were constructed in order to replace these residues with smaller variants, thereby increasing space in the hydrophobic pocket. It was proposed that, in a similar manner to the 'phenyllactate dehydrogenase' described by Wilks *et al.*, the substrate preference of the mutant enzyme would be shifted towards larger 2-hydroxy acids. The wild-type and mutant enzymes were all characterised using a series of straight chained 2-hydroxy acids, from the smallest 2-hydroxy acid, glycolate, to the 8-carbon 2-hydroxyoctanoate. Three singly substituted variants (A198G, L230A and I326A) were successfully overexpressed in *E. coli*, and each retained some activity with L-lactate. The double mutant A198GL230A was also tested.

For the wild type and mutant enzymes, their steady state turnover rate was measured with each hydroxyacid and the artificial electron acceptor used was potassium ferricyanide (1mM). This was used in preference to the physiological electron acceptor, cytochrome *c*, because of the higher relative activities and lower K_m for ferricyanide compared to cytochrome *c*. Values for k_{cat}/ K_m were used as a measure of the catalytic efficiency of the enzyme and so called 'substrate specificity profiles' were constructed, with substrate chain-length plotted against catalytic efficiency.

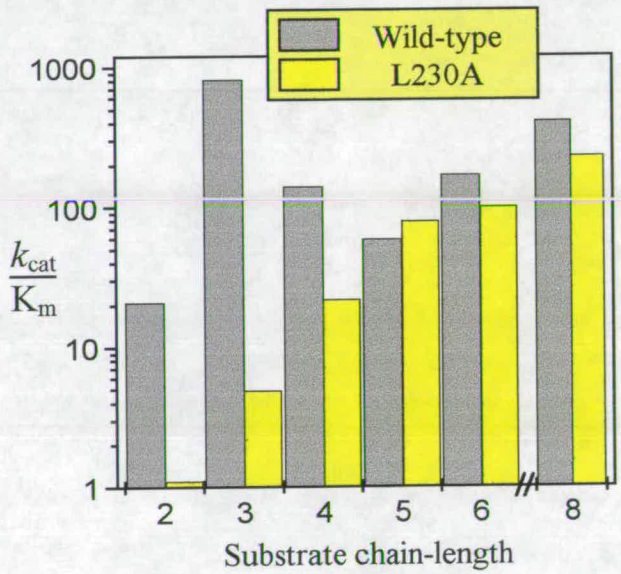

Figure 3.3 The substrate specificity profile of WT L-ldh and L230A The actual k_{cat} and K_m values for each substrate can be found in (Daff *et al.*, 1994). The k_{cat}/K_m values are represented as $mM^{-1}s^{-1}$ on a log scale. Substrate chain lengths correspond to the number of carbons in the range 2-hydroxy acids tested with 2 equals glycolate and 8 equals hydroxyoctanoate.

For the wild-type enzyme, (see figure 3.3) it was obvious that the enzyme was fairly non-specific with the 2-hydroxy acids and would still turnover extremely large and small substrates at measurable rates. However, the enzyme would preferentially

turnover L-lactate over all the others. There was also a decrease in K_m values with the long chain 2-hydroxy acids as substrates compared to the smaller 2-hydroxy acids. This is probably due to larger side-chains binding more effectively in the largely hydrophobic protein interior.

Leu230 is thought to interact with the methyl side-chain of lactate so mutation of this to a smaller alanine residue should reduce this contact. This residue is not well conserved between related 2-hydroxy acid dehydrogenases/oxidases and there appears to be a relationship between the size of substrate side-chain used by a particular enzyme and the size of the amino-acid side-chain at that position. In enzymes that have L-lactate as a primary substrate (*S. cerevisiae* L-ldh, *H. anomala* L-ldh, *E. coli* L-ldh and L-lactate monooxygenase from *Mycobacterium smegmatis* leucine is conserved, while in spinach glycolate oxidase (glycolate has a hydrogen at the α-carbon instead of a methyl group) the position of Leu230 is occupied by a larger tryptophan residue. In L-mandelate dehydrogenase from *Pseudomonas putida,* Leu230 is replaced by smaller alanine residue and in the same enzyme the residue corresponding to Ala198 is also replaced by glycine. Therefore it seems likely that this residue plays a role in controlling substrate specificity. For the mutant L230A, catalytic efficiency increased progressively with substrate chain length (see figure 3.3). However, this mutation has all but destroyed the enzyme's ability to oxidise lactate with k_{cat}/K_m falling from 810 $mM^{-1}s^{-1}$ (WT) to 4.90 $mM^{-1}s^{-1}$ with L230A. On the other hand, the enzyme's ability to turn over the longest 2-hydroxyacid tested, 2-hydroxyoctanoate was now 40 fold better than with lactate. In comparison wild type L-ldh was twice as efficient with lactate as 2-hydroxyoctanoate. In other words there has been an **80**-fold swing in substrate specificity.

Ala198 was also thought to be within contact range of the substrate methyl group. Alteration of this alanine to glycine removed a single methyl group from the active site of the enzyme. The A198G had a less specific effect than L230A with the enzyme efficiencies for all substrates decreasing by roughly the same amount resulting in a substrate specificity profile that has essentially the same shape as wild type, *i.e*, a

maximum at L-lactate. The double mutant A198GL230A was also constructed and this substrate specifity profile was similar to the one generated for L230A, but because of the contribution of the A198G mutant, the efficiencies with each mutant were much lower with each substrate (see diagram 3.4).

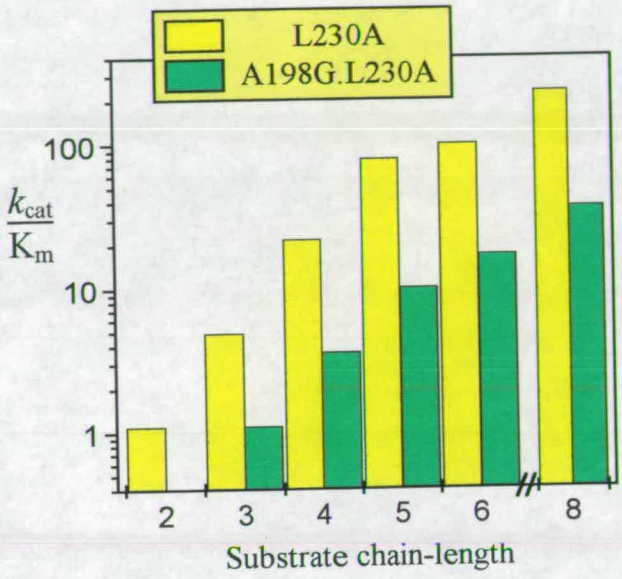

Figure 3.4 Substrate specificity profiles of L230A and A198GL230A mutant enzymes (Daff *et al.*, 1994)

Another active-site residue, Ile 326, is slightly further away from the substrate than either Ala198 or Leu230, but within contact range of a larger 2-hydroxy acid substituent. The mutation of isoleucine to alanine also removed bulk from the active site and the substrate specificty profile for the I326A mutant was dramatically different to that for the wild-type (see figure 3.5). The largest peak at 2-hydroxyoctanoate was due to a large decrease in the K_m value, which was ten-fold less than with the wild type enzyme. The I326A mutant was found to be over 80 times more efficient with 2-hydroxyoctanoate than with L-lactate (representing a **160**-fold swing in the selection of 2-hydroxyoctanoate over L-lactate by the enzyme).

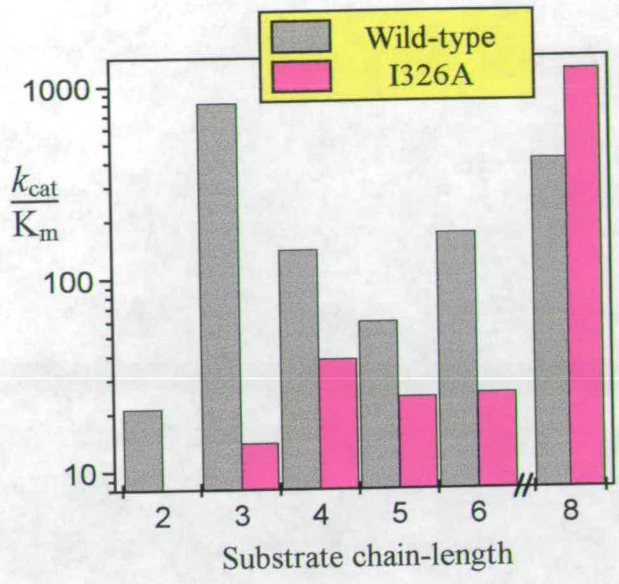

Figure 3.5 Substrate specificity profile of WT and I326A mutant enzymes (Chapman *et al.*, 1993)

These results indicate that it is possible to manipulate the substrate specificity of an enzyme, with a high degree of success, by simply mutating one or two well chosen active-site residues. Even the Ala198G mutation, which led to an overall decrease in enzyme catalytic efficiency, demonstrated how K_m values could be increased for a range of substrates. This work may also provide useful information on enzyme evolution, for example, how has L-lactate dehydrogenase evolved its preference for L-lactate over another 2-hydroxy acid, L- mandelate? This question is not as simple as it might at first seem, since L-lactate dehydrogenase can turnover a wide variety of substrates with an *aliphatic* side chain, at rates that are almost within the same order of magnitude as its turnover rate with L-lactate, but can only turnover L-mandelate, which has an *aromatic* side group at barely detectable levels. This is all the more surprising, given that the L-mandelate dehydrogenase (L-mdh) found in the yeast *Rhodotorula graminis* shares many of the characteristics of the *S. cerevisiae* L-lactate dehydrogenase (see section 1.4.2). In a previous study (Smékal *et al.*, 1993) the kinetic characteristics of the two *b*-type flavocytochromes were compared. The authors found that L-ldh was unable to oxidize L-mandelate and similarily L-mdh was unable to oxidize L-lactate. Moreover they found L-lactate to be a competitive

inhibitor of L-mdh and L-mandelate a competitve inhibitor of L-ldh, with K_i values which were very similar to the K_m values obtained when the compounds were used as substrates for L-mdh and L-ldh respectively. Since the inhibition they observed was competitive in nature, the authors suggested that the discrimination between the two substrates was not due to a lack of binding, but due to differences in either the orientation of the compounds at their active sites or that the two enzymes' transition states were different. Another interesting difference between the two enzymes was that L-ldh could use phenyllactate as a substrate whereas L-mdh could not. It appears that by the insertion of a CH_2 group between the α-carbon and the aromatic ring of mandelate to give phenyllactate prevents L-mdh from utilising the compound as a substrate.

3.5 Results

The role of the active site residues of L-ldh in controlling this substrate discrimination, has been further examined in the light of new sequence information on the L-mandelate dehydrogenase from *R. graminis* (R. Illias, 1997).

	L-LDH	**L-MDH**
k_{cat} (s^{-1}) L-lactate	400 ±10	0.50 ± 0.10
K_m (mM)	0.49 ± 0.05	0.40 ± 0.05
k_{cat}(s^{-1}) L-mandelate	0.02 ± 0.01	550 ± 25
K_m (mM)	*	0.35 ± 0.02

Table 3.1 The kinetic parameters of L-ldh and *R. graminis* L-mandelate dehydrogenase (L-mdh) with L-lactate and L-mandelate as substrates The L-ldh/ L-lactate values taken from Miles *et al.*, 1992. Assays were performed in Tris.HCl buffer at 25°C (see section 2.8.1) and 1 mM ferricyanide as acceptor. Errors in K_m are

standard deviations from least-squares fitting and errors in k_{cat} are standard deviations from multiple assays at saturating substrate concentration.* Unable to determine accurate value for K_m (see text for details).

As a starting point, the turnover rate of L-ldh with L-mandelate was calculated and compared to the value obtained with L-lactate as substrate. The value for k_{cat} quantifies the maximum rate of turnover in the presence of saturating amounts of substrate and electron acceptor (1mM potassium ferricyanide). However, the activity of L-ldh with L-mandelate can barely be detected (see table 3.1) and because of this it has proved particularly difficult to determine a K_m value with this substrate. The inhibition constant, K_i for L-ldh with L-mandelate has been determined (Smekal *et al.*, 1993) and has a value of 0.26 ± 0.08mM. This result, combined with the fact that the K_m values for L-mdh with both substrates are similar suggest that the K_m value for L-ldh with L-mandelate would probably be in the region of 0.2-0.6 mM. These results illustrate that, in contrast to previous reports, L-ldh can utilise L-mandelate as a substrate.

There is, however, a large difference between the turnover numbers generated in the presence of the two substrates. With L-lactate, the physiological substrate of L-ldh, the k_{cat} is 400 s^{-1}. With L-mandelate the k_{cat} is over 4 orders of magnitude slower at 0.02s^{-1}. It has been suggested that the different substrate specificities of L-mdh and L-ldh were due to differences in the relative energies of the transition states for L-lactate and L-mandelate dehydrogenation (Smekal *et al.*, 1993). It was previously demonstrated that the steady state turnover of L-ldh with L-[2-^{1}H]lactate and L-[2-^{2}H]lactate gave a kinetic isotope effect (KIE) of 4.7 ± 0.4 (Miles *et al.*, 1992). The authors synthesised what they took to be DL-[2-^{2}H]mandelate and carried out similar steady state experiments on L-mdh. The KIE value of 1.1 ± 0.1 indicated that there was no [2-^{2}H] isotope effect and that the transition states of the two enzymes must be different. As will be discussed in chapter 4, these experiments were repeated with

DL-[2-^{2}H]-mandelate that was unambiguously assigned to be isotopically correct (A. Neu, unpublished results), and a kinetic isotope effect value of 3.5 ± 0.2 was measured. Therefore, it is clear that there is little difference betweeen the KIEs obtained for L-ldh and L-mdh, and the reason for the slightly smaller KIE for L-mdh with mandelate is probably due to the fact that the removal of the H at the C-2 position of mandelate would be facilitated by the stabilising effect of the aromatic ring in mandelate. How then can we account for the near mutually exclusive substrate specificity that is found between these two enzymes?

Examination of the three dimensional crystal structure of L-ldh, which has been solved to 2.4 Å, showed the product molecule bound at the active site. By replacing this molecule with phenylglyoxalate (the product of mandelate dehydrogenation), we can see that productive binding of L-mandelate at the active site might be impeded by steric interactions between the phenyl ring of L-mandelate and the side chains of Leu 230, Ala 198, and to a smaller degree, Ile 326 (see figure 3.6). These are the same residues that were found by Daff *et al.*, to control the substrate specificity of L-ldh in favour of L-lactate. The mutants which had been previously constructed (A198G, L230A, A198GL230A and I326A) were also tested with L-mandelate. By comparing the k_{cat} and K_m values obtained for the various mutant enzymes, we can clearly see that these mutations have an effect on both the rate of turnover and the binding affinity for L-mandelate. In the following section increases in k_{cat} are our primary concern, rather than the combined effect of k_{cat}/ K_m. This is due to to the fact that the main difference between the two enzymes is in the turnover rates with each other's substrate rather than substrate binding.

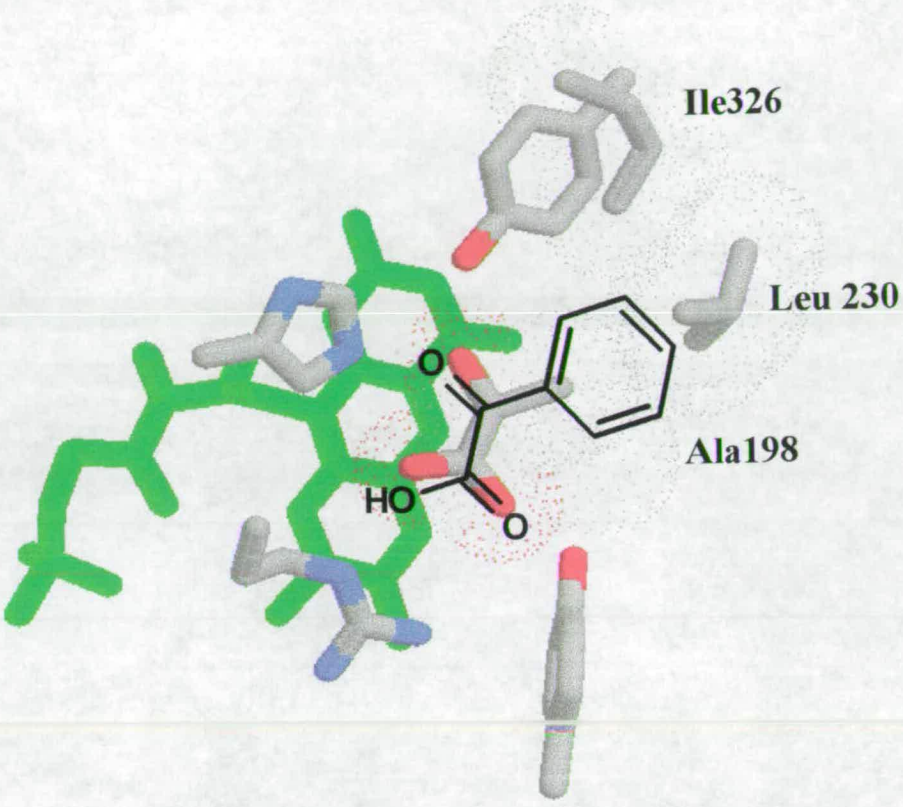

Figure 3.6 The active site of *S.cerevisiae* L-ldh derived from X-ray crystallography (Xia and Mathews, 1990) illustrating the steric interference between the side groups of Ala198, Leu 230 and Ile326 and the phenyl ring of phenylglyoxalate

	k_{cat} (s^{-1})	K_m (mM)	k_{cat} (s^{-1})	K_m (mM)
	L-mandelate		L-lactate	
Wild Type	0.02 ± 0.01	0.25 ± 0.60	400 ± 10	0.49 ± 0.05
I326A	0.04 ± 0.02	0.25 ± 0.60	11 ± 0.1	0.76 ± 0.07
L230A	0.11 ± 0.05	0.16 ± 0.01	30 ± 3	6.10 ± 0.20
A198G	0.40 ± 0.05	1.00 ± 0.20	185 ± 5	4.10 ± 0.40
L230G	0.80 ± 0.20	0.70 ± 0.10	100 ± 5	1.90 ± 0.30
A198GL230A	8.50 ± 0.50	1.36 ± 0.10	41± 2	38 ± 4

Table 3.2 The kinetic parameters of L-ldh WT and mutant enzymes with L-mandelate and L-lactate as substrates. The parameters were determined as described in table 3.1

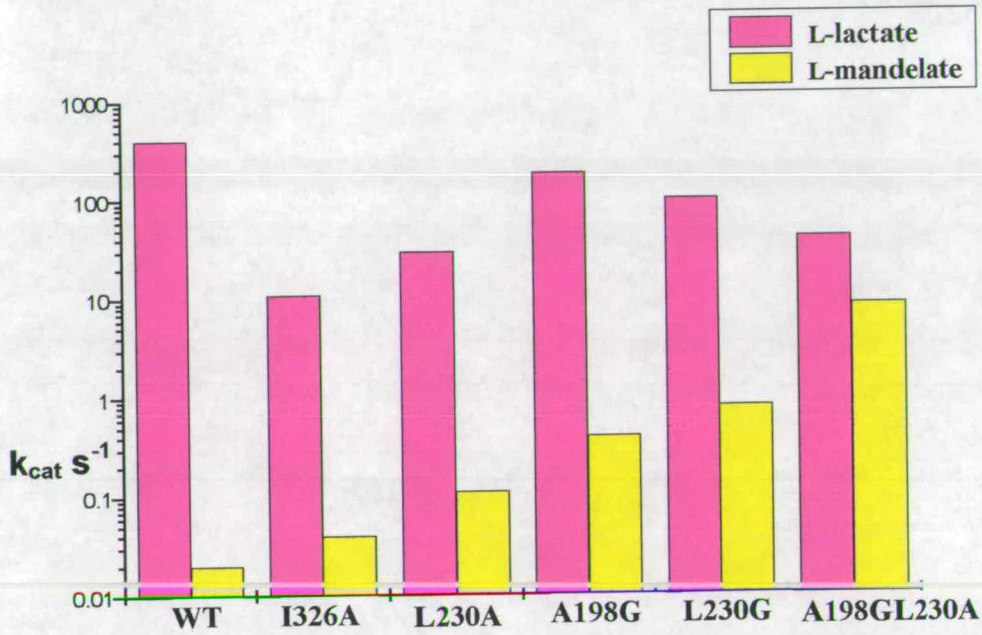

Figure 3.7 A comparison of the activities of L-ldh WT and mutant enzymes with L-lactate and L-mandelate, tabulated above

Table 3.2 and figure 3.7 illustrate the progress made so far in constructing an L-mandelate dehydrogenase. The reactivity of wild type and mutant enzymes for both lactate and mandelate are compared. The first mutant tested was I326A. This residue is a little further away than the other two residues, but would certainly be within contact range of bulkier substrate side groups. Additionally, the side chain of Ile326 appears to make contact with Leu230 and may help position this residue relative to the substrate. The effect of this mutation was to create a dramatic swing in specificity towards 2-hydroxy octanoate. However, when tested with L-mandelate there is no increase in the k_{cat} value compared to wild type, which suggests that there

are subtle differences between the positioning of the aromatic side group of mandelate in the active site compared to substrates with aliphatic side chains.

The L230A mutant was also shown to be more specific for the long-chain 2-hydroxy acids and has a **10**-fold decrease in activity with L-lactate compared to wild type. There is a slight increase in k_{cat} with L-mandelate compared to the value for wild type ($0.02s^{-1}$ to $0.11s^{-1}$) though perhaps not a large enough increase to be considered significant. There is also a decrease in the K_m value, suggesting that this mutation stabilises the Michaelis complex.

The A198G mutation also results in an increased turnover rate with L-mandelate and has a larger K_m value compared to the postulated value for wild type L-ldh. This increase in K_m is also found for the other mutants using either L-lactate or L -mandelate as substrate. This is perhaps to be expected since by creating a larger volume for the substrate to reside in the active site there will be an overall weakening of the interactions which anchor the substrate in place. This is particularly apparent for the double mutant, A198GL230A.

Yorita *et al.*, (1996) mutated the residue equivalent to alanine 198 in *Aerococcus viridans* L-lactate oxidase to glycine (A95G). This homologous flavoenzyme also catalyses the oxidation of L-lactate to pyruvate, and the flavin molecule is reoxidised by reduction of molecular oxygen to hydrogen peroxide. The effect of this mutation was to increase the enzyme's reactivity towards long chain hydroxy acids and L-mandelate. The turnover number of A95G with mandelate (measured in mol O_2/min/mol FMN) was increased almost 5000-fold. However this mutation also resulted in an increased K_m value with mandelate (from 0.30-20 mM). Thus although the effect of the Ala→Gly mutation in L-lactate oxidase is more dramatic than in L-ldh, the importance of this particular residue to the substrate specificity of both enzymes is assured.

Recently the gene encoding L-mandelate dehydrogenase from *R.graminis* has been isolated and sequenced (R. Illias, 1997). Figure 3.8 aligns the *R.graminis* L-mdh coding sequence along with several other related flavoenzymes. At the position corresponding to the Leu 230 of L-ldh, there is a glycine residue rather than the slightly larger alanine found in the *Pseudomonas* L-mandelate dehydrogenase. Perhaps it is necessary to remove the hydrocarbon side chain of leucine 230 completely at this position to enable the substrate to bind in a more favourable position. To test this the mutant L230G was constructed and assayed with L-mandelate. The L230G mutation was constructed using the oligonucelotide L230G (5′ GAT ATC TAC TGG TGC TTC ATG ATG T 3′) (Oswel DNA Service). After identifying a clone which contained the L230G mutation (GGT replaced TTG), the entire L-ldh gene was sequenced using a combination of oligonucleotide primers (see section 2.3.5) to check for any unwanted mutations elsewhere in the sequence. The entire gene was then excised from the phagemid pGR401 on an *Eco*RI-*Hin*dIII fragment and ligated into the expression vector pDS6 to form pDSL230G (see section 2.4).

This mutation resulted in a k_{cat} value of around 0.80 s^{-1}, which represents a significant increase (**40**-fold) compared to the value obtained with wild type. This mutant enzyme was also tested with 2-hydroxy acids with increasing length of side chain and a substrate specificity profile was generated in a similar manner to the work carried out by Daff *et al.*, 1994 (table 3.3).

Figure 3.8 Amino acid sequence comparison between *S. cerevisiae* L-ldh (Scb2), *H. anomala* L-ldh (Hab2), Spinach glycolate oxidase (Gox), rat hydroxy acid oxidase (Hao), *Pseudomonas putida* L-mdh (Mdh), *Mycobacterium smegmatis* lactate oxidase (Lox), *E. coli* L-ldh (LctD) and *R.graminis* L-mdh

Table 3.3 and fig 3.9. Substrate specificity profiles of WT and L230G mutant enzyme. Values for k_{cat}/K_m (tabulated below) are represented in $mM^{-1}s^{-1}$ on a log. scale. Substrate chain length (2-8), as described in figure 3.3.

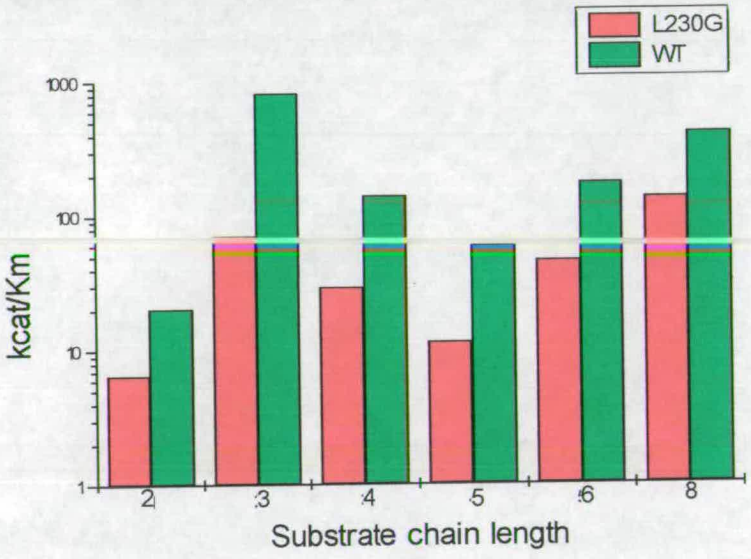

	chain length	k_{cat} (s^{-1}) L230G	K_m L230G	k_{cat} (s^{-1}) WT	K_m WT
glycolate	2	10.8 ± 1	1.65 ± 0.02	7.1± 1	0.34 ± 0.05
L-lactate	3	100 ± 5	1.42 ± 0.01	400 ± 10	0.49 ± 0.05
s-2-hydroxybutyrate	4	56.5 ± 2	1.93 ± 0.04	82 ± 7	0.59 ± 0.04
s-2-hydroxyvalerate	5	21.1 ± 1	1.84± 0.05	13 ± 1	0.22± 0.02
s-2-hydroxycaproate	6	27.1 ± 2	0.59 ± 0.02	19 ± 1	0.11 ± 0.01
s-2-hydroxyoctanoate	8	32.4 ± 3	0.24 ± 0.01	45± 5	0.11 ± 0.01

The values presented in table 3.3 and fig. 3.9 reveal that the shape of the profile is similar to wild type, but due to a universal increase in K_m values the column heights are slightly smaller. However, as in L230A, there is a swing in substrate specificity away from L-lactate towards L-2-hydroxyoctanoate, though the swing is of a smaller magnitude (only 4-fold compared to the 80-fold swing observed in L230A). The reason why the L230G mutant enzyme should be better at turning over shorter 2-hydroxy acids than L230A is unclear, when one would almost expect the opposite to be the case. However, as these data illustrate, predicting the effect of a mutation in the active site is not as straightforward as it at first seems, since we can not predict the effect that changing one residue may have on neighbouring residues. Furthermore, despite this mutant being generally poorer at turning over long chain aliphatic hydroxy acids, there has certainly been a marked increase in the k_{cat} value with an aromatic substrate, L-mandelate (see table 3.2).

As mentioned previously, the effect of the double mutant (A198GL230A) when tested with long-chain 2-hydroxy acids was that the k_{cat} values were reminiscent of the values obtained with L230A for all the substrates. However, the K_m values, which had all increased, were similar to the K_m values obtained with A198G. It appears that the individual effects of the two mutations were combined within the double mutant. However, when the double mutant was tested with mandelate, we saw a dramatic increase in activity, from 0.02 s^{-1} for wild type to rates of around 8.50 s^{-1}, representing a **450** fold increase in reactivity towards L-mandelate. In conclusion, it appears that one needs to remove bulk from Ala198 *and* Leu230 in order to accommodate the phenyl side chain of the substrate. Therefore in this situation we are not seeing the individual contributions of the two single mutations (which is the situation with the long chain hydroxy acids), but that each mutation must have a direct effect on the other in enabling the mutant enzyme to turnover mandelate at a rate which is considerably faster than wild type. The next logical step would be to

remove the side chains completely (ie) A198GL230G. The double mutant has been constructed, but attempts to overexpress this protein have so far been unsuccessful. It may be that by creating such a large hole in the enzyme's active site has a destabilising effect on protein folding, ultimately leading to little or no production of active enzyme.

However, there remain other, more distant residues at the active site which may be suitable candidates to undergo site directed mutagenesis in order to enhance mandelate dehydrogenase activity. One such possibility would be to replace an active site residue with one which has an aromatic side chain, for example, phenylalanine, in order to induce stacking between the amino acid aromatic ring and the aromatic side group of mandelate. Other possibilities include generating random, rather than site-directed, mutants of L-ldh by PCR and then screening for mandelate metabolism. However, there are several problems with generating a mandelate dehydrogenase by this process. Firstly, if the protein is to be over-produced in a bacterial strain, such as *E. coli*, the physiological electron acceptor of L-mdh, cytochrome *c* will not be produced. Furthermore, the product of mandelate oxidation, phenylglyoxalate, is not a substrate for any *E. coli* enzymes. An alternative would be to express the protein in a species which contains the enzymes of the mandelate pathway, such as *Pseudomonas putida*, however, there still remains the problem of an electron acceptor if this bacterium were used.

3.6 Mandelate activity of the flavin domain of L-ldh (FDH)

Figure 3.10 shows the relative orientations of the flavin and haem groups in L-ldh. The prosthetic groups are approximately coplanar, with a 20° twist to their planes. The closest edge to edge distance in subunit 1 is 9.7 Å, between N5 of FMN and C2a of the porphyin haem edge. This haem propionate 'finger' protrudes far into the active site, which presumably facilitates electron transfer between the flavin and

Chapter 4: L-mandelate dehydrogenase

Purification and Characterisation of *R. graminis* L-mandelate dehydrogenase

4.1 Introduction

This chapter describes the expression, purification and kinetic characterisation of the L-mandelate dehydrogenase from *R..graminis*. Where possible, the kinetic properties of this enzyme are compared to those of the L-lactate dehydrogenase from *S. cerevisiae*. As explained earlier, the two enzymes share many similarities (see section 1.4.2), including subunit size, location in the cell, and the incorporation of flavin mononucleotide and haem molecules as prosthetic groups. From the results obtained on the enzyme redesign work described in chapter 3, we can see that the major difference between the enzymes is in their substrate specificity. In this chapter, any further similarities/differences in the kinetic properties of the two enzymes are described.

4.11 Expression of the L-mandelate dehydrogenase gene

The *R. graminis* L-*mdh* gene was isolated, cloned and sequenced by R. Illias (1997). The genomic form of the gene was found to contain eleven introns in the region encoding the mature enzyme. In order to avoid these, single stranded cDNA, reverse transcribed from the total RNA of *R. graminis* was used as a template for the amplification of the coding sequence of L-mdh. Two specific primers were designed based on the N- and C- terminal amino acid sequences of the genomic form of the enzyme. A fragment of about 1.5 kb was amplified and the fragment ligated to pTZ19R cut with *Xma*I and *Hin*dIII, to generate the recombinant plasmid pLM5.

4.12 Amino acid sequence comparisons

Figure 4.1 shows the entire amino acid sequence of the L-mdh gene. The mature protein contains 492 amino acids and the subunit molecular weight was calculated to be 54,604 Daltons. Alignment of the amino acid sequence of L-mdh with other FMN dependent 2-hydroxy acid dehydrogenases/oxidases (also Figure 4.1) demonstrates that there is a high degree of sequence similarity. There is 42 % sequence identity with the L-lactate dehydrogenase from *S.cerevisiae*. As described in Section 1.7.7, most of the residues involved in cofactor and substrate binding in L-ldh are also found in L-mdh, as are the catalytically important residues described in Section 1.7.9. However, there are two areas in which the sequences differ greatly: these are the regions corresponding to the interdomain hinge and protease-sensitive loop of L-ldh (approximately residues 92-103 and 298-314 respectively, numbering as in L-ldh).

4.13 Expression of L-mandelate dehydrogenase.

The L-mdh cDNA insert in pTZ19R was cut with the restriction enzymes *Xma*I and *Hin*dIII, cloned into the expression vector pKK22-33 cut with the same restriction enzymes to generate the recombinant plasmid pLM7 (R. Illias, 1997) and transformed into *E.coli* JM105 cells. Production of the L-mdh protein was induced by addition of IPTG when the cells were at mid log phase (OD_{600} =0.6). Western blotting of the cell extracts with anti L-mdh antibody failed to detect any expression.

The cDNA insert from LM7 was removed by cutting with *Eco*RI and *Hind*III, cloned into the expression vector pRC23 to generate the recombinant plasmid pLM8. and then transformed into *E. coli* NF1 cells. The plasmid pRC23 contains the thermoinducible lamda P_L promoter (Crowl *et al.*, 1985), which is repressed by the lamda cI*857* at 30°C. The plasmid bearing NF1 cells were grown in LB media at 30°C then shifted to 42°C to express the L-mandelate dehydrogenase when the O.D reached 0.6.

The average yield of L-mdh found in the cell lysate of 1 litre of culture, was approximately 10 mg, corresponding to around 2% of the total cell protein. This represents a significant increase in L-mdh production compared to the levels of the native form of the enzyme synthesised by *R. graminis* (estimated to be around 0.1%, Yasin and Fewson, 1993). This increase in overexpression was also indicated by the pink colour of the NF1 cells, caused by the raised levels of haem containing protein. Western blotting was used to the confirm that the overproduced protein was L-mdh.

Figure 4.1 Amino-acid sequence comparison between *R. graminis* L-mandelate dehydrogenase and other 2-hydroxy acid dehydrogenases / oxidases

Spinach glycolate oxidase (gox-spiol: Volokita and Somerville, 1988), rat kidney hydroxy-acid oxidase (Hao: Lê and Lederer, 1991), *H.anomala* L-ldh (Ha: Black *et al.*, 1989), *S. cerevisae* L-ldh (b2: Guiard, 1995), *R. graminis* L-mdh (cdnalmdh: R. Illias, 1997), *P.putida* L-mdh (mdlb-psepu: Tsou *et al.*, 1990), and *M. smegmatis* lactate mono-oxygenase (la2m-mycsm: Giegel *et al.*, 1990). Amino-acids which are catalytically important are marked (numbering as in *S. cerevisiae* L-ldh)

```
                                                  1
Gox_Spiol  .......... .......... .......... .......... ..........
      Hao  .......... .......... .......... .......... ..........
       Ha  NSLIALAIS. .LSAVSSSYY L.YQKDKFIS ADVPHWKDIE LTPEIVSQHN
       B2  QSWTALRVGA ILAATSSVAY LNWHNGQIDN EPKLDMNKQK ISPAEVAKHN
  Lmdhcdna .......... .......... ......DAQL PVKQRGRARS ISAAEVAKHN
 Mdlb_Psepu .......... .......... .......... .......... ..........
 La2m_Mycsm .......... .......... .......... .......... ..........

                                        43                      66
Gox_Spiol  .......... .......... .......... .......... ..........
      Hao  .......... .......... .......... .......... ..... ....
       Ha  KKDDLWVVLN GQVYDLTDFL PNHPGGQKII IRYAGKDATK IFVPIHPPDT
       B2  KPDDCWVVIN GYVYDLTRFL PNHPGGQDVI KFNAGKDVTA IFEPLHAPNV
  Lmdhcdna SRDSMWVCID DEVWDITNFV ELHPGGAKVL EQNAGKDVTK VFKSIHPPKT
 Mdlb_Psepu .......... .......... .......... .......... ..........
 La2m_Mycsm .......... .......... .......... .......... ..........


Gox_Spiol  .......... .......... .......... .......... .........M
      Hao  .......... .......... .......... .......... ..........
       Ha  IEKFIPPEKH LGPLVGEFEQ E......EEE LSDEEIDRLE RIER.KPPLS
       B2  IDKYIAPEKK LGPLQGSMPP ELVCPPYAPG ETKEDIARKE QLKSLLPPLD
  Lmdhcdna LEKFLTDDNF VGRIDVDEVT KIGGGKNAED L......RIE QARKELRNVE
 Mdlb_Psepu .......... .......... .......... .......... .......MSQ
 La2m_Mycsm ..........  .......... .........SN WGDYENEIYG QGLVGVAPTL

                                       143
Gox_Spiol  EITNVNEYEA IAKQKLPKMV YDYYASGAED QWTLAENRNA FSRILFRPRI
      Hao  PLVCLADFKA HAQKQLSKTS WDFIEGEADD GITYSENIAA FKRIRLRPRY
       Ha  QMINLHDFET IARQILPPPA LAYYCSAADD EVTLRENHNA YHRIFFNPKI
       B2  NIINLYDFEY LASQTLTKQA WAYYSSGAND EVTHRENHNA YHRIFFKPKI
  Lmdhcdna TVVCLDEFEE ISQKILSEMA MAYYGTGAET EQTLRDEREA WQRVRFRPRV
 Mdlb_Psepu NLFNVEDYRK LRQKRLPKMV YDYLEGGAED EYGVKHNRDV FQQWRFKPKR
 La2m_Mycsm PM.SYADWEA HAQQALPPGV LSYVAGGSGD EHTQRANVEA FKHWGLMPRM

                                       198
Gox_Spiol  LIDVTNIDMT TTILGFKISM PIMIAPTAMQ KMAHP.EGEY ATARAASAA.
      Hao  LRDMSKVDTR TTIQGQEISA PICISPTAFH SIAWP.DGEK STARAAQEA.
       Ha  LIDVKDVDIS TEFFGEKTSA PFYISATALA KLGHP.EGEV AIAKGAGRE.
       B2  LVDVRKVDIS TDMLGSHVDV PFYVSATALC KLGNPLEGEK DVARGCGQGV
  Lmdhcdna LRKMRHIDTN TTFLGIPTPL PIFVAPAGLA RLGHP.DGEQ NIVRGVAKH.
 Mdlb_Psepu LVDVSRRSLQ AEVLGKRQSM PLLIGPTGLN GALWP.KGDL ALARAATKA.
 La2m_Mycsm LMAATERDLS VELWGKTWAA PMFFAPIGVI ALC.AQDGHG DAASAQASAR

                230                                   254
Gox_Spiol  .GTIMTLSSW ATSSVEEVAS TGP.G..IRF FQLYVYKDRN VVAQLVRRAE
      Hao  .NICYVISSY ASYSLEDIVA AAPEG..FRW FQLYMKSDWD FNKQMVQRAE
       Ha  .DVVQMISTL ASCSFDEIAD ARIPGQQ.QW YQLYVNADRS ITEKAVRHAE
       B2  TKVPQMISTL ASCSPEEIIE AAPSDKQIQW YQLYVNSDRK ITDDLVKNVE
  Lmdhcdna .DILQVVSSG ASCSIDEIFE VKEPDQNLAW .QFYVHSDKK IAEEKLKRAL
 Mdlb_Psepu .GIPFVLSTA SNMSIEDLAR QCDGDL...W FQLYV.IHRE IAQGMVLKAL
 La2m_Mycsm TGVPYITSTL AVSSLEDI.. RKHAGDTPAY FQLYYPEDRD LAESFIRRAE


Gox_Spiol  RAGFKAIALT VDTPRLGRRE ADIKNRFVL. ...PPFLTLK N.........
      Hao  ALGFKALVIT IDTPVLGNRR RDKRNQLNL. ...EANILLK D.........
       Ha  ERGMKGLFIT VDAPSLGRRE KDMKMK.... .FEADSDVQG ..........
       B2  KLGVKALFVT VDAPSLGQRE KDMKLK.... .FSNTKAGPK A.........
  Lmdhcdna ALGAKAIFVT VDVPVLGKRE RDLKLKARSQ NYEHPIAAQW K.........
 Mdlb_Psepu HTGYTTLVLT TDVAVNGYRE RDLHNRFKIP MSYSAKVVLD GCLHPRWSLD
```

```
La2m_Mycsm  EAGYDGLVIT LDTWIFGWRP RDLTI..... ...SNFPFLR GLCLTNYVTD

 Gox_Spiol  ......FEGI DLGKMDK..A NDSGLSSYVA GQIDRSLSWK DVAWLQTITS
       Hao  ......LRAL ...KEEK..P TQSVPVSFPK A....SFCWN DLSLLQSITR
        Ha  .......DDE DIDRSQG..A SRALSSF... ..IDPSLSWK DIAFIKSITK
        B2  ......MKKT NVEESQG..A SRALSKF... ..IDPSLTWK DIEELKKKTK
  Lmdhcdna  ......AAGS KVEET.I..A KRGVSDIPDT AHIDANLNWD DIAWIKERAP
 Mdlb_Psepu FVRHGMPQLA NFVSSQT..S SLEMQAALMS RQMDASFNWE ALRWLRDL.W
 La2m_Mycsm PVFQKKFKAH SGVEAEGLRD NPRLAADFWH GLFGHSVTWE DIDWVRSITK

                                                373 376
 Gox_Spiol  .LPILVKGVI TAEDARLAVQ HGAAGIIVSN HGARQLDYVP ATIMALEEVV
       Hao  .LPIILKGIL TKEDAELAMK HNVQGIVVSN HGGRQLDEVS ASIDALREVV
        Ha  .MPIVIKGVQ RKEDVLLAAE HGLQGVVLSN HGGRQLDYTR APVEVLAEVM
        B2  .LPIVIKGVQ RTEDVIKAAE IGVSGVVLSN HGGRQLDFSR APIEVLAETM
  Lmdhcdna  GVPIVIKGVG CVEDVELAKQ YGADGVVLST HGARQLDGAR APLDVLIEVR
 Mdlb_Psepu PHKLLVKGLL SAEDADRCIA EGADGVILSN HGGRQLDCAI SPMEVLAQSV
 La2m_Mycsm .MPVILKGIQ HPDDARRAVD SGVDGIYCSN HGGRQANGGL PALDCLPEVV

 Gox_Spiol  K.....AAQG RIPVFLDGGV RRGTDVFKAL ALGAAGVFIG RPVVFSLAAE
       Hao  A.....AVKG KIEVYMDGGV RTGTDVLKAL ALGARCIFLG RPILWGLACK
        Ha  PILKERGLDQ KIDIFVDGGV RRGTDVLKAL CLGAKGVGLG RPFLYAMSSY
        B2  PILEQRNLKD KLEVFVDGGV RRGTDVLKAL CLGAKGVGLG RPFLYANSCY
  Lmdhcdna  R..KNPALLK EIEVYVDGQA RRGTDVLKAL CLGARGVGFG RGFLYAQSAY
 Mdlb_Psepu A.......KT GKPVLIDSGF RRGSDIVKAL ALGAEAVLLG RATLYGLAAR
 La2m_Mycsm K......ASG DTPVLFDSGI RTGADVVKAL AMGASAVGIG RPYAWGAALG

 Gox_Spiol  GEAGVKKVLQ MMRDEFELTM ALSGCRSLKE ISRSHIAADW DGPSSRAVAR
       Hao  GEDGVKEVLD ILTAELHRCM TLSGCQSVAE ISPDLIQFSR L.........
        Ha  GDKGVTKAIQ LLKDEIEMNM RLLGVNKIEE LTPELLDTRS IHNRAVPVAK
        B2  GRNGVEKAIE ILRDEIEMSM RLLGVTSIAE LKPDLLDLST LKARTVGVPN
  Lmdhcdna  GADGVDKAIR ILENEIQNAM RLLGANTLAD LKPEMVE.CS FPERWVPE..
 Mdlb_Psepu GETGVDEVLT LLKADIDRTL AQIGCPDITS LSPDYLQNEG VTNTAPVDHL
 La2m_Mycsm GSKGIEHVAR SLLAEADLIM AVDGYRNLKE LTIDALRPTR ..........

 Gox_Spiol  L......... .......... ..
       Hao  .......... .......... ..
        Ha  DYLYEQNYQR MSGAEFRPGI ED
        B2  DVLYNEVYEG PTLTEFEDA. ..
  Lmdhcdna  .......... .......... ..
 Mdlb_Psepu IGKGTHA... .......... ..
 La2m_Mycsm .......... .......... ..
```

However the attempts by Illias to obtain high levels of L-mdh protein proved only partially successful. While there is a notable increase in the amount of protein being produced compared to the native enzyme, the vast majority of the proteins produced by the cell are not L-mdh, which greatly hinders any attempted purification of the enzyme.

Several approaches were used to increase the production levels of L-mdh. The first of these was to change the growth medium. Initially all the cells were grown in Luria-Bertani (LB) media. The main components of this broth are tryptone and yeast extract. Cells were also grown in 'Terrific broth', which has twice the concentration of tryptone and yeast extract, compared to LB, but is phosphate buffered and lacks NaCl. By using Terrific broth instead of LB the cells produced approximately twice as much L-mdh (per unit volume).

A second condition which one can alter is the point at which the cells are induced (temperature shifted). Surprisingly, the cells which produced the most enzyme were the ones which were grown continually at 42°C. This is indicated in figure 4.2 which shows the different intensities of the protein band of the Western blot of cells induced at different stages in their growth. This suggests that the best expression of the enzyme is by constitutive (continual) growth. To test this, the *L-mdh* containing plasmid, (pLM8) was tranformed into an *E. coli* strain which allowed constitutive growth only. The Western blot of figure 4.2 shows that continual growth in JM109 cells at 37°C, in Terrific broth leads to a dramatic increase in the amount of protein being produced, to levels around 14% of the total cell protein.

Figure 4.2 Western blot of *E. coli* cell extracts indicating the different levels of L-mdh overexpression (Approximately 50μg total protein in each lane)

A Partially purified L-mdh expressed in JM109, grown at 37°C in Terrific broth.

B As A, except grown at 42°C.

C As B, except grown in Luria broth

D Partially purified L-mdh expressed in NF1, grown continually at 42°C in Terrific broth

E As D, except temperature shifted at $OD_{600nm} = 0.6$

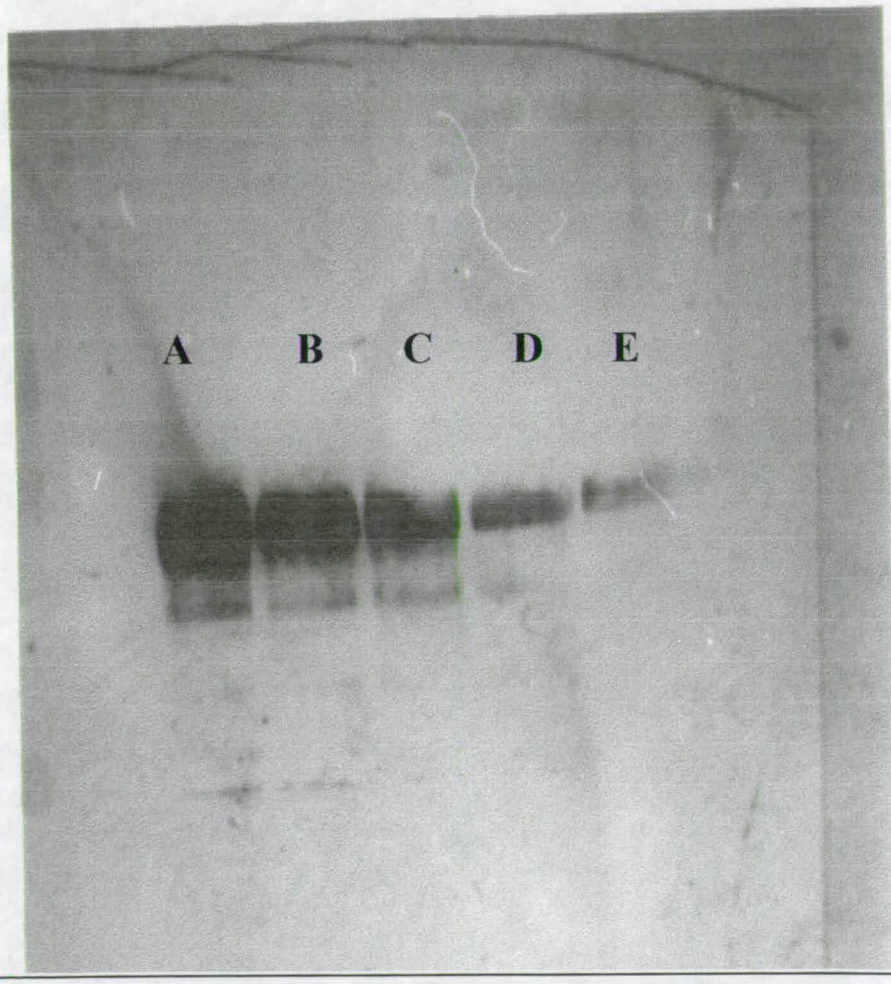

4.2 Growth of L-mandelate dehydrogenase

500 ml of Terrific broth medium, containing 150 μgml^{-1} of the antibiotic ampicillin as a selectable marker, was inoculated with a single bacterial colony and incubated at 37°C, with shaking. The cells were allowed to grow to stationary phase. Usually 5 litres of culture were grown for each preparation. The cells were then harvested in a Sorvall RC-5B centrifuge with a GS3 rotor run at 5000 ***g*** for 10 minutes. The resulting wet pellet of cells was stored at -20°C until required.

4.3 Purification of L-mandelate dehydrogenase

Early attempts to purify L-mdh were based on the purification procedure for recombinant L-ldh (Section 2.5.2). However, despite both enzymes having such a high degree of sequence identity, they behave differently on the ion exchange columns used. The overall charge of L-mdh is slightly more negative (+3 instead of +5) than L-ldh, which may contribute to the inability of this enzyme to bind to a hydroxyapatite column except at very low ionic strength conditions.

Previous attempts to purify the enzyme to homogeneity had included the following steps. The frozen pellet of cells containing overexpressed protein was thawed and resuspended in 0.1M phosphate buffer. The cells were lysed by sonication using a Heat Systems Ultra Sonicator, for 3 x 30 seconds at full power. The protein solution was centrifuged in a Sorvall RC-5B centrifuge (SS34 rotor) at 39,000 ***g*** for 10 minutes. After lysis, the supernatant was adjusted to 30 % ammonium sulphate (176 gl^{-1}) saturation and the precipitated proteins removed by centrifugation at 39,000 ***g*** for 10 minutes. This supernatant was further adjusted to 50 % saturation (an additional 127 gl^{-1}) which precipitates the L-mdh protein and the protein removed by centrifugation.

To lower the ionic strength of the protein solution prior to loading on the hydroxyapatite column and to remove any low molecular weight contaminants, the

solution was dialysed for 2 hours against a 10 X volume of 10 mM phosphate buffer in tubing with a molecular weight exclusion limit of 12 kDa. Following dialysis, the solution was loaded onto a 7.5 x 2.5 cm hydroxyapatite column which had been previously equilibrated with 0.1 M phosphate buffer. The protein was eluted using a 10-100 mM phosphate buffer gradient. The eluted protein solution was precipitated with 50 % ammonium sulphate and pelleted again by centrifugation. The protein was redissolved in a minimum volume of 10 mM Tris.HCl buffer and the concentrated enzyme solution was then loaded onto a 10 x 1.5 cm Sephadex G25 column, equilibrated and eluted with Tris buffer. This method of purification would usually result in a protein solution that was between 30-50% pure. There were, however, major losses of L-mdh protein at each step in the purification, and several modifications were made in order to increase protein yield and purity.

4.3.1 Cell lysis and DEAE cellulose column (Whatman DE52)

The initial stage of the purification procedure, cell lysis by sonication was the first step to be altered. Sonication appears to be too effective a method of lysis since it can solublise proteins that are normally held within the cell membranes. By using a less rigourous form of lysis, such as snap-freezing in liquid nitrogen (Section 2.5.3), less protein will be released into the lysate. It was also found that a substantial source of L-mdh loss occurred during the ammonium sulphate precipitation step, since a significant amount of enzyme would remain in solution, even when the ammonium sulphate concentration was adjusted to 100% saturation. This step was replaced by washing the protein solution through a DEAE (diethylaminoethyl, functional group $CH_2CH_2N^+H(CH_2CH_3)_2$) cellulose anion exchange column (10 x 4.5 cm) equilibrated at 100 mM phosphate buffer. L-mdh does not bind to DEAE at this ionic strength, but passes straight through the column. However, other impurities, such as DNA, are retained on the column. Any eluted protein fractions which were red in colour were then collected.

4.3.2 DEAE sephacel column (Sigma)

After being dialysed for 2 hours against a 10 fold greater volume of 30 mM phosphate buffer the protein was loaded onto a 20 x 3 cm DEAE Sephacel column which had previously been equilibrated with 30mM phosphate. The protein bound in a tight band at the top of the column and was washed again with several column volumes of 30 mM phosphate buffer. The enzyme was eluted using a 0 - 0.3 M NaCl gradient in 30mM phosphate buffer (1 litre total volume). Fractions that contained around 30 % pure L-mdh were pooled and dialysed against a 10-fold greater volume of 30 mM phosphate buffer.

4.3.3 Quaternary ammonium (Q) sepharose column (Sigma)

A 10 x 2.5 cm Q Sepharose anion exchange column (functional group, - $CH_2N^+(CH_3)_3$) was poured The protein fractions were then loaded onto the column, which had previously been equilibrated with 30 mM phosphate buffer. A 0-0.3 M NaCl gradient in 30 mM phosphate buffer (600ml total volume) was used to elute the protein. Fractions containing roughly 50 % pure L-mdh were pooled and dialysed again as before in 30 mM phosphate. To concentrate the protein solution, the pooled fractions were loaded onto a small DEAE cellulose column (3 x 3 cm) and immediately eluted with 150 mM phosphate buffer.

4.3.4 S300-HR Sephacryl gel filtration column (Sigma)

The concentrated protein solution was loaded onto an S300 sephacryl column (100 cm x 2.5 cm) which had previously been washed with 10 mM Tris.HCl buffer (pH 7.5 *I* 0.1). The protein was eluted after washing with 1litre of buffer and fractions containing 90-100 % pure L-mdh were saved and frozen in liquid nitrogen.

Table 4.1 Purification table of L-mdh

The purity of each fraction was determined by measuring the ratio of the peak heights at $A_{269\,nm}$ (total protein) and $A_{423\,nm}$ (L-mdh reduced haem Soret peak). A pure protein solution has an A_{269}/A_{423} ratio of 0.5. Figure 4.3 shows the visible absorption spectra of pure oxidised and reduced L-mdh. (1,2, Errors for these data are quite large, ~10%).

STEP	Total protein (mg)/ per litre of culture[1]	L-mdh (mg)/per litre of culture[2]	Yield of L-mdh (%)[3]	Purification (fold)[4]
Cell lysate	~ 1000	~ 140	100	1
DEAE cellulose	~750	~110	80	1.1
DEAE Sephacel	~ 250	~ 80	60	2.3
Q Sepharose	~100	~ 50	40	3.6
S300 Sephacryl	~ 20	~20	15	7.1

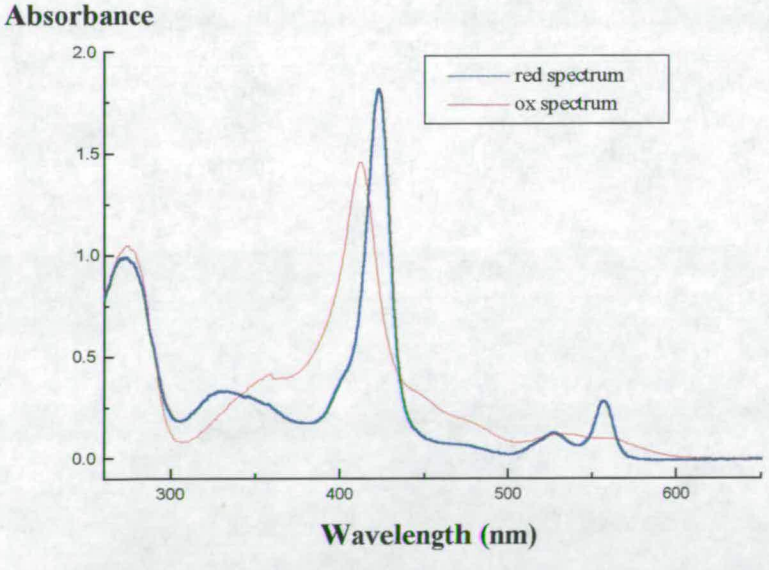

Figure 4.3 The oxidised and reduced spectra of pure L-mdh ε (413nm) = 129500 $M^{-1}cm^{-1}$ ε (423 nm) = 183000 M^{-1} cm^{-1} (Pajot and Groudinsky, 1970)

Figure 4.4 SDS PAGE gel of purified L-mdh Lane 1 protein markers Lane 2 Approx. 20 μg L-mdh (apparent M_r = 59 kDa)

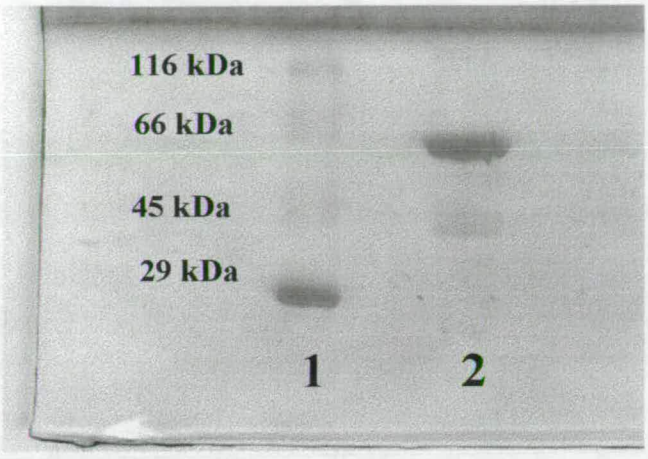

4.4Steady-state kinetic properties of L-mdh

4.4.1 Introduction

Like L-ldh, L-mdh catalyses a two electron oxidation and is capable of transferring electrons to a wide variety of electron acceptors. The turnover of the enzyme has been measured under steady-state conditions by monitoring the reduction of an external electron acceptor under saturating conditions. The physiological electron acceptor of L-mdh and L-ldh is cytochrome *c*. Assays were carried out using either this electron acceptor, or the artificial electron acceptor, potassium ferricyanide. In order to compare these results to the previously determined kinetic data for L-ldh, all steady-state experiments were carried out under the same conditions as those for L-ldh; that is, at 25 ± 0.1°C, in 10 mM Tris.HCl at pH 7.5 (*I* 0.1). The kinetic parameters for substrate were determined by carrying out assays at varying substrate concentrations. All the data were analysed by non-linear least-squares regression using the Michaelis-Menten equation (Section 2.8)

Tables 4.2 to 4.5 present the results of the steady state kinetic measurements of L-mdh using L-mandelate, DL-[2-^{1}H]-mandelate and [2-^{2}H]-mandelate as substrates, and with ferricyanide and cytochrome *c* as electron acceptors. These

results are compared to previously reported values for the enzyme isolated from *R. graminis.*

4.4.2 Ferricyanide as electron acceptor

From the data in table 4.2, it is clear that the recombinant form of L-mdh can effectively turn over L-mandelate, judged from the k_{cat} value with ferricyanide as electron acceptor (500 ± 25 s^{-1}). This value is higher than the values previously obtained for native (109 ± 3 s^{-1}, Smekal *et al.*,1993) and partially purified recombinant enzymes (351 ± 9 s^{-1}; R. Illias, 1997). This is probably due to significant activity losses during the purification procedures of these two enzymes, probably because of flavin loss which will be favoured at lower enzyme concentrations and by the longer time-scale of earlier purification protocols.

The kinetic results for the oxidation of L-mandelate and L-lactate by L-mdh or L-ldh with ferricyanide as electron acceptor are presented in table 4.2. Values of k_{cat} for the enzymes with their primary substrates are of a similar magnitude. The K_m value for the recombinant form of L-mdh is also within good agreement with the values obtained with both the native (0.27 ± 0.03 mM) and partially purified L-mdh (0.35 ± 0.03 mM) and again are within the same range as L-ldh with L-lactate, suggesting that there is little difference between the substrate binding mechanisms of the two enzymes with their physiological substrates. Furthermore, neither enzyme showed any ferricyanide concentration dependence above 100 μM ferricyanide. In each assay saturating concentrations of potassium ferricyanide (1mM) were used.

As described previously, (section 3.5), L-mdh and L-ldh can turnover each other's substrate only at very low rates. In the case of L-ldh, this is thought to be due to steric interference between the side groups of certain active site residues with the aromatic side group of mandelate.

4.4.3 Steady-state kinetic isotope effect values (with D. Robertson)

It is frequently observed that the rate of a reaction in which hydrogen is being transferred is several times faster than that of the corresponding reaction in which deuterium is transferred. The most important reason for this 'deuterium isotope effect' (k_H/k_D, see section 2.7) is due to the difference in the zero-point energies of bonds to hydrogen and to deuterium. Since the size of a bond's zero-point energy is dependent on the vibrational frequency (ν) of the bond, and ν is proportional to $1/\sqrt{mass}$, the zero point energy of the CD bond will be lower. This difference in energy minima is approximately 5 $kJmol^{-1}$ (Jencks, 1969). However the undeuterated and deuterated compounds reach the same energy *maximum*, which corresponds to the transition state of the reaction. This difference in Δ E corresponds to a difference in rate of sevenfold at room temperature. Therefore the deuterium isotope effect can be used as evidence for or against the occurrence of hydrogen transfer in the rate-limiting step of a reaction, with the size of the change in rate giving us an idea of the extent of the breaking of the CH bond in the transition state. For example, in wild type L-ldh, using L-lactate ^2H labelled at the C2 position, a kinetic isotope effect of 5 was obtained (Pompon *et al.*, 1980). Thus, cleavage of the H-C2 bond of L-lactate does rate limit the oxidation of lactate. Previous steady-state experiments with native L-mdh (Smekal *et al.*, 1993) obtained no significant isotope effect and this was interpreted as clear evidence that the transition states in the two enzymes were different. In this work, the steady state turnover of DL-[2-^2H] mandelate by the recombinant form of L-mdh was measured. Because the deuterated form of mandelate was a racemic mix of the D- and L- isomers , the steady state turnover of DL-mandelate was also measured (D-mandelate is a competitve inhibitor of L-mdh with a K_i value of 1.98 mM, Yasin and Fewson, 1993). From the data presented in table 4.3, it can be seen that L-mdh has almost the same deuterium kinetic isotope effect as L-ldh.

Figure 4.5 A Michaelis-Menten plot for L-mdh with L-mandelate.

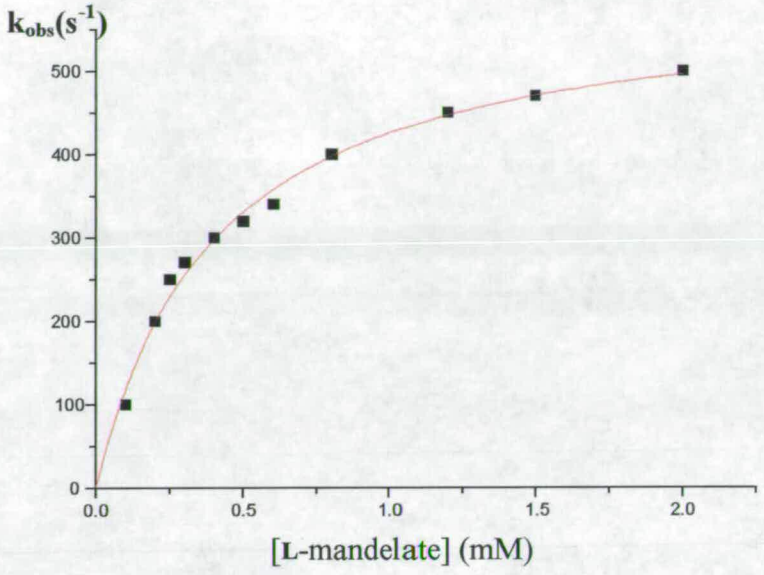

Table 4.2 Steady-state kinetic parameters for L-mdh and L-ldh with ferricyanide as electron acceptor All experiments were carried out at 25.0 ±0.1°C in Tris.HCl buffer, pH 7.5, (*I* 0.10). Values for k_{cat} represent the rates of reduction, at saturating substrate concentration, of 1 mM ferricyanide in electrons transferred / s per molecule of enzyme. Errors quoted represent standard deviations from a non-linear least-squares fit

	L-ldh	**L-mdh**
k_{cat} (s^{-1}) **L-lactate**	400 ± 10	0.50 ± 0.10
K_m (mM)	0.49 ± 0.05	0.40 ±0.05
k_{cat} (s^{-1}) **L-mandelate**	0.02 ± 0.01	550 ± 25
K_m (mM)	see section 3.*	0.35 ± 0.02

Table 4.3 The steady state kinetic isotope effect values for L-mdh and L-ldh with ferricyanide (conditions as above)

	L-mdh	L-ldh
^1H substrate k_{cat} (s^{-1})	300 ± 5	400 ± 10
^2H substrate k_{cat} (s^{-1})	88 ± 4	86 ± 5
^1H substrate K_m (mM)	0.47 ±0.03	0.49 ± 0.05
^2H substrate K_m (mM)	0.53 ± 0.05	0.76 ± 0.06
KIE	**3.5 ± 0.2**	**4.7 ± 0.4**

4.4.3 Cytochrome *c* as the electron acceptor

The ferricyanide reduction data suggests that there are no major differences between L-mdh and L-ldh with their respective substrates when this molecule is used as electron acceptor. However, do the two enzymes behave differently with their physiological electron acceptor, cytochrome *c* ? Table 4.4 presents the results of the steady-state turnover of L-mdh and L-ldh with cytochrome *c*. The values for k_{cat} and K_m are again within the same range as the values obtained with L-ldh, suggesting that both enzymes interact with cytochrome *c* in a similar way. Both enzymes show a dependence of reaction rate on the concentration of cytochrome *c*. The K_m values for cytochrome *c* seen for L-mdh and L-ldh are identical (10 ± 1μM). This is consistent with both enzymes interacting with cytochrome *c* in the same way.

The deuterium KIE value for L-mdh with cytochrome *c* is similar to the reported value for L-ldh (table 4.5) Values for the KIEs of L-mdh and L-ldh are both smaller than the values obtained with ferricyanide indicating that for both enzymes, there are electron-transfer steps following the H-C2 cleavage which also limit the turnover rate of the enzyme.

Table 4.4 Steady-state kinetic parameters for L-mdh and L-ldh with cytochrome *c* as electron acceptor Assays performed at 25.0 ± 0.1°C in Tris.HCl buffer, pH 7.5 *(I* 0.10). Horse heart cytochrome *c* was used as electron acceptor, at a concentration of 35 μM.

	L-mdh	**L-ldh**
k_{cat} (s^{-1}) **L-lactate**		207 ±10
K_m (mM)		0.24 ±0.04
k_{cat} (s^{-1}) **L-mandelate**	225 ±15	
K_m (mM)	0.35 ±0.05	

Table 4.5 The steady-state kinetic isotope effect values with cytochrome *c* (conditions as above)

	L-mdh	**L-ldh**
^1H substrate k_{cat} (s^{-1})	155 ± 5	207 ± 10
^2H substrate k_{cat} (s^{-1})	92 ± 10	70 ±10
^1H substrate K_m (mM)	0.78 ± 0.02	0.24 ± 0.04
^2H substrate K_m (mM)	1.33 ± 0.10	0.48 ± 0.10
KIE	**1.68 ± 0.3**	**3.0 ± 0.6**

4.5 Pre-steady-state kinetic parameters for L-mandelate oxidation by L-mdh

4.5.1 Introduction

Under pre-steady-state conditions, in the absence of any external electron acceptors, the full reduction of L-mdh is expected to proceed as illustrated in figure 1.11. Stopped-flow spectrophotometry has been used previously to monitor the reduction of L-ldh by L-lactate. Miles *et al.*, (1992) determined the rate constants for this process by monitoring FMN reduction at an isosbestic in the absorption spectrum of b_2-haem (438.3 nm) and haem reduction at 557 nm where FMN absorbance is negligible. These experiments were carried out as described in section 2.9. The rate constants for reduction of the flavin and haem prosthetic groups of L-mdh by ^{1}H and ^{2}H-mandelate have also been determined using this method (with D. Robertson).

4.5.2 FMN reduction

A typical L-mdh FMN reduction trace is illustrated below (figure 4.7). The kinetic traces can be satisfactorily analysed as the sum of two exponential functions and a model has been proposed to explain the reduction process (Capeillere-Blandin *et al.*, 1975). The rapid first phase is a two step process, in which two electrons from the substrate reduce the flavin molecule and then redistribute between the flavin and haem (see section 1.7.10). The slower second phase is due to the entry of the third electron per subunit, which is made possible by intersubunit electron transfer (see figure 4.5) generating fully reduced enzyme. The rate constant for L-ldh FMN reduction (the fast phase rate) is $604 \pm 60\ s^{-1}$. The rate constant for the reduction of the L-mdh flavin, is $280 \pm 20\ s^{-1}$, approximately 50 % of the value obtained with L-ldh. The K_m values for both enzymes with their respective substrates are, within error, the same.

The reason for the unexpectedly low rate of L-mdh FMN reduction was at first thought to be due to the protein sample containing a heterogenous mix of flavin free and fully incorporated enzyme, which would lead to lower observed rates. However, this was obviously not the case since the enzyme contained a full

The reason for the unexpectedly low rate of L-mdh FMN reduction was at first thought to be due to the protein sample containing a heterogenous mix of flavin free and fully incorporated enzyme, which would lead to lower observed rates. However, this was obviously not the case since the enzyme contained a full complement of flavin (determined by separating denatured protein and FMN on a gel filtration column and measuring the haem and flavin concentration spectrophotometrically). Furthermore, the flavin reduction experiments were repeated at different enzyme concentrations (not shown). Decreasing the L-mdh concentration had no effect upon the rate constants for flavin reduction, implying that none of the phases observed were due to interprotein electron transfer.

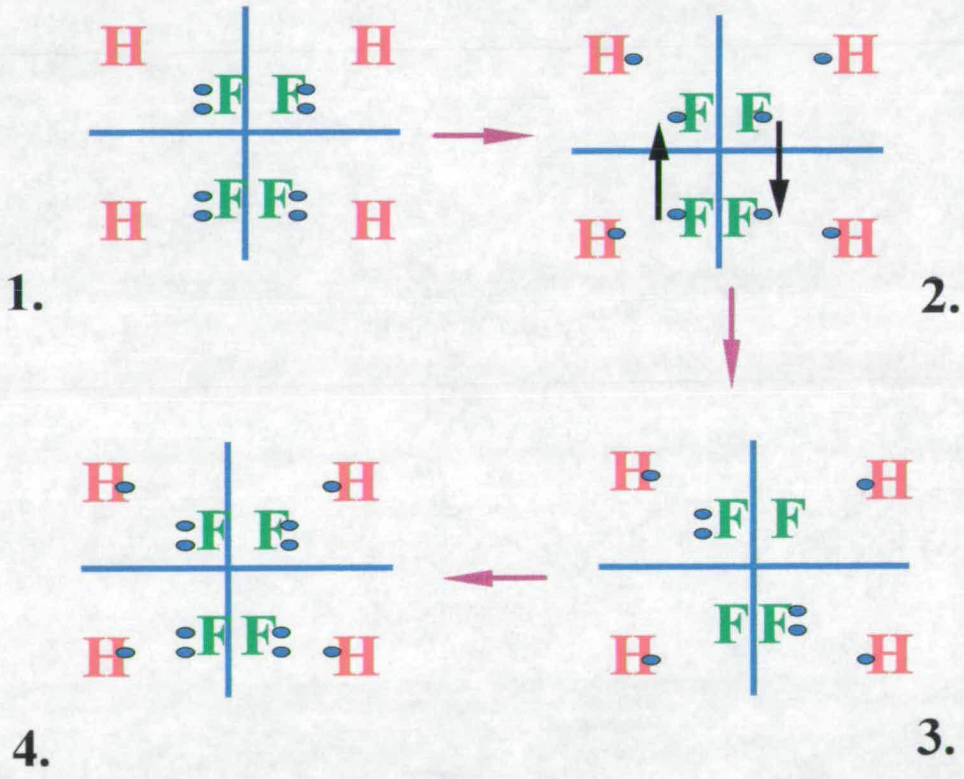

Figure 4.5 Schematic representation of the reduction of the L-mdh tetramer

Step 1. Reduction of the FMN molecules by mandelate

Step 2. Electron transfer between flavin and haem groups

Step 3. Intersubunit electron transfer between flavin semiquinones

Step 4. Full reduction of the L-mdh tetramer by two molecules of mandelate

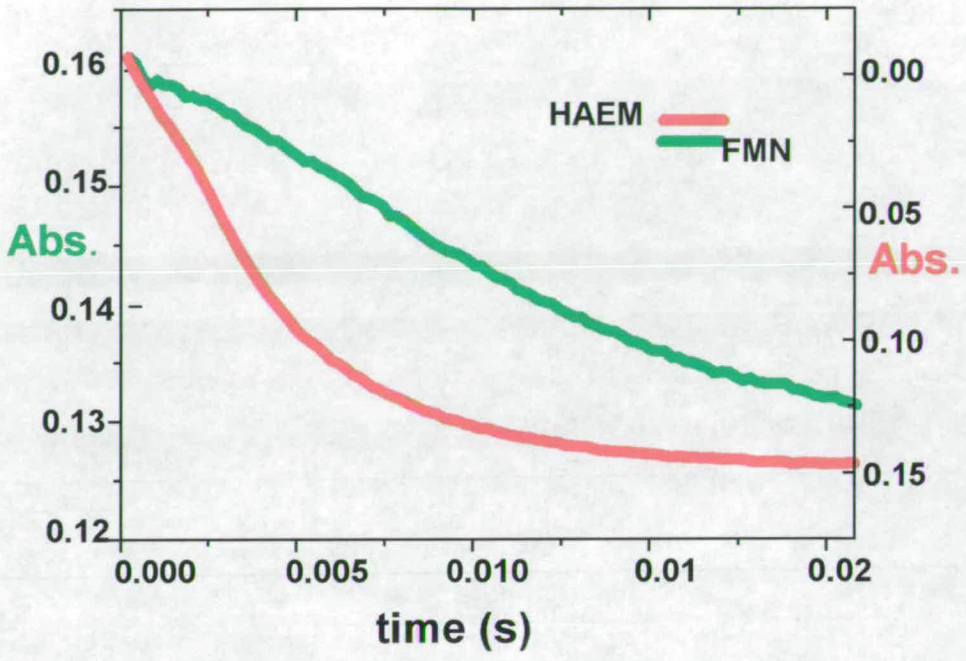

Figure 4.6 Stopped-flow traces for FMN (green) and haem (red) reduction of L-mdh collected at 438.3 nm and 557 nm respectively. Both traces (averages of 5) were generated on mixing 10 μM enzyme with 10 mM L-mandelate in Tris. HCl buffer at 25°C.

Table 4.6 Pre steady-state kinetic parameters for the reduction of FMN in L-mdh and L-ldh. (Values for L-ldh from Miles, 1992)

	L-ldh	**L-mdh**
k_{obs} (s^{-1}) **L-lactate**	604 ± 60	
K_m (mM)	0.84 ± 0.20	
k_{obs} (s^{-1}) **L-mandelate**		280 ± 20
K_m (mM)		0.35 ±0.10

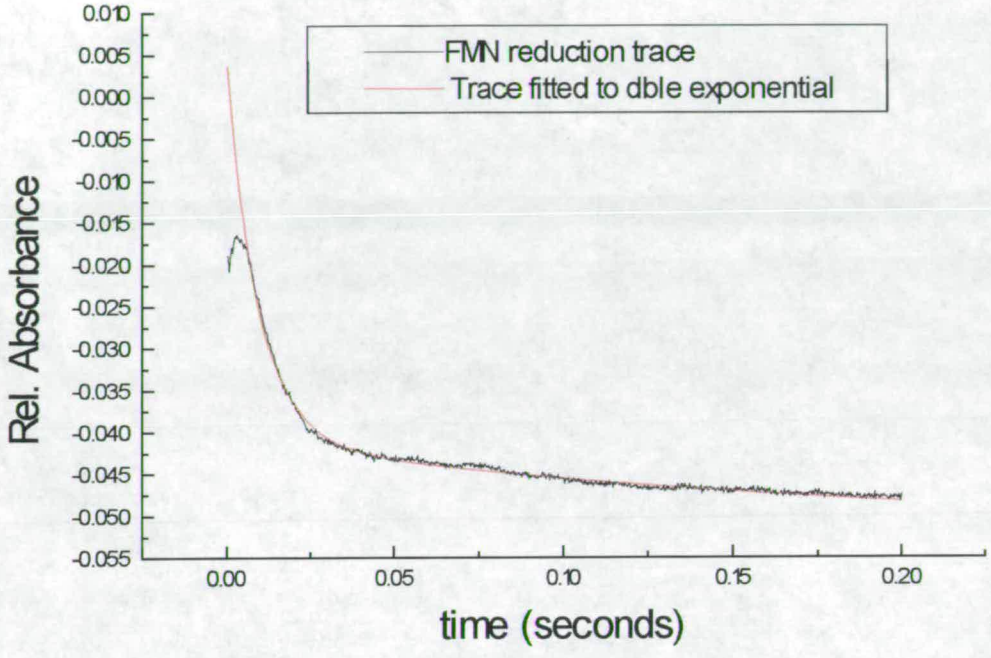

Figure 4.7 FMN reduction trace fitted to a double exponential equation Traces were generated by mixing 10 μM L-mdh with 10 mM L-mandelate in Tris.HCl buffer at 25°C

Table 4.7 Pre steady-state kinetic isotope effects for the reduction of FMN in L-mdh and L-ldh

	L-mdh	**L-ldh**
^{1}H substrate k_{cat} (s^{-1})	210 ± 10	604 ± 60
^{2}H substrate k_{cat} (s^{-1})	43 ± 5	75 ± 5
^{1}H substrate K_m (mM)	0.47 ± 0.10	0.84 ± 0.20
^{2}H substrate K_m (mM)	0.35 ± 0.05	1.33 ± 0.28
KIE	**4.9 ± 1.0**	**8.1 ± 1.4**

The flavin reduction experiments were repeated using DL[2-^{1}H]- and DL[2-^{2}H-mandelate (table 4.7). The measured deuterium isotope effect value is again within the same range as that for L-ldh. The magnitude of this value suggests that during the process of FMN reduction, H abstraction from C2 of L-mandelate is almost entirely rate limiting. This value is higher than the value obtained after the steady state turnover of cytochrome *c*, implying that there are other steps in the catalytic cycle of L-mdh which contribute to the rate limitation of the catalytic turnover rate.

4.5.3 Haem reduction

A typical L-mdh haem reduction trace is shown in Fig 4.8 The k_{cat} values for the haem reduction of L-ldh and L-mdh are similar, and are in good agreement with the values obtained with the steady state kinetics. However, this value for L-mdh haem reduction ($605 \pm 50\ s^{-1}$) is significantly larger than the rate of FMN reduction, a curious result since electrons have to pass through the flavin molecule before they reach the haem. It is nonsensical to assume that the electrons speed up before they reach the haem molecule. It seems more likely that the reduction of the flavin molecules of the L-mdh tetramer is not observed spectrophotometrically until after the intersubunit electron transfer and the disproportionation of flavin semiquinones (see figure 4.5). This would be the case, if the electron transfer rate between the flavin and haem molecule was extremely rapid.

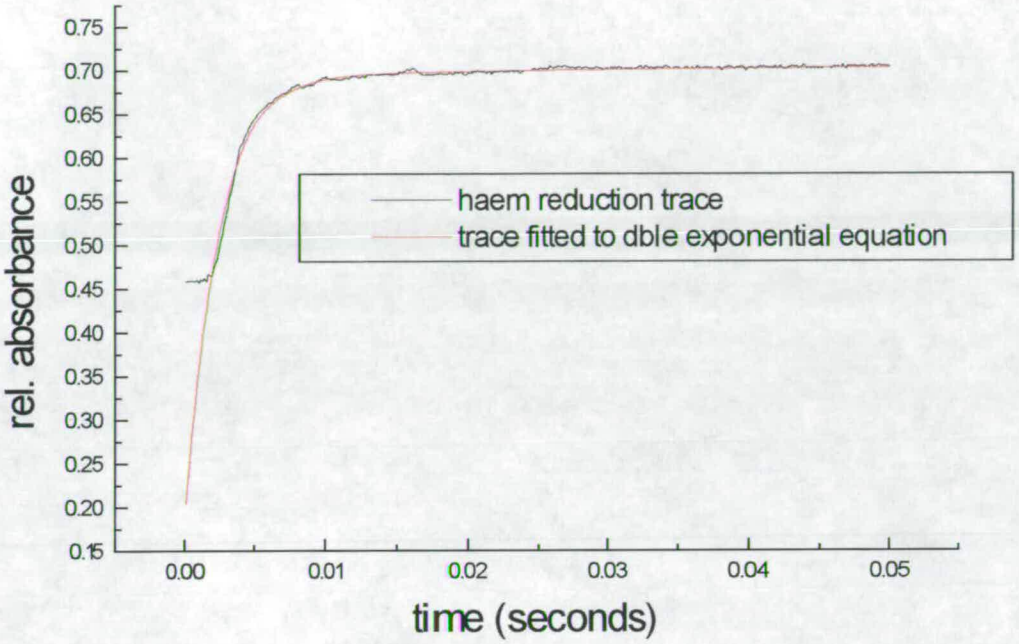

Figure 4.8 Stopped flow haem reduction trace of L-mdh collected at 557 nm. Traces were generated by mixing 10 μM L-mdh with 10 mM L-mandelate in Tris. HCl buffer at 25°C

Table 4.8 Pre-steady state L-mdh and L-ldh haem reduction

	L-ldh	**L-mdh**
k_{obs} (s^{-1}) **L-lactate**	445 ± 50	
K_m (mM)	0.53 ± 0.05	
k_{obs} (s^{-1}) **L-mandelate**		605 ± 50
K_m (mM)		0.39 ± 0.1

Table 4.9 Pre steady-state kinetic isotope effects for the reduction of haem in L-mdh and L-ldh

	L-mdh	**L-ldh**
^{1}H substrate $k_{obs}(s^{-1})$	505 ± 20	445 ± 50
^{2}H substrate k_{obs} (s^{-1})	115 ± 10	71 ± 5
^{1}H substrate K_m (mM)	0.49 ± 0.1	0.53 ± 0.05
^{2}H substrateK_m (mM)	0.56 ± 0.05	0.68 ± 0.05
KIE	**4.39 ± 0.5**	**6.3 ± 1.2**

4.5.4 Cytochrome *c* reduction by L-mdh

The reduction of cytochrome *c* by L-mdh was also measured using stopped-flow spectrophotometry (as described in section 2.9.2). A substoichiometric amount of cytochrome *c* (0.75 μM) was mixed with reduced L-mdh (1.5-15 μM after mixing) and the increase in absorbance at 416.5 nm (an L-mdh haem isosbestic) monitored. The bimolecular rate constants for cytochrome *c* reduction are shown in table 4. 10 Figure 4.9 shows plots of k_{obs} for cytochrome *c* reduction against L-mdh concentration fitted to a linear regression analysis. These data measure the formation of a catalytically competent electron transferring complex between L-mdh and cytochrome *c* and do not reflect the rate of electron transfer from L-mdh haem to cytochrome *c* haem in the preformed complex. The second order rate constant is within the same order of magnitude as L-ldh. The cytochrome *c* reduction traces fitted well to monophasic exponential equations for both L-mdh and L-ldh as expected for a one electron transfer reaction between b_2-haem and cytochrome *c*.

Table 4.10 Reduction of cytochrome *c* by reduced L-mdh / L-ldh Horse heart cytochrome c (0.75 μM) was mixed with fully reduced (10 mM L-mandelate) L-mdh Traces collected at the L-mdh isobestic of 416.5 nm

	2nd order rate constant for cytochrome *c* reduction
L-mdh	$41.5 \pm 2\ \mu M^{-1}\ s^{-1}$
L-ldh (S.Daff, 1996)	$34.8 \pm 0.9\ \mu M^{-1}\ s^{-1}$

Figure 4.9 A plot of the rate of cytochrome c reduction against concentration of L-mdh. The gradient gives the second-order rate constant for this process

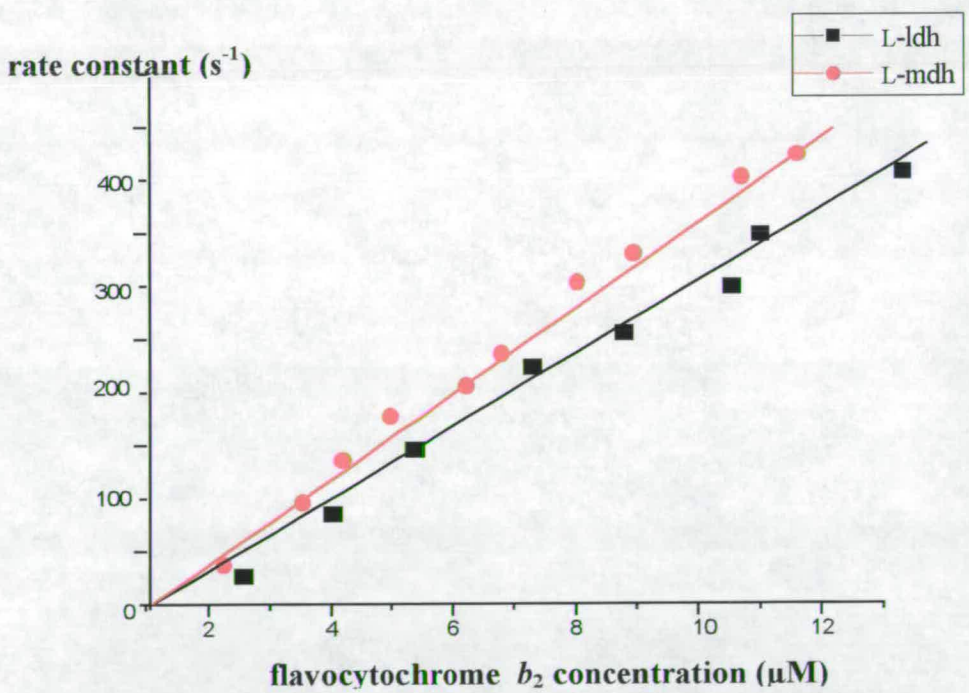

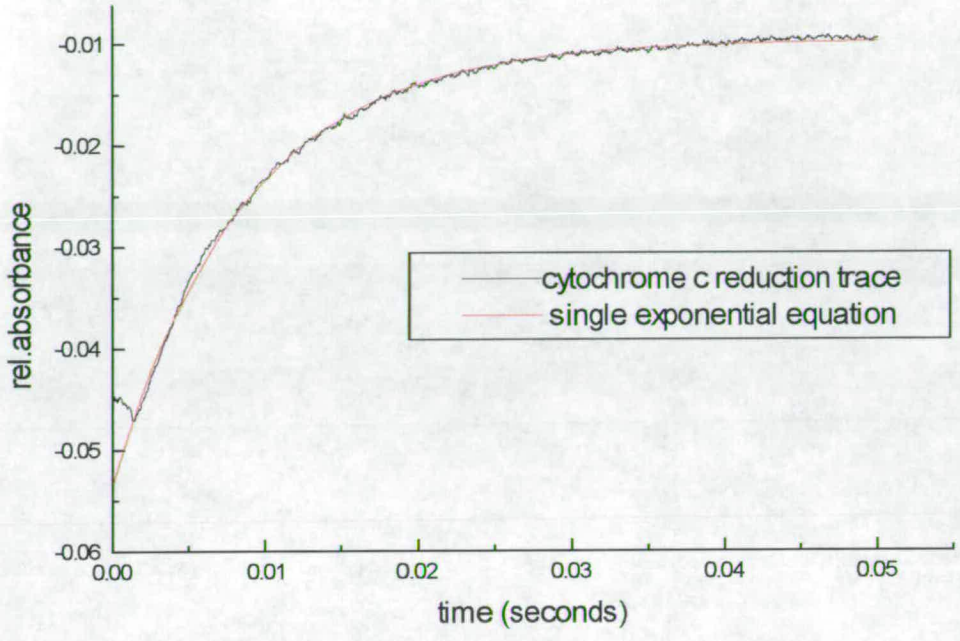

Figure 4.10 Reduction of cytochrome *c* by10 μM L-mdh Horse heart cytochrome *c* (0.75 μM) was mixed with fully reduced (10 mM L-mandelate) L-mdh. Trace collected at the L-mdh isosbestic of 416.5 nm

4.10 Haem midpoint potential of L-mdh

It seemed possible that the reason for the different observed flavin and haem reduction rates was due to differences in the haem midpoint redox potential of L-mdh compared to the corresponding midpoint potential in L-ldh. The midpoint potential of a redox couple is a measure of the tendency of a molecule to donate or accept electrons. This value gives an indication of the relative stability of the oxidised and reduced states. If the haem group of L-mdh was a better electron acceptor then this would have a more positive redox potential than the L-ldh haem. The method described by Dutton (1978) coupled with spectrophotometry was used to measure the haem midpoint potential. Measurements were carried out as described in section 2.10.

Table 4.11 The redox potentials of haem groups of L-mdh (L-ldh haem group, Miles *et al*, 1992)

	L-mdh	L-ldh
haem	-10 ± 2 mV	-17 ± 3 mV

The enzyme has a slightly more positive midpoint potential (by about 7 mV) than the value for L-ldh haem. However, the difference in midpoint potentials is too small to account for the different observed flavin reduction rates of the two enzymes. This result is consistent with the proposal that the haem domains of L-mdh and L-ldh are virtually identical. In order to compare the flavin domains of L-mdh and L-ldh without any interference from the haem groups, the flavin domain of L-mdh has been cloned and expressed in *E. coli*. This is described further in chapter 5.

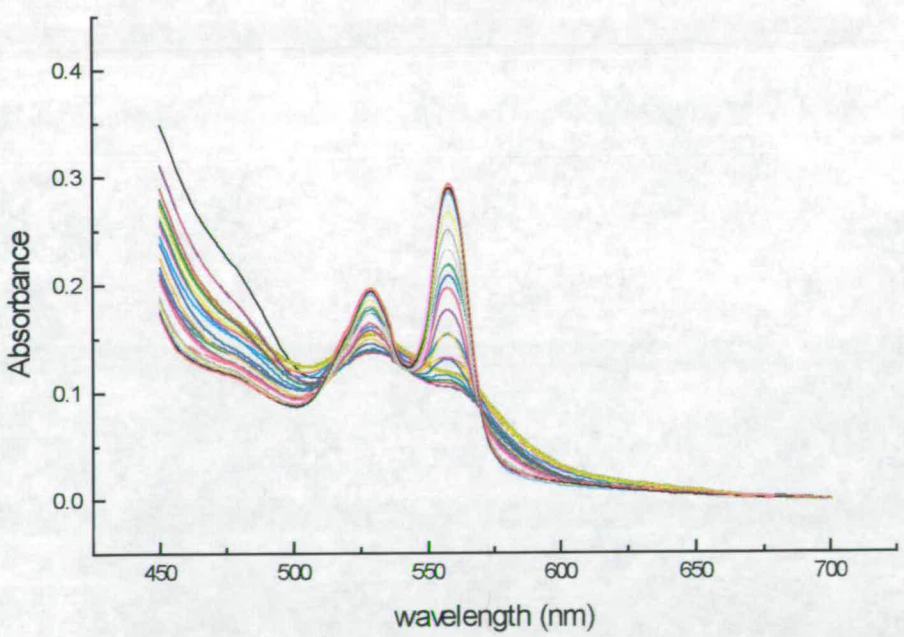

Figure 4.11 Redox titration of the L-mdh haem domain, observing absorbance changes at 557nm.

Figure 4.12 Modified Nernst plot of electrode potential *vs.* Mean Abs (570-540 nm)

See section 2.10.4

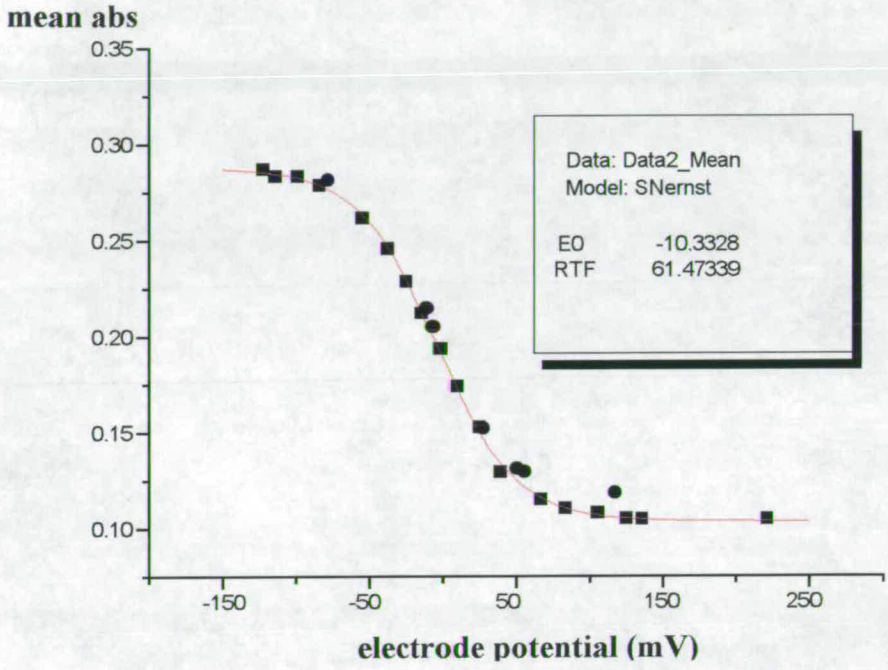

4.7 Conclusion

The recombinant form of the L-mdh enzyme has been successfully overexpressed in *E. coli*. The enzyme has been purified to homogeneity, and the kinetic parameters of the enzyme calculated.The enzyme functions as an L-mandelate dehydrogenase with either ferricyanide or cytochrome *c* as the electron acceptor, at rates comparable to *S.cerevisae* L-ldh with L-lactate. The steady-state and pre steady-state KIE values of the two enzymes are also similar, which suggests that removal of the substrate αH bond rate limits the overall turnover rate of both enzymes to the same degree. The haem midpoint potentials of both enzymes are also, within error, the same. The two enzymes differ dramatically, however, in their pre steady-state FMN reduction rates. This is investigated further in chapter 5.

Chapter 5: L-mandelate dehydrogenase flavin domain

Cloning, expression, purification and characterisation of the flavin domain of L-mandelate dehydrogenase.

5.1 Introduction

Residues 100-486 of the L-mdh amino acid sequence comprise the flavinmononucleotide containing domain. As described earlier (section 1.7.7), the location of the enzyme's active site is within the flavin domain. In the intact enzyme, the first step of the electron transfer pathway of L-mdh is from bound L-mandelate to FMN, oxidising mandelate to phenylglyoxalate and reducing FMN (a two-electron transfer step). The reduced FMN then transfers each electron individually to the haem, from which electrons are transferred to cytochrome *c*. The FMN cofactor is able to act as a mediator between the two electron transfer reaction (mandelate→FMN) and the one electron transfer reaction (haem→cyt *c*) because of its ability to exist as a semiquinone, (see section 1.6).

In the intact enzyme, the flavin absorbance is swamped by the much more intense haem absorbances so that it is extremely difficult to monitor the spectroscopic properties of the flavin. Hence, in order to study the properties of the flavin molecule in L-mdh more closely it would be useful to separate the flavin domain from the rest of the protein In the following chapter, the expression, purification and kinetic characterisation of the L-mdh flavin domain is described.

5.2 Isolation of the flavin binding domain

There are several ways to study in isolation the flavin domain of L-mdh: denaturation of the holoenzyme followed by reconstitution in the presence of FMN; treatment with proteases; or cleavage of the L-mdh coding sequence by restriction enzymes. The first method had been previously used (Iwatsubo *et. al* 1977) in an

attempt to isolate the flavin binding domain of L-ldh. However, this approach was rejected after it appeared that there were conformational differences between the native and reconstituted forms of L-ldh. Cleavage of the L-ldh flavin domain with proteases has also been attempted (Gervais *et al.*, 1980) however, this region of the protein contains a proteinase-sensitive area (known as the proteolytically-sensitive, or disordered loop, residues 293-314) which resulted in the flavin domain being separated further into two fragments. More recently, however the flavin domain of L-ldh has been successfully isolated after independent expression of a modified L-ldh coding sequence. (Balme *et al.*, 1995). A similar approach was used to isolate the flavin domain of L-mdh.

5.3 Isolation of L-mdh fdh DNA

The L-mdh coding sequence was modified by site directed mutagenesis as described previously (see section 2.3), using the oligonucleotide GAT TGG CGG CGA ATT CAT GGG CAA GAA TGC. This oligonucleotide introduces an *Eco*RI cleavage site between the sequences encoding the haem and flavin containing domains and places an ATG inititation codon immediately preceding the codon for Gly99, the first residue of the flavin domain. Resulting clones were screened for the introduction of the *Eco*RI site and the entire flavin domain sequenced to ensure that there were no further, unwanted mutations introduced.

DNA seq	**ATT**	**GGC**	**GGC**	**GAA**	**TTC**	**ATG**	**GGC**	**AAG**	**AAT**	**GCA**
amino acid seq	**I**	**G**	**G**	***Eco*RI**	**site**	**M**	**G**	**K**	**N**	**A**

HAEM domain **FLAVIN domain**

Figure 5.1 Gene modification used in the expression of the flavin domain of L-mdh in *E. coli*

Table 5.1 Oligonucleotide Primers used to sequence L-mdh fdh

Sequence 5′3′:	Name:	Priming position relative to start of L-mdh coding sequence:
AAGCAGCACCGCACGACGCC	LMDH1	212-232
GAGCTGAGTAGAAGCAG	LMDH2	239-377
CGAGGTGACCAAGATTG	LMDH3	827-843
GACACGACTTGCAAGAT	LMDH4	1479-1463
ATCTTGCAAGTCGTGTC	LMDH5	1463-1479
TGCCGACCTTGCGAAG	LMDH6	474-489

5.4 Cloning and expression of L-mdh fdh

The DNA encoding the flavin containing domain was transferred to the expression vector pRC23 as an *Eco*RI-*Hin*dIII fragment. The recombinant plasmid was transformed into *E. coli* JM109 cells and transformants were grown overnight at 37°C, with shaking, until the cells reached stationary phase. As with the intact enzyme, cells were grown in Terrific broth medium with ampicillin. The cells were harvested by centrifugation in a Sorvall RC-5B centrifuge with a GS3 rotor at 5000 ***g*** for 10 minutes. The resulting wet pellet of cells was yellow in colour.

5.5 Cell lysis and column chromatography

The pellet of cells was snap-cooled in liquid nitrogen and resuspended in 0.1 M phosphate buffer (pH 7) + EDTA. The solution was centrifuged (39000 ***g***, 10 minutes) to remove insoluble cell debris and unlysed cells.

A DEAE ion-exchange column

The isolated L-mdh flavin domain was purified by column chromatography using DE-52 (Whatman), the same microgranular cellulose anion exchange material used during the purification of the intact enzyme. Cell lysate was loaded onto a DE52 column (10 cm x 4.5 cm), which had been previously equilibrated in 0.1 M phosphate buffer (pH7). The protein was eluted after washing the column with several column volumes of buffer. Protein fractions which were yellow in colour were immediately collected. The eluted fracions of L-mdh fdh had a UV/Vis ratio (A_{269nm}/A_{450nm}) of around 15.

B DEAE sephacel column

The eluted fractions were pooled and dialysed for ~2hours against a 10 fold greater volume of 30 mM phosphate. The protein solution was then loaded onto a 20 x 3 cm DEAE sephacel column which had previously been equilibrated with 30 mM phosphate buffer. The enzyme was eluted using a 30 mM phosphate - 0.3 mM NaCl in 30mM phosphate buffer gradient (1 litre total volume). Fractions with a A_{269nm}/A_{450nm} ratio of ~7.5 were pooled, adjusted to 80 % ammonium sulphate saturation and spun at 39000 ***g*** for 10 minutes.

C Sephadex G25 gel filtration column

The ammonium sulphate pellet was redissolved in 0.01 M Tris buffer (pH 7.5) and loaded onto a G25 20 x 2 cm gel filtration column. This final column desalts the protein solution. The eluted protein was in aliquoted in liquid nitrogen and frozen.

Table 5.2 The purification of L-mdh fdh (1,2 The errors for this set of data are quite large, approx.10%)

STEP	Total protein (mg) per litre of culture[1]	L-mdh fdh (mg) per litre of culture[2]	Yield of L-mdh (%)[3]	Purification (fold)[4]
Lysate	~1000	~210	100	1
DE-52	~320	~144	69	2.1
Sephacel	~130	~115	55	4.2
G25	~100	~90	42	4.8

Figure 5.2 SDS PAGE gel of purified L-mdh fdh lane 1. Approx 30 μg L-mdh fdh. Apparent M_r 47000. Lane 2 protein markers

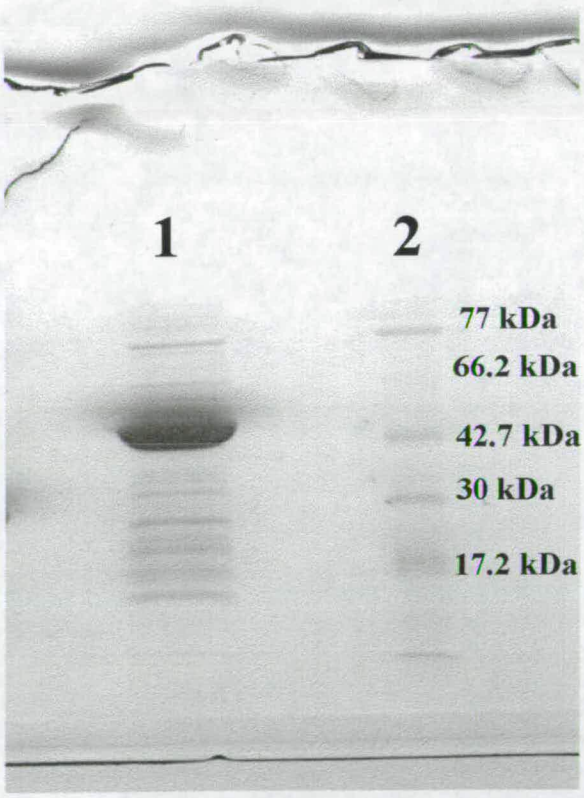

5.6 Native molecular weight determination

From SDS PAGE the monomer molecular weight of the L-mdh flavin domain was found to be ~47000. However, this does not resolve the question of whether the enzyme behaves as a tetramer in the cell. Determination of the molecular weight of native flavin domain (that is, not denatured as in SDS PAGE) was estimated using a sephacryl S300 column . A plot of V_e versus log (molecular weight), where V_e is the elution volume (volume at which the most active fraction is eluted) is linear (see section 2.6). The enzyme behaves as a species of M_r 210 000 on the gel filtration column. Therefore the native flavin binding domain of L-mdh behaves as a tetramer. This was expected, since the flavin domain of L-ldh also behaves as a tetramer.

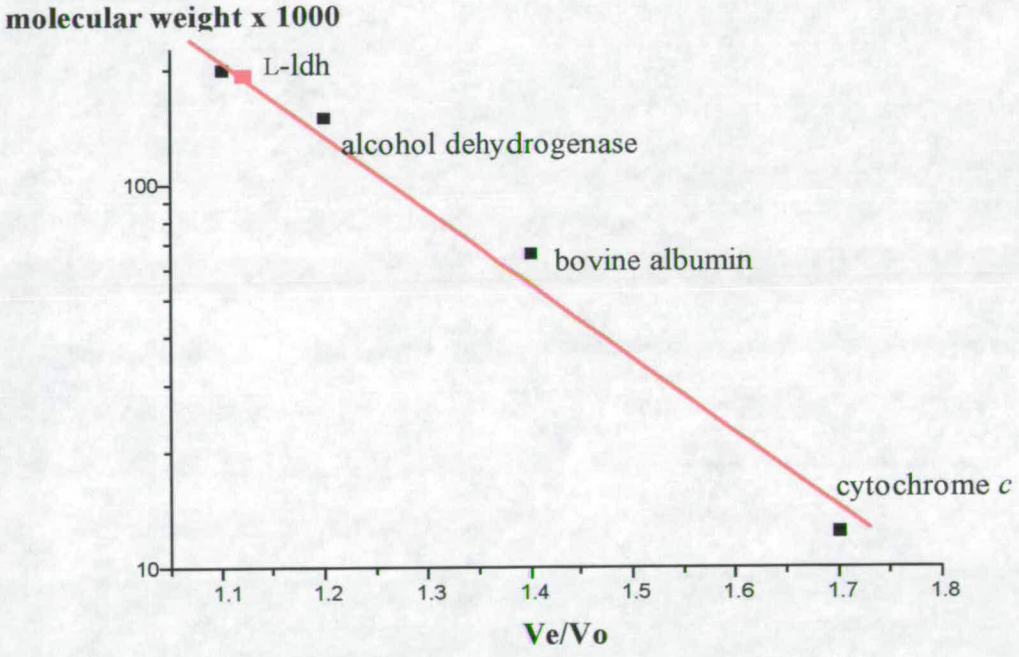

Figure 5.3 Calibration curve obtained using L-ldh (M_r 250 000), alcohol dehydrogenase (M_r 150 000) , bovine serum albumin (M_r 66 000) and horse heart cytochrome *c* (M_r 12 400). L-mdh fdh elutes at approximately the same volume as L-ldh.

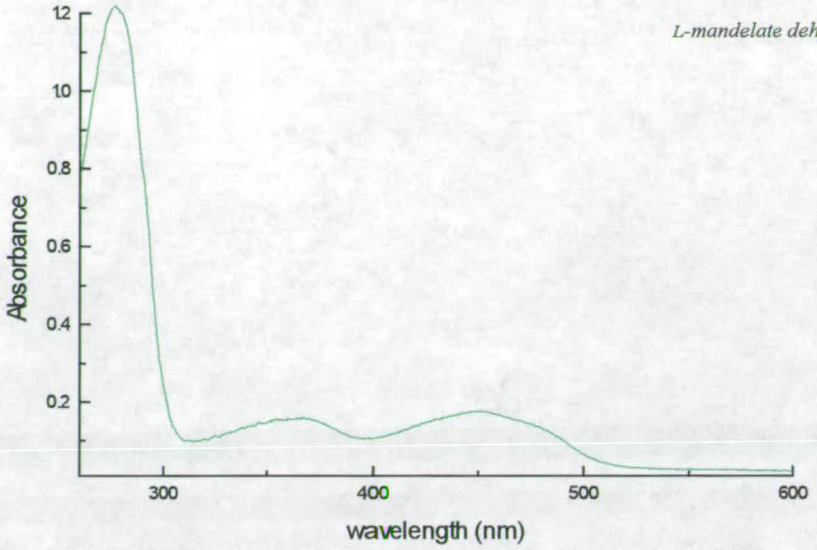

Figure 5.4 Visible absorption spectra of 18μM L-mdh fdh (oxidised) in 0.1 M Tris. HCl buffer: ε (453 nm) = 11100 M^{-1} cm^{-1}

5.7 Electronic absorption spectrum

The spectroscopic properties of the FMN group of L-mdh had been impossible to observe prior to the expression of L-mdh fdh due to the dominant haem absorbances in the visible spectrum. The contribution of the flavin absorbance in the visible spectrum of the intact enzyme was predicted by the sulphite-induced difference spectroscopy method described by Lederer (1978). Expression of the flavin domain in *E. coli* enables the spectrum to be measured directly.

The electronic absorption of the L-mdh flavin domain (oxidised) is shown in figure 5.4. The yellow oxidised enzyme has absorbance maxima at 375 and 450 nm. This spectrum is identical to that observed for L-ldh fdh, for which extinction coefficients have been published (Iwatsubo *et al.*, 1977).

5.8 Steady-state kinetic analysis

The isolated flavin domain of L-mdh has L-mandelate dehydrogenase activity when ferricyanide is used as the electron acceptor, but not when cytochrome *c* is used, despite the large driving force for the reaction. This result underlies the importance of the haem domain for the effective transfer of electrons to cytochrome *c*. The steady state parameters for the flavin domain and intact L-mdh with

ferricyanide are of similar magnitude, with the k_{cat} observed for the L-mdh fdh being around 90 % of that recorded for the intact enzyme. This slight decrease in activity is explained by the fact that in the intact enzyme, electrons can be transferred to ferricyanide from the haem as well as the flavin group. However, it thus appears that removal of the haem domain of L-mdh has a negligible effect on catalysis at the active site of the flavin domain. The L-mandelate:ferricyanide reductase activity of intact L-mdh is saturated at very low ferricyanide concentrations (K_m<<0.1 mM), so all steady state experiments were carried out using 1 mM ferricyanide. However, with the flavin domain of L-mdh, the observed rate of reaction appeared to be dependent on the ferricyanide concentration, with a K_m for ferriyanide of 0.34 mM. Similar behaviour had also been reported with the flavin domain of L-ldh. Consequently all experiments were carried out at 3.33 mM ferriyanide concentrations.

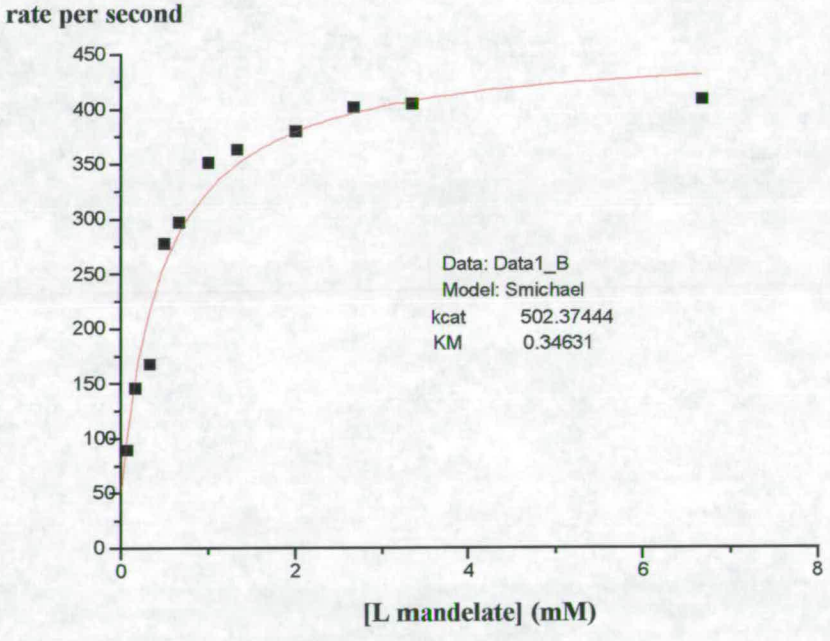

Figure 5.5 A Michaelis-Menten plot for L-mdh fdh with L-mandelate. 0.01 M Tris. HCl buffer, pH7.5 (*I* 0.10) was used in each experiment. 3.33mM ferricyanide was used as electron acceptor. All assays were carried out at 25 ± 0.1 °C.

	k_{cat} (s^{-1})	K_m (mM)
flavin domain	500 ± 50	0.35 ± 0.02
intact enzyme	550 ± 25	0.33 ± 0.05

Table 5.3 Steady state kinetic parameters for the isolated flavin domain and intact L-mdh with ferricyanide as electron acceptor (see section 2.8 for details)

The steady state parameters of the L-mdh flavin domain are also compared to those of the flavin domain of L-ldh. As in the intact enzyme, the k_{cat} and K_m values are of a similar magnitude for both enzymes.

Table 5.4 Steady state turnover of L-mdh fdh and L-ldh fdh with ferricyanide as electron acceptor (3.33mM ferricyanide for L-mdh fdh, 6 mM ferricyanide for L-ldh fdh) Values for L-ldh fdh taken from Balme *et al.*, 1995. See Fig 5.4 for details

	L-mdh fdh	**L-ldh fdh**
k_{cat} (s^{-1}) **L-lactate**		273 ± 6
K_m (mM)		0.22 ± 0.05
k_{cat} (s^{-1}) **L-mandelate**	500 ± 50	
K_m (mM)	0.33 ±0.05	

Table 5.5 Steady-state kinetic parameters of the flavin domains of L-mdh with DL-[2-^{1}H] and [2-^{2}H] mandelate Kinetic isotope effects were calculated by dividing k_{cat} values. L-ldh fdh/L-lactate values taken from Balme *et al.*, 1995(steady state and pre steady-state KIE values for L-ldh fdh, Balme *et al.*, 1995)

	L-mdh fdh	**L-ldh fdh**
^{1}H substrate k_{cat} (s^{-1})	316 ± 18	273 ± 6
^{2}H substrate k_{cat} (s^{-1})	99 ± 4	72 ± 2
^{1}H substrate K_m (mM)	0.74 ± 0.11	0.22 ± 0.05
^{2}H substrateK_m (mM)	0.79 ± 0.08	0.41 ± 0.06
KIE	**3.2 ± 0.32**	**3.8 ± 0.2**

5.8.1 Steady-state kinetic isotope effect values

These steady-state experiments were also repeated using DL-[2-^{2}H] and [2-^{1}H] mandelate as substrates, in order to determine whether there was a significant kinetic isotope effect after the enzyme had reduced ferricyanide (see table 5.5). As mentioned previously, in L-ldh the abstraction of the αH by the FMN limits the overall turnover of the enzyme and is the major rate limiting step at the level of flavin reduction. The KIE observed in the isolated flavin binding domain of L-ldh is 3.8 ± 0.2. This is slightly lower than the value obtained for the intact enzyme (4.7 ± 0.3), indicating that the αH abstraction is not solely rate limiting. A similar situation was found with the intact L-mdh and the isolated flavin domain, in which there is a decrease in KIE values from 3.5 ± 0.2 to 3.21 ± 0.32.

5.9 Stopped-flow kinetics

The reduction of the flavin domain of L-mdh by L-mandelate was measured by stopped-flow spectrophotometry. In the intact enzyme, biphasic kinetics were observed during the reduction of the FMN, with the slow second phase due to the subsequent reduction of the haem and the intersubunit electron transfer between flavins. In the isolated flavin domain, the reduction traces obtained fitted more accurately to a monoexponential equation. This can be explained by the fact that there are no haem groups to accept electrons, therefore the flavin moleules cannot be re reduced by mandelate. The rate constants and K_m values for the reduction of the FMN molecules in L-ldh and L-mdh are, within error, identical. The rate obtained for flavin reduction in L-mdh fdh is actually greater than the value obtained with intact L-mdh. This result confirms the previous suggestion (see section 4.5.2) that the real rate of flavin reduction in the intact enzyme was in fact much greater than the observed rate of only 280 ± 20 s^{-1}, (i.e) the observed rate is lower because of the rapid reoxidation of the flavin.

Table 5.6 Rate constants for pre-steady state FMN reduction of L-mdh fdh and L-ldh fdh by L-mandelate and L-lactate respectively The latter value determined by Miles *et al.*, 1992 (see section 2.9, page for details)

	L-mdh fdh	**L-ldh fdh**
$k_{obs}(s^{-1})$ **L-lactate**		400 ± 40
K_m (mM)		0.26 ±0.07
k_{obs} (s^{-1}) **L-mandelate**	450 ± 30	
K_m (mM)	0.39 ± 0.1	

Table 5.7 Pre steady-state kinetic isotope values for the flavin domains of L-mdh and L-ldh L-ldh fdh/L-lactate values taken from Balme *et al.*, 1995. (See table 5.5 for details)

	L-mdh	L-ldh
^{1}H substrate k_{cat} (s^{-1})	339 ± 9.0	400 ± 40
^{2}H substrate k_{cat} (s^{-1})	81 ± 3.0	69 ± 3
^{1}H substrate K_m (mM)	0.45 ± 0.07	0.26 ± 0.07
^{2}H substrate K_m (mM)	0.33 ± 0.05	0.38 ± 0.09
KIE	**4.20 ±0.30**	**5.8 ± 0.9**

5.9.1 Kinetic isotope effect values for flavin reduction

The KIE values for the flavin reduction of L-mdh fdh (see table 5.7) again show that αH abstraction from L-mandelate totally rate limits the rate of flavin reduction. This value is in good agreement with the KIE value obtained for the flavin reduction in the intact enzyme (4.9 ± 1.0). This result is also similar to the value previously obtained with the flavin domain of L-ldh. In conclusion, all of the kinetic isotope experiments, on the intact and flavin domain of L-mdh, indicate that both enzymes have similar transition states.

5.10 The midpoint potential of the flavin domain of L-mdh

In the preceding chapter, measurement of the haem redox potential was described. This was determined by titrating, under anaerobic conditions, small volumes of reductant to a solution of oxidised enzyme. Visible absorption spectra were measured sequentially and the electrode potential was also noted after addition

of titrant. The ratios of oxidised and reduced enzyme were determined and the midpoint potential calculated after fitting the data to the Nernst equation.

$$E = E_O + RT/nF \log [ox]/[red].$$

RT/nF is a constant, and for a single electron process, n = 1 and RT/nF = 59mV. However, there are two independent one electron couples which have to be considered for the flavin molecule: F_O/F_S and F_S/F_r where o = oxidised, s = semiquinone and r = reduced. For a two electron process we need to combine two Nernst equations:

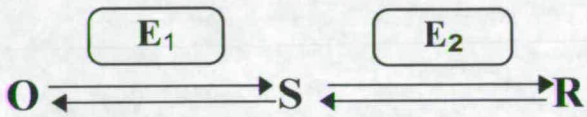

and $[O]/[S] = 10^{(E-E1/59)}$ and $[S]/[R] = 10^{(E-E2/59)}$

combining these with the conservation of mass law:

$$[O] + [S] + [R] = 1$$

Giving each species an extinction coefficient (O_{abs}, S_{abs} and R_{abs}), the total absorbance is equal to

$$\frac{O_{abs}10^{(E-E1/59)} + S_{abs} + R_{abs}10^{(E-E2/59)}}{1 + 10^{(E-E1/59)} + 10^{(E-E2/59)}}$$

Setting E1 to a large negative value and E2 to a large positive value would reduce the above equation to a 2 electron process. The 2 electron equation should work for any wavelength in the flavin spectrum and give the same values for E1 and E2 although obviously the values for O_{abs}, S_{abs} and R_{abs} will vary.

Monitoring the blue (neutral) semiquinone formation of *Bacillus megaterium* flavocytochrome P450 BM3, for example, at 600 nm will give an $O_{abs} \approx 0$ and $R_{abs} \approx 0$ whereas the S_{abs} will be large (see figure 5.6) The semiquinone is stable over a large range of potentials and it is possible to measure the first and second one electron reduction potentials of the FMN cofactor, with E_1 more positive than E_2.

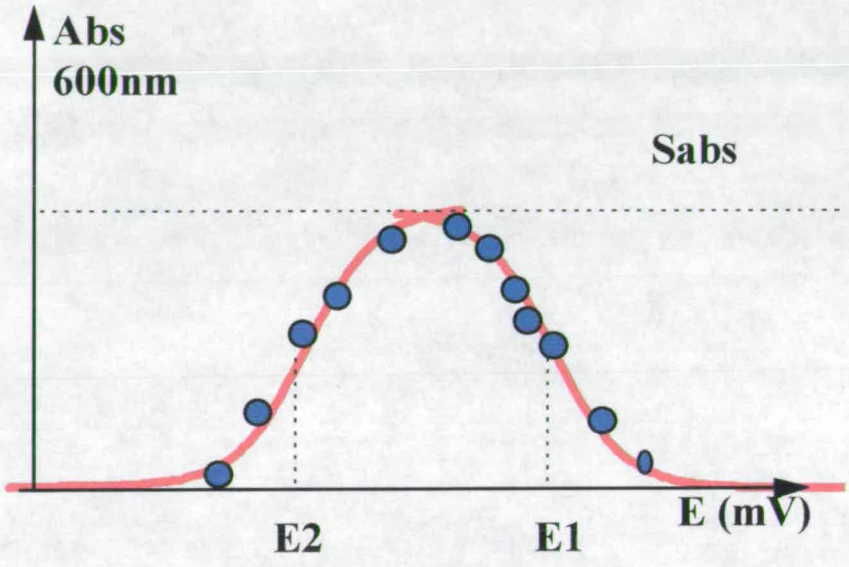

Figure 5.6 Formation of a blue neutral semiquinone at 600 nm

The proportion of semiquinone observed during the titration of L-ldh however, is thought to be as little as 10 % due to large differences in the values of E_1 and E_2 (See figure 5.7). In this case however, E_2 is more positive than E_1, (Walker and Tollin 1991). This makes it virtually impossible to calculate values for the single reduction couples of the FMN. It was calculated that a difference of -60 mV or more between E_1 and E_2 would result in the accumulation of such a small proportion of semiquinone. Values of -94 and -34 mV for E_1 and E_2 were calculated based on the two-electron midpoint potential for the FMN cofactor (-64 mV, this equals $(E_1 + E_2)/2$).

However, previous studies performed with *H. anomala* L-ldh (Tegoni *et al.*, 1984, 1986) demonstrated that the semiquinone could be stabilised in the presence of pyruvate, the product of L-lactate oxidation. This results from an increase in the midpoint potenial of the F_O/F_S redox couple (-23 $\rightarrow$ +74 mV) and a decrease in the midpoint potential of the F_S/F_T couple (-45 $\rightarrow$ -133 mV). With the flavin domain of L-

mdh, it was also possible to measure the midpoint potential of the F_O/F_S couple in the presence of the product molecule, phenylglyoxalate. This thermodynamic stabilisation of the semiquinone form of FMN in the presence of phenylglyoxalate alters the driving force for the intramolecular electron transfer between the FMN and haem cofactor, and could be a factor in controlling the rate of this process. This will be described more fully later.

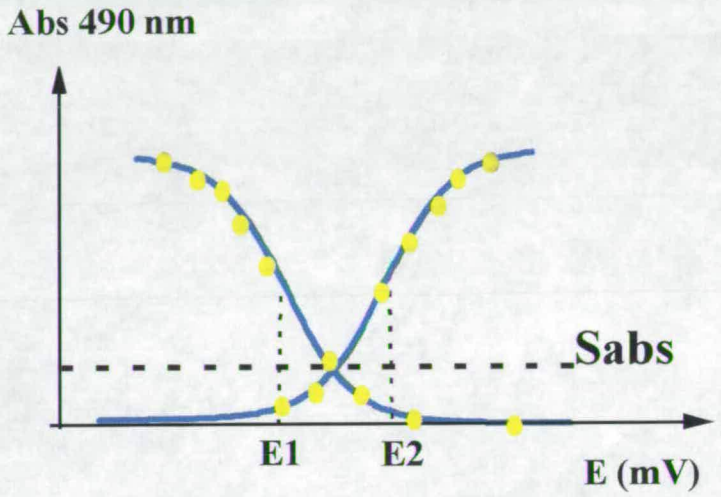

Figure 5.7 Formation of the red anionic semiquinone at 490 nm

Table 5.8 The midpoint potentials of various redox couples (mV; pH7, 25°C; *vs* Pt/H_2)

	Eox/red	Eox/sq	Esq/red
$FMN/FMNH_2$ (free) (a)	-205	-238	-172
S.c L-ldh (FMN) 24°C (b)	-64	-94	-34
H.a L-ldh (FMN) 30°C (c)	-34 ± 10	-23 ± 10	-45 ± 12
H.a L-ldh (FMN) 18°C + pyruvate (d)	-31 ± 5	+74 ± 4	-133 ± 7
R. g L-ldh (haem)This work, page 125	-10 ± 2		
S.c L-ldh (haem) (e)	-17 ± 3		
lactate/pyruvate (f)	-185		

a = Stankovich, 1991 b = Walker and Tollin, 1991 c = Cappelleire-Blandin *et al.*, 1986 d = Tegoni *et al.*, 1986 e = White *et al.*, 1993 f = Loach (1971)

5.10.1 The midpoint potential for the Fox/red couple

Table 5.8 lists the redox potentials of various species. The midpoint potential values of the free flavin and lactate/pyruvate couples are close together, whereas the potential of the flavin couple bound in L-ldh is more than 100 mV more positive. Therefore the enzyme is able to catalyse L-lactate dehydrogenation by facilitating flavin reduction (presumably the same situation is found with L-mdh/L-mandelate). The midpoint potential of the flavin in intact L-ldh has been measured using photoinduced deazariboflavin semiquinone as reductant (Walker and Tollin, 1991). Flavin reduction levels were determined from the absorbance changes at 450 nm, following removal of the absorbance contribution due to the haem. However, since the absorbance contribution from the haem at this wavelength accounted for half of the total absorbance loss observed upon reduction of the enzyme, this method of flavin midpoint potential measurement has its drawbacks. Nernst plots constructed from the absorbance changes at 450 nm gave a two electron midpoint potential (F_O/F_R) of -64 mV. However, the more recently determined midpoint potential of the isolated flavin domain of L-ldh (-78 ± 10 mV) is probably a more realistic result. (Martine Meyer, unpublished results).

The calculated rate constant for the intramolecular electron transfer between FMN and haem represents the sum of the forward and reverse microsopic rate constants for electron transfer between reduced flavin and oxidised haem (see section 1 7.10).

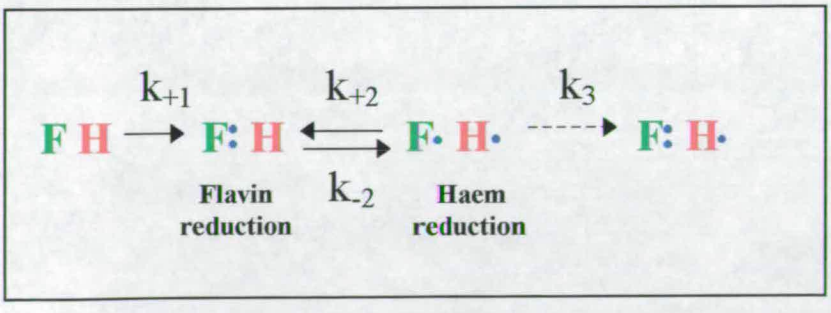

The individual electron-transfer steps leading to the reduction of L-mdh by L-mandelate. k_3 is extremely slow and makes no contribution to the catalytic cycle

From the previously calculated midpoint potentials of L-ldh haem and flavin (-17mV and -64mV) respectively, the equilibrium constant (i.e the ratio of k_{+2} to k_{-2}) was calculated to be 5.5 using the equation

$$\ln K_{eq} = nF\Delta E/RT, \qquad (\Delta E = 47 \text{ mV})$$

This meant that the equilibrium lay 85 % in favour of reduced haem. Using the midpoint potential of the flavin couple of the L-ldh flavin domain (Fo/r = -78 mV, therefore ΔE = 61 mV) resulted in an equilibrium constant for the reaction of around 10 (which is equivalent to the equilibrium actually lying around 90 % in favour of reduced haem. The redox couple of the FMN molecule of the L-mdh flavin domain was also measured (-120 ± 10 mV). This is 42 mV more negative than the flavin molecule of L-ldh. Furthermore, the midpoint potential of the haem group of L-mdh is slightly more positive than the haem of L-ldh. Both of these factors combine to give a greater ΔE value (110 mV) than L-ldh. This gives a K_{eq} = 49 which is equivalent to the equilibrium between the flavin and haem molecules of L-mdh lying 98 % in favour of reduced haem. This may partly explain the erroneous flavin reduction traces measured with the intact enzyme. Because there is a greater ΔE between the prosthetic groups of L-mdh compared to L-ldh, electrons will driven towards the haem groups so that flavin reduction is grossly underestimated. (see section 4.5.2)

Figure 5.8 Redox titration of L-mdh flavin domain, observing absorbance changes at 450 nm

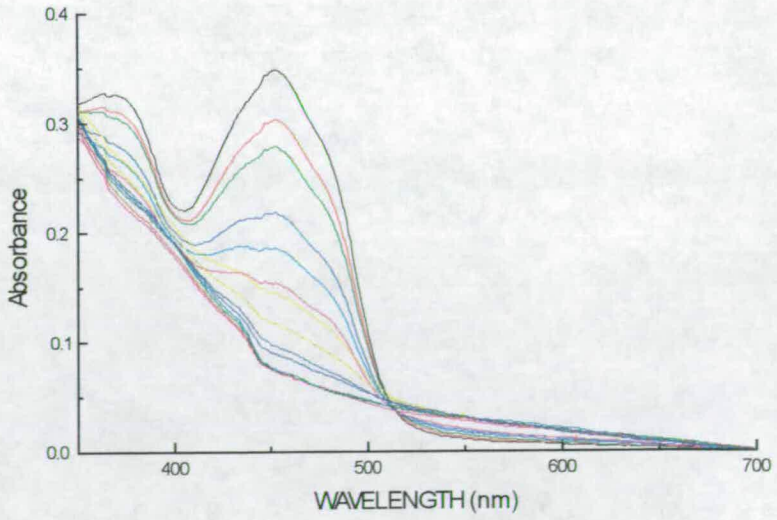

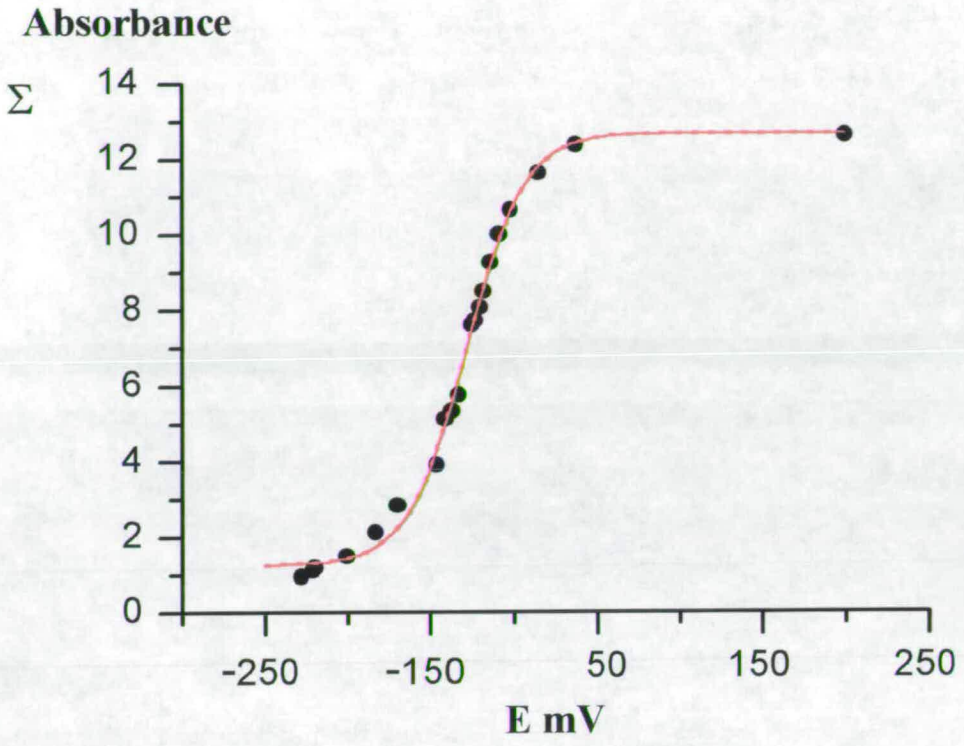

Figure 5.9 Nernst plot for the redox titration of L-mdh flavin domain E = 119.48 mV

Table 5.9 The midpoint potentials of L-mdh fdh and L-ldh fdh (see section 2.10.4 for details) The redox couples of L-ldh fdh FMN measured by Martine Meyer, unpublished results.

	Eox/red	**Eox/sq** (+ 10 mM product)
L-MDH FDH	-120 ± 5mV	-90 ± 10 mV
L-LDH FDH	-78 ± 4 mV	-60 ±10 mV

Figure 5.10 The stabilised semiquinone of L-mdh fdh after addition of 10 mM phenylglyoxalate (see section 2.10.4 for details)

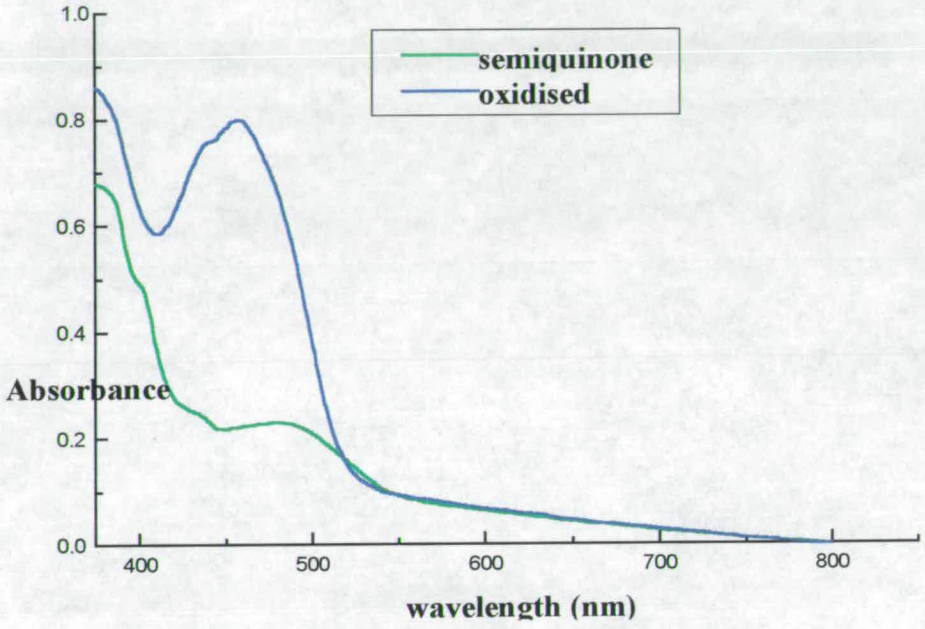

5.10.2 The midpoint potential of the Fox/Fsq couple in the presence of phenylglyoxalate

Potentiometric titrations performed with *S. cerevisiae* L-ldh in the absence and presence of pyruvate indicated that profound changes in the redox behaviour occur as a result of pyruvate binding (Walker & Tollin, 1991). Similar results have been observed using the protein from *H. anomala* (Tegoni *et al.*, 1986). With the latter enzyme, the flavin semiquinone proportion was estimated using electron paramagnetic resonance measurements. It was found that pyruvate bound preferentially to the semiquinone form of the FMN with the gap between the midpoint potentials of the two monoelectronic couples going from 50mV to more than 230 mV. The bielectronic couples, Fo/r and Ho/r, on the other hand, had the same midpoint

potentials whether pyruvate was present or not. This increase in midpoint potential of the Fo/s couple was more positive than the haem couple which meant that $F_s \rightarrow H_{ox}$ electron transfer was no longer thermodynamically feasible. It was suggested that this modulation of the Fo/s redox potential ensured that enzyme activity could be regulated by a form of feedback control. Thus it was of interest to determine the midpoint potentials of the FMN cofactor of L-mdh in the presence of its product, phenylglyoxalate.

Mandelate was added to a solution of oxidised enzyme (enzyme and substrate were equimolar). The potential of the solution fell to around -200 mV. Approximately 10 mM phenylglyoxalate was then added to the solution. The addition of product resulted in several observable changes. Firstly, the yellow oxidised enzyme solution had been first reduced by mandelate and the absorbance at 450 nm was bleached resulting in a colourless solution, then by addition of phenylglyoxalate the semiquinone was formed which resulted in the solution turning pink. This was due to the anionic semiquinone absorbing around 490 nm. This also resulted in the electrode potential becoming more positive, though unlike the intact *H. anomala* L-ldh, there was not a significant increase in potential when product was added. The enzyme was eventually reoxidised by the titration of ferricyanide, and the midpoint potential for the Fo/s couple was determined to be around -90 $\pm$ 10 mV. When phenylglyoxalate was present at a concentration of 10 mM it was not possible to reduce the flavin semiquinone to the fully reduced flavin species even when electrode potential values reached around -300 mV. It was possible to decrease the potential further by the addition of dithionite in amounts roughly corresponding to the L-mdh concentration. However this decrease in potential was then followed by a progressive increase, approximately restoring the preceding equilibrium level. This can be explained as the consumption of dithionite coupled to phenylglyoxalate reduction, yielding L-mandelate, as catalysed by the enzyme. Addition of even more dithionite resulted in the precipitation of denatured enzyme. Therefore it was impossible to titrate the second flavin redox transition by dithionite. One must assume however, that because there is only a small increase in the stability of the Fo/s couple

the phenylglyoxalate must have a major destabiling effect on the Fs/r couple. The reason for the different effects seen in the two enzymes is unclear. However, the equivalent experiment was also carried out on the flavin domain of *S. cerevisae* L-ldh (Martine Meyer, unpublished results). This showed that there is in fact only a small increase in the Fo/s couple of L-ldh, from -78 mV to -60 mV.

The reason for the enhanced stability of the FMN semiquinone in the presence of phenylglyoxalate may be due to retention of the proton from the hydroxyl group of mandelate on the active site histidine (His 377), which would position a positive charge adjacent to the FMN ring. There may also be electronic stabilisation between the conjugated systems of the phenylglyoxalate molecule and the FMN ring. Whatever the reason, we can assume that phenylglyoxalate targets the flavin semiquinone→haem electron transfer step in much the same way as pyruvate inhibits the same step in L-ldh. An inhibition constant value of 40 ± 17 mM (S. Daff, 1997) was obtained after measuring the rate of flavin oxidation of L-ldh in the presence of pyruvate. This is comparible to the constant derived for the non-competitive steady-state inhibition (30 mM, Lederer, 1978) of the same enzyme.

5.11 Conclusion

The flavin domain of L-mdh was cloned and expressed to high levels (~ 20% of the total cell protein) in *E. coli*. The enzyme was purified using almost the same procedure as described for the intact L-mdh. Steady-state analysis revealed that L-mdh fdh can oxidise L-mandelate, almost as efficiently as the intact form of the enzyme. However, L-mdh fdh is unable to reduce the physiological electron acceptor, cytochrome *c*, suggesting that the role of the haem domain of L-mdh is to facilitate the transfer of electrons from the reduced FMN to cytochrome *c*. The kinetic isotope effect values obtained using [2-^{2}H] and [2-^{1}H]mandelate indicated that cleavage of the αC-H bond limits the overall turnover of the enzyme. The midpoint potential of the Fo/r couple was also measured. This was slightly lower than the value obtained for the flavin domain of L-ldh. The semiquinone form of the FMN molecule can be stabilised by an excess of the product, phenylglyoxalate.

Final Conclusion

The work described in this thesis mainly concerns the kinetic characterisation of the L-mandelate dehydrogenase from *R.graminis* (recombinant form). Previous work on the yeast expressed L-mdh revealed that the enzyme turns over L-mandelate at rates comparible to the L-lactate dehydrogenase from *S.cerevisiae*. This was also found to be the case for the recombinant form of L-mdh expressed in *E.coli*, with the steady-state parameters of the enzyme (*ie*, k_{cat} and K_m) calculated to be 550 ± 25s^{-1} and 0.35 ± 0.02 mM respectively, using potassium ferricyanide as electron acceptor. The corresponding values for *S. cerevisiae* L-ldh with L-lactate were 400 ± 10s^{-1} and 0.49 ± 0.05 mM. The two enzymes also show similar steady-state behaviour with their physiological electron acceptor, cytochrome *c* (L-mdh: k_{cat} = 225 ± 15s^{-1}; K_m = 0.35 ± 0.05 mM. L-ldh: k_{cat} = 207 ± 10s^{-1}; K_m = 0.24 ± 0.04 mM).

However, the pre-steady-state values for the reduction of L-mdh, measured by stopped-flow spectrophotometry, differs considerably to the previously calculated values for the reduction of L-ldh. The reduction of the flavin prosthetic group of L-mdh was analysed as the sum of two exponential functions. The rate constant calculated for the first (fast) phase was 280 ± 20s^{-1}, approximately half the value of the flavin reduction rate in L-ldh (604 ± 60 s^{-1}). However, the rate constants for the haem reduction of L-mdh and L-ldh are similar, and are in good agreement with their steady-state values (L-mdh: 605 ± 50s^{-1}; L-ldh 445 ± 50s^{-1}). The proposed explanation for the difference in the rate constants for the flavin reduction rates was that there was a greater potential difference between the flavin and haem prosthetic groups in L-mdh (110 mV,) than in L-ldh (61 mV, values calculated by measuring the midpoint potentials of the prosthetic groups). This results in an increased rate of electron transfer between the flavin and haem of L-mdh compared to L-ldh. The reason for the unexpectantly low flavin reduction rate is that flavin reduction is only observed spectrophotometrically *after* the rapid intramolecular electron transfer step

from the flavin to the haem, resulting in reduced haem and flavin semiquinone, followed by electron transfer between the semiquinones, producing two oxidised and two reduced flavin molecules per tetramer. The tetramer is then fully reduced by a further two molecules of L-mandelate. This proposal was in part supported by the flavin reduction rates of the isolated flavin domain of L-mdh (450 ± 30 s^{-1}) which is significantly greater than the value obtained in the intact enzyme.

The reduction of cytochrome *c* by L-mdh was also measured using stopped-flow spectrophotometry and the second order rate constant, which represented the on-rate for the formation of a catalytically competent complex between L-mdh and cytochrome *c*, was determined to be within error the same as the previously obtained value with L-ldh and cytochrome *c* (L-mdh: 41.5 ± 2 $\mu M^{-1}s^{-1}$. L-ldh: 34.8 ± 0.9 $\mu M^{-1}s^{-1}$). This result, along with the similar values for the haem reduction rates and midpoint potentials of the haem groups of the two enzymes (L-mdh: -10 ± 2mV, L-ldh: -17 ± 3 mV) suggested that any differences in the kinetic properties of the two enzymes would be attributable to differences in their flavin domains.

One important feature is the almost mutually exclusive substrate specificities of L-mdh and L-ldh. (L-mdh with L-lactate as substrate: $k_{cat} = 0.02 \pm 0.01 s^{-1}$. L-ldh with L-mandelate as substrate: $k_{cat} = 0.50 \pm 0.1$ s^{-1}). In order to provide an explanation for these values, the 3D crystal structure of L-ldh (product bound) was examined. It appears that there are several active site residues which are in close proximity to the methyl side group of L-lactate. By mutating two of these residues (Ala198 and Leu230) to smaller variants it was possible to swing the substrate specificity of the L-ldh mutant enzymes towards L-mandelate. This was presumably achieved by there being less steric hinderence between the phenyl ring of L-mandelate and the shorter side chains of the mutated residues. The most significant increase in turnover with L-mandelate in the intact enzyme was seen with the double mutant, A198GL230A (an approximate 450 fold increase in k_{cat} from 0.02 ± 0.01 s^{-1} to 8.50 ± 0.50 s^{-1}). This was increased further when the isolated flavin domain of L-ldh was

constructed containing the same mutations. (A198GL230A flavin domain k_{cat} = 15.5 ± 1 s^{-1}). As mentioned previously, there are several other possible candidates for site directed mutagenesis, for example, Phe 325. However, it may also be possible to increase enzyme activity with mandelate by random mutagenesis. Perhaps the best way to introduce random mutations into the *L-ldh* gene is by PCR, since mutations may be targeted to specific areas. Altering dNTP concentration, pH, or adding $MnCl_2$ to the PCR reaction mixture can increase the mutational frequency of the reaction. The yeast *Rhodotorula graminis* may be a suitable host organism for the mutant enzymes. However, in order to screen the various mutants for their ability to utilise L-mandelate, the *R. graminis L-mdh* gene would first have to be removed using, for example, an appropriate suicide vector containing the entire gene and a kanamycin resistance cassette.

It has been proposed (Smekal *et al.* 1993) based on the kinetic isotope values obtained that L-ldh and L-mdh are unable to turnover each other's substrates because they adopt different transition states with their respective substrates. For example, in the case of L-ldh the rate limiting step was predicted to involve removal of the hydrogen of the C2 carbon of L-lactate, after measurement of the steady-state turnover of the enzyme using deuterated [2-^{2}H] L-lactate resulted in a 5 fold decrease in rate. The steady-state turnover rate of native L-mdh with what researchers took to be deuterated mandelate, however, was within error, the same as the value obtained with undeuterated mandelate. This result suggested that cleavage of the C2-H did not rate limit the turnover of mandelate by L-mdh and that some other step, possibly polarisation of the C2 carbon was the major rate determining step. These experiments have been repeated using recombinant L-mdh and the differences in the rate of flavin reduction using [2-^{1}H] (k_{obs} = 210 ± 10 s^{-1}) and [2-^{2}H] DL-mandelate (k_{obs} = 43 ± 5 s^{-1}) suggest that cleavage of the C2-H bond of mandelate does in fact limit the rate of flavin reduction. The kinetic isotope effect value was calculated to be 4.9 ± 2, which is only slightly lower than the previously determined isotope effect value for the reduction of L-ldh flavin by L-lactate (8.1 ± 1.4). It is reasonable to assume then, that both enzymes have similar transition states with their physiological substrates. Future

work on L-mdh will include investigating the possible nature of the transition state. By measuring the rate of L-mdh flavin reduction by substituted mandelates, it is possible to predict whether the C2 carbon is electron rich (*ie*, a carbanion intermediate has been formed) or electron deficient (the C2 hydrogen is removed as a hydride ion). If the latter situation is found in L-mdh, then the rate of flavin reduction ought to be increased when the substituted mandelate has an electron donating group para to the C2 carbon. This group would be able to stabilise the resultant positive charge after the hydrogen is removed as a hydride. Initial experiments by D. Robertson have shown that the rate of flavin reduction is dramatically increased using substrates such as 4-hydroxy mandelate.

Finally, it is important that in the future we will be able to directly compare the three dimensional structures of L-mdh and L-ldh, since this will provide us with vital information on the structural basis for the kinetic differences between the two enzymes. In order to obtain crystals we need to have pure protein. Previous attempts to purify native and recombinant L-mdh have been only partially successfull, probably due to the extremely low levels of L-mdh protein production by the cells. In this work the amount of active L-mdh and L-mdh flavin domain expressed have been increased significantly (between 14 and 20 % of the total cell proteins), and both the intact and flavin domain of L-mdh have been purified to homogeneity with only a minor loss in activity. Preliminary crystal trials suggest that L-mdh may crystallise under similar conditions to L-ldh (recombinant form).

Appendices

1. References

Allison, N. and Fewson, C. A. (1986). *FEMS Microbiol. Lett.* **36**, 183-186.

Allison, N., O' Donnell, M. J. and Fewson, C. A. (1985a). *Biochem. J.* **227**, 753-757.

Allison, N., O' Donnell, M. J. and Fewson, C. A. (1985b). *Biochem. J.* **231**, 407-416.

Appleby, C.A. and Morton, R.K. (1954) *Nature* (London) **173**, 749-752.

Bach, S.J., Dixon, M. and Keilin, D. (1942a) *Nature* (Letters to the Editor) **149**, 21.

Baker, D. P. and Fewson, C. A. (1989). *J. Gen. Microbiol.* **135**, 2305-2044.

Baldwin, J.E. and Krebs, H. (1981) *Nature* **291**, 381-382.

Balme, A., Brunt, C. E., Pallister, R. L., Chapman, S. K. and Reid, G. A. (1995). *Biochem. J.* **309,** 601-605.

Banner, D.W., Bloomer, A.C., Petsko, G.A., Phillips, D.C., Pogson, C.I., Wilson, I.A., Corran, P.H., Furth, A.J., Milman, J.D., Offord, R.E., Priddle, J.D. and Waley, S.G. (1975) *Nature* **255**, 609-614.

Baudras, A. (1962). *Biochim. Biophys. Res. Commun.* **7**, 310-313.

Bernheim, F. (1928) *Biochem. J.* **22**, 1178-1192.

Bhat, S. G., Ramanayaganan, M, and Vaidyanathan, C. S. (1973). *Biophys. Res. Commun.* **52**, 834-842.

Bhat, S. G., and Vaidyanathan, C. S. (1976). *J. Bacteriol.* **127**, 1108-1118.

Birnboim, H. C and Doly, J. (1979). *Nuc. Acid. Res.* **7**, 1513-1523.

Black, M. T., Gunn, F. J., Chapman, S. K. and Reid, G. A. (1989a) *Biochem. J.* **263**, 973-976.

Black, M.T., White, S.A., Reid, G.A. & Chapman, S.K. (1989) *Biochem. J.* **258**, 255-259.

Brunt, C.E., Cox, M.C., Thurgood, A.G.P., Moore, G.R., Reid, G.A. and Chapman, S.K. (1992) *Biochem. J.* **283,** 87-90.

Capeillere-Blandin, C. (1975) *Eur. J. Biochem.* **56**, 91-101.

Capeillere-Blandin, C., Bray, R.C., Iwatsubo, M., and Labeyrie, F. (1975b) *Eur. J. Biochem.* **56**, 91-101.

Chakrabarti, S. K. (1979). *Clin. Chem.* **25**, 592-595.

Chalmers, R. M., Keen, J. N., and Fewson, C. A. (1991). *Biochem. J.*, **273**, 99-102.

Chapman, S. K., Reid, G. A., Bell, C., Short, D. M. and Daff, S. N. (1996). *Biochem. Soc. Trans.* **24**, 73-77.

Chapman, S.K, Reid, G.A., Daff, S., Sharp, R.E., White, P.W., Manson, F.D.C. and Lederer, F. (1994) *Biochem. Soc. Trans.* **22**, 713-718.

Chapman, S. K., White, S. A. and Reid, G. A. (1991). *Adv.Inorg. Chem.* **36,** 257-301.

Chen, Y. P., Dilworth, M. J. and Glenn, A. R. (1989). *Arch. Microbiol.* **151**, 520.

Clarke, A. R., Smith, C. J., Hart, K. W., Wilks, H. M., Chia, W. N., Lee, T. V., Birktoft, J. J., Banaszak, L. J., Barstow, D. A., Atkinson, T. and Holbrook, J. J. (1987). *Biochem. Biophys. Res. Commun.* **148**, 15-23.

Clarke, A.R., Atkinson, T. and Holbrook, J.J. (1989) *Trends Biochem. Sci.* **14**, 145-148.

Colagrande, O. (1959). *Ann. Microbiol. Enzymol.* **9**, 62-72.

Crawford, N. M., Smith, M., Bellissimo, D. and Davis, R. W. (1988). *Pro. Natl. Acad. Sci. USA.* **85,** 5006-5010.

Cristiano, R. J. and Steggles, A. W. (1989). *Nucl. Acid. Res.* **17**,799.

Crowl, R., Seamans, C., Lomedico, P. and McAndrew, S. (1985). *Gene.* **38**, 31-38.

Daff, S. N., *PhD Thesis*, University of Edinburgh, (1996).

Daff, S., Manson, F.D.C., Reid, G.A. and Chapman, S.K. (1994) *Biochem. J.* **301**, 829-834.

Daff, S. N., Sharp, R. E., Short, D.M, Bell, C., White, P.W., Manson, F. D. C., Reid, G. A. and Chapman, S. K. (1996). *Biochemistry.* **35,** 6351-6355.

Dong, J.M., Taylor, J.S., Latour, D.J., Iuchi, S., and Lin, E.C.C. (1993) *J. Bacteriol.* **175,** 6671-6678

Durham, D. R., McNamee, C. G. and Stewart, D. B. (1984). *J. Bacteriol.* **160**, 771-777.

Dutton, P. L. (1978). *Meth. Enz.* **54**, 41.

Fewson, C. A. In: *The Evolution of Metabolic Function*, edited by Mortlock, R. P: Boca Raton, CRC Press, 1992. pp. 115-141.

Fewson, C. A. (1988). *FEMS Microbiol. Rev.* **54**, 85-110.

Fewson , C. A., Baker, D. P., Chalmers, R. M., Keen, J. N., Hamilton, I. D., Scott, A. J. and Yasin, M. (1993). *J. Gen. Microbiol.* **139**, 1345-1352.

Futai, M. (1973). *Biochemistry.* **12**, 2468-2474.

Gervais, M. and Tegoni, M. (1980). *Eur. J. Biochem.* **34**, 268.

Gibson, T. J. (1984). *PhD Thesis.* Cambridge University.

Gibson, D.T (1968). *Sci.* **161**, 1093-1097.

Giegel, D.A., Williams, C.H.Jr. and Massey, V. (1990), *J. Biol. Chem.* **256**, 6626-6632.

Goldberg, J. D., Yoshida, T. and Brick, P. (1994). *J. Mol. Biol.* **236**, 1123-1140.

Goodall, M. and Alton, H. (1969). *Biochem. Pharmacol.* **18**, 295-302.

Guiard, B. (1985). *EMBO, J.* **4**, 3265-3272.

Guiard, B. and Lederer, F. (1977). *Eur. J. Biochem.* **74,** 181-186.

Hageman, G. D., Rosenberg, E. Y. and Kenyon, G. L. (1970). *Biochemistry*. **9**, 4029-4036.

Harwood, C. S. and Parales, R. E (1996). *Ann. Microbiol.* **50**, 553-590.

Hockenhall, D. J. D., Walker, A. D., Wilkin, G. D. and Winder, F. G. (1952). *Biochem. J.* **50**, 605-609.

Hoey, M. E., Allison, N., Scott, A. J. and Fewson, C. A. (1987). *Biochem. J.* **50**, 605-609.

Holmgren, A. (1985). *Ann. Rev. Biochem.* **54**, 237-271.

Hummel, W., Schiitte, H. and Kula, M-R. (1988). *Appl. Microbiol. Biotech.* **28**, 433-439.

Illias, R. MD. (1997) *PhD. Thesis*. University of Edinburgh.

Iwatsubo, M., Mevel-Ninio, M. and Labeyrie, F. (1977) *Biochemistry* **16**, 3558-3566.

Iyayi, C. B. and Dart, R. K. (1980). *Microbiol. Lett.* **15**, 127-133.

Jacq, C. & Lederer, F. (1972) *Eur. J. Biochem.* **25**, 41-48.

Jamaluddin, M., Subba Rao, P. V.and Vaidyanathan, C. S. (1970). *J. Bacteriol.* **101,** 786-793.

Jenks, W.P (1969). *Catalysis in Chemical Enzymology*. McGraw Hill, NY.

Kennedy, S. I. T, and Fewson, C. A. (1968). *Biochem. J.* **107**, 497-506.

Kishore, G., Sugumaran, M. and Vaidyanathan, C.S. (1974). *Biochem. Biophys. Res. Commun.* **56**, 851-859.

Kunkel, T.A. (1985) *Proc. Natl. Acad. Sci. U.S.A.* 82, 488-492.

Labeyrie, F. and Baydras, A. (1972). *Eur. J. Biochem.* **25**, 33-40.

Labeyrie, F., Baudras, A. and Lederer, F. (1978) in *Methods in Enzymology* (S. Fleischer & L. Packer eds., Academic Press, New York) **53**, 238-256.

Laemmli, U. K. (1970). *Nature.* **227**, 680-685.

Le, K.H.D. and Lederer, F. (1991) *J. Biol. Chem.* **266**, 20877-20881.

Lederer, F. (1978) *Eur. J. Biochem.* **88**, 425-431.

Lederer, F.(1991) in *Chemistry and Biochemistry of Flavoenzymes* vol II Ch.7, (F. Muller ed., CRC Press, Boca Raton, Florida).

Lederer, F. and Simon, A-M.(1971) *Eur. J. Biochem.* **20**, 469-474.

Lindqvist, Y., Branden, C-I., Mathews, F. S. and Lederer, F. (1991*). J. Biol. Chem.* **266,** 3198-3207.

Loach, P.A. (1976) in *Handbook of Biochemistry and Molecular Biology* (Physical and Chemical Data Vol. 1) 3rd. Edn. (Fasman G.D. ed.), CRC Press Inc., Cleveland, 122-130.

Mayhew, S.G. and Ludwig, M.L. (1975) *Enzymes* (3rd Ed.) **12**, 57-118.

Middleton, B., Middleton, A., Micink, A., White, D. A. and Bell, G. D. (1983). *Biochem. Pharmacol.* **32**, 649-651.

Miles, C.S., *PhD Thesis*, University of Edinburgh, (1992).

Miles, C. S., Manson, F. D. C., Reid, G. A. and Chapman, S. K. (1993). *Biochim. et Biophys. Acta.* **1202,** 82-86.

Miles, C.S., Rouviere, N., Lederer, F., Mathews, F.S., Reid, G.A., Black, M.T., and Chapman, S.K. (1992) *Biochem. J.* **285**, 187-192.

Muh, U., Williams, C.H. and Massey, V. (1994a) *J. Biol. Chem.* **269**, 7982-7988.

Muh, U., Williams, C.H. and Massey, V. (1994b) *J. Biol. Chem.* **269**, 7994-8000.

Muh, U., Williams, C.H. and Massey, V. (1994c) *J. Biol. Chem.* **269**, 7989-7993.

Ornston, L. N and Stanier, R. Y. (1964). *Nature.* **26,** 1279-1283.

Ornston, L.N and Stanier, R.Y. (1966). *J. Biol. Chem.* **241**, 3776-3786.

Pai, E. F., Karplus, P. A. and Schultz, G. E. (1988*). Biochemistry*. **27**, 4465-4474.

Pajot, P. and Claisse, M. (1974). *Eur. J. Biochem.* **49**, 275-285.

Pajot, P. and Groudinsky, O. (1970) *Eur. J. Biochem.* **12**, 158-164.

Perham, R. N., Scrutton, N. S. and Berry, A. (1991). *Bioessays.* **10**, 515-525.

Pompon, D. (1980) *Eur. J. Biochem.* **106**, 151-159.

Pompon, D. and Lederer, F. (1979) *Eur. J. Biochem.* **96**, 571-579.

Ramakrishna Rao, D. N. and Vaidyanathan, C. S. (1977). *Can. J. Microbiol.* **23,** 1496-1499.

Reid, G.A.,White, S.A., Black, M.T., Lederer, F., Mathews, F.S. and Chapman, S.K. (1988) *Eur. J. Biochem.* **178,** 329-333.

Rokeach, L. A., Haselby, J. A. and Hoch, S. O. (1988). *Proc. Natl. Acad. Sci. USA.* **85**, 4832-4836.

Scrutton, N. S., Berry, A. and Perham, R. N. (1990). *Nature*, **343**, 38-43.

Short, D. M., Walkinshaw, M. D., Taylor, P., Reid, G.A. and Chapman, S. K. (1997) in *Flavins and Flavoproteins* 1996. University of Calgary press

Smekal, Reid, G. A. and Chapman, S. K. (1994). *Biochem. J.* **297**, 647-652.

Smekal, O., Yasin, M., Fewson, C. A., Reid, G. A. and Chapman, S. K. (1993). *Biochem. J.* **290**, 103-107.

Stanier, R. Y and Ornston, L. N (1973). *Microbiol. Physiol.* **9**, 89-151.

Stanier, R. Y., Palleroni, N. J. and Doudoroff, M. (1966). *J. Gen. Microbiol.* 43, 159-271.

Stankovich, M. and Fox, B. (1983) *Biochemistry* **22**, 4466-4472.

Stanley, K. K. and Luzio, J. P. (1984). *EMBO. J.* **3**, 1429-1434.

Tegoni, M., Janot, J.M. and Labeyrie, F. (1986) *Eur. J. Biochem.* **155**, 491-503.

Tegoni, M., Silvestrini, M. C., Labeyrie, F. and Brunosi, M. (1984) *Eur. J. Biochem.* **140**, 39-45.

Tegoni, M., White, S.A., Roussel, A., Mathews, F.S. & Cambillau, C. (1993) *Proteins* **16**, 408-422.

Tsou, A. Y., Ransom, S. C. and Gerlt, J. A. (1990). *Biochemistry.* **29**, 9856-9862.

Viera, J. and Messing, J, (1987). *Gene.* **19**, 259-268.

Volokita, M. and Somerville, C.R. (1987) *J. Biol. Chem.* **262**, 15825-15828.

Walker, M. C., and Tollin, G. (1991) *Biochemistry* **30**, 5546-5555.

White, P., Manson, F.D.C., Brunt, C.E., Chapman, S.K. and Reid, G.A. (1993) *Biochem. J*, **291**, 89-94.

Wierenga, R. K., de Maeyer, M. C. and Hol, W. G. J. (1985). *Biochemistry.* **24**, 1346-1357.

Wigley, D.B., Gamblin, S.J., Turkenburg, J.P., Dodson, E.J., Piontek, K., Muirhead, H. and Holbrook, J.J., (1992) *J. Mol. Biol.* **223**, 317.

Wilks, H.M., Halsall, D.J., Atkinson, T., Chia, W.N., Clarke, A.R. and Holbrook, J.J. (1990) *Biochemistry* **29**, 8587-8591.

Wilks, H.M., Hart, K.W., Feeney, R., Dunn, C.R., Muirhead, H., Chia, W.N., Barstow, D.A., Atkinson, T., Clarke, A.R. and Holbrook, J.J. (1988) *Science* **242**, 1541-1544.

Wilks, H.M. and Holbrook, J.J. (1991) *Curr. Opin. Biochem.* **2**, 561.

Wilks, H.M., Moreton, K.M., Halsall, D.J., Hart, K.W., Sessions, R.D., Clarke, A.R. and Holbrook, J.J. (1992) *Biochemistry* **31**, 7802-7806.

Williams R.F. and Bruice T.C. (1976) *J. Am. Chem. Soc.* **98**, 7752-7768.

Xia, Z-X. & Mathews, F.S., (1990) *J. Mol. Biol.* 212, 837-863.

Yamazaki, Y. and Maeda, H. (1986). *Agri. Biol. Chem.* **50**, 2621-2631.

Yasin, M. and Fewson, C. A. (1993). *Biochem. J.* **293**, 455-460.

Yorita, K., Aki, K., Ohkuma-Soyejima, T., Kokubo, T, Misaki, H. and Massey, V. (1996). *J. Biol. Chem.* **271**, 28300-28305.

2. Abbreviations

Amino acids

	Code	Symbol
Alanine	Ala	A
Arginine	Arg	R
Asparagine	Asn	N
Aspartic acid	Asp	D
Cysteine	Cys	C
Glutamic acid	Glu	E
Glutamine	Gln	Q
Glycine	Gly	G
Histidine	His	H
Isoleucine	Ile	I
Leucine	Leu	L
Lysine	Lys	K
Methionine	Met	M
Phenylalanine	Phe	F
Proline	Pro	P
Serine	Ser	S
Threonine	Thr	T
Tryptophan	Trp	W
Tyrosine	Tyr	Y
Valine	Val	V

Mutations

When referring to oligonucleotides, the following abbreviations are used:

A, adenine; T, Thymidine; C, Cytosine and G, Guanine

Amino acid mutations are represented as: code | number→code where the number gives the position on the polypeptide chain. The mutant enzymes produced are referred to as in the following example:

Leu230→Gly would generate the mutant L230G

Kinetic Parameters

K_m	Michaelis constant
k_{cat}	Rate constant at saturation
K_i	Inhibition constant
K_d	Dissociation constant
k_{et}	Electron transfer rate constant
t	Time

Standard units

m	metre	°C	degree Celsius
g	gram	M	molar
s	second	V	volt
l	litre	Å	Angstrom

Textual abbreviations

Abs.	Absorbance
APS	Ammonium persulphate
ATP	Adenosine-5'-triphosphate
BSA	Bovine serum albumin
B. stearothemophilus	*Bacillus stearothermophilus*
B. megaterium	*Bacillus megaterium*
Da	Daltons
DAD	2,3,5,6-tetramethyl-p-phenylenediamine
dATP	Deoxyadenosine
dCTP	Deoxycytosine
dGTP	Deoxyguanidine
dTTP	Deoxythymidine
ddATP	Dideoxyadenosine
ddCTP	Dideoxycytosine
ddGTP	Dideoxyguanidine
ddTTP	Dideoxythymidine
dH_2O	Distilled water
DNA	Deoxyribonucleic acid
DTT	Dithiothreitol
E. coli	*Escherichia coli*
EDTA	Ethylenediaminetetraacetic acid
EPR	Electron paramagnetic resonance (spectroscopy)
FMN	Flavin mononucleotide
ΔG	Free energy change
H. anomala	*Hansenula anomala*
HNQ	2-hydroxy-1,4-napthoquinone

HRP	Horse radish peroxidase
I	Ionic strength
KIE	Kinetic isotope effect
LB	Luria broth
LDH	Lactate dehydrogenase
M_r	Molecular weight
M. smegmatis	*Mycobacterium smegmatis*
NMR	Nuclear magnetic resonance (spectroscopy)
NAD	β-Nicotinamide adenine dinucleotide
OD	Optical density
PAGE	Polyacrylamide gel electrophoresis
PEG	Polyethylene glycol
PES	Phenazine ethosulphate
PMS	Phenazinesulphate
P. putida	*Pseudomonas putida*
PTFE	Polytetrafluoroethene
RNA	Ribonucleic acid
R. graminis	*Rhodotorula graminis*
S. cerevisiae	*Saccharomyces cerevisiae*
SDS	Sodium dodecyl sulphate
SHE	Standard hydrogen electrode
TEMED	N,N,N',N'-Tetramethylethylene diamine
Tris	Tris(hydroxymethyl)aminomethane
UV	Ultraviolet
Vis	Visible

3. Conferences attended

FLAPS Network Meetings:

Wageningen, Netherlands (1995)

Dourdan, France (*Poster presented*, 1996)

Biochemical Society Meeting at University College Dublin (*Poster presented*,1995)

Inorganic Chemistry Group Meetings, Firbush, Scotland (*As speaker, posters presented*,1995-1997)

Institute of Cell and Molecular Biology Group Meetings, St. Andrews, Scotland. (*As speaker*, 1995-1997)

4. Publications

Sinclair, R., Reid, G.A., Daff, S.N. and Chapman, S.K. (1997) in *Flavins and Flavoproteins 1996*, University of Calgary Press, pp 579-582.

Constructing a Mandelate Dehydrogenase

Rhona Sinclair, Graeme A. Reid
Institute of Cell and Molecular Biology, University of Edinburgh, Edinburgh EH9 3JJ, Scotland.

Simon Daff, Stephen K. Chapman
Department of Chemistry, University of Edinburgh, Edinburgh EH9 3JJ, Scotland.

INTRODUCTION

Flavocytochrome b_2 from *Saccharomyces cerevisiae* is a well characterised L-lactate dehydrogenase/cytochrome c reductase. Its X-ray crystal structure has been determined to 2.4 Å (1) allowing the active site for dehydrogenation to be identified. This is constructed around the non-covalently bound FMN cofactor. In one of the two crystallographically distinguishable subunits of the enzyme (which is a homotetramer), the product of dehydrogenation, pyruvate, can be resolved. A representation of this is shown in Figure 1.

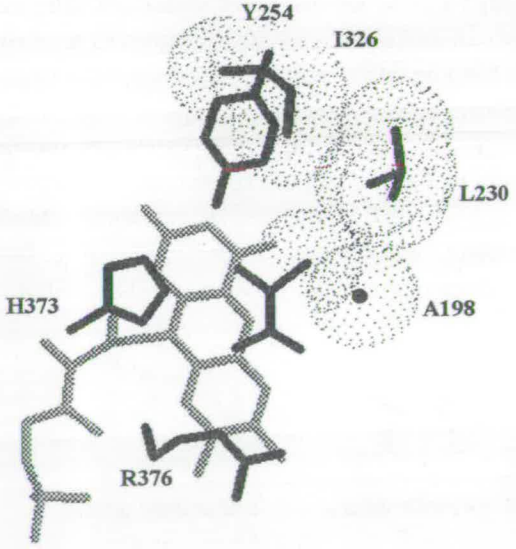

FIG. 1. The active site structure of *S. cerevisiae* flavocytochrome b_2 (1) indicating the hydrophobic interactions between substrate methyl group and alkyl amino-acid side-chains.

```
                    198                                 230
S. cere. b2  VPFYVSATAL CKLGNPLEGE KDVARGCGQG VTKVPQMIST LASCSPEEII  239
H. anom. b2  APFYISATAL AKLGHP.EGE VAIAKGAGRE ..DVVQMIST LASCSFDEIA  228
P. put. MDH  MPLLIGPTGL NGALWP.KGD LALARAATKA ..GIPFVLST ASNMSIEDLA  119
  Spin. GOX  MPIMIAPTAM QKMAHP.EGE YATARAASAA ..GTIMTLSS WATSSVEEVA  117
R. Gram. b2  LPIFVAPAGL ARLGHP.DGE QNIVRGVAKH ..DILQVVSS GASCSIDEIF  243
```

FIG. 2. Amino-acid sequence comparison between *S. cerevisiae* flavocytochrome b_2 (lactate dehydrogenase), *H. anomala* flavocytochrome b_2 (lactate dehydrogenase), *Pseudomonas putida* mandelate dehydrogenase, Spinach glycolate oxidase and *Rhodotorula graminis* flavocytochrome b_2 (mandelate dehydrogenase), over a region implicated in defining substrate specificity (see 4, 5).

S. cerevisiae flavocytochrome b_2 is related both structurally and by sequence to a number of other FMN-containing α-hydroxy-acid dehydrogenases/oxidases, including spinach glycolate oxidase (2) and L-mandelate dehydrogenase from *R. graminis* (3). However, both these enzymes exhibit a kinetic preference for alternative substrates. The position of pyruvate in Figure 1 indicates that the methyl group of the substrate makes contact with the hydrophobic side-chains of Ala198 and Leu230, while being a little more distant from Ile326. As demonstrated in Figure 2, Ala198 and Leu230 are not well conserved in the glycolate or mandelate dependent enzymes and this applies to the overall sequence surrounding Ile326. It was postulated therefore that these interactions were responsible for the selection of L-lactate by the enzyme in preference to other α-hydroxy-acids. In a previous study (4 & 5) several point mutations were made to test this notion. The residues were all replaced by smaller variants in an attempt to increase the size of the substrate binding cavity and thereby disrupt the close steric contacts. The mutants were all characterised by using a range of straight-chain α-hydroxy-acids (chain-length 2 to 8) to generate 'substrate specificity profiles', as illustrated in Figure 3. Substitution of Leu230 for Ala converted the enzyme into a non-specific long-chain α-hydroxy-acid dehydrogenase by essentially deselecting the physiological substrate L-lactate. Substitution of Ile326 for Ala, however, generated a specific (S)-α-hydroxyoctanoate dehydrogenase. The influence of

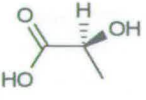

L-Lactic acid

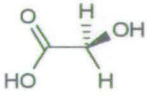

Glycolic acid

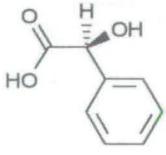

L-Mandelic acid

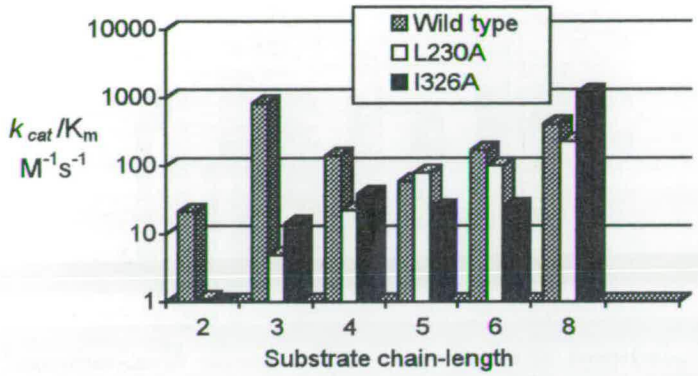

FIG. 3. Substrate specificity profiles for *S. cerevisiae* flavocytochrome b_2 mutants constructed using steady-state data for a series of straight-chain α-hydroxy-acids (4 & 5).

Ile326 is likely to be two-fold as it lies in direct contact with Leu230 and probably contacts the alkyl substituents of large substrates.

RESULTS AND DISCUSSION

The flavocytochromes b_2 from *S. cerevisiae* and *R. Graminis* have previously been considered as having mutually exclusive substrates: L-lactate and L-mandelate respectively (6). However, small activities can be detected in both cases with the alternate substrate. For the *S. cerevisiae* variant, the k_{cat} is around 0.07 s^{-1} with L-mandelate compared to 400 s^{-1} with L-lactate. The structural basis for this acute discrimination is the subject of an extended study by protein engineering, aided by the recent acquisition of the amino-acid sequence for the *R. graminis* enzyme (3). Alignment of the two enzymes' sequences (see Figure 2) reveals a 40% identity, with significant differences highlighted at positions 198(Ala-Gly) and 230(Leu-Gly). Generation of the Leu230→Gly mutant in the *S. cerevisiae* enzyme increased its activity with L-mandelate by an order of magnitude to 0.89 s^{-1}, while the double mutation of Ala198→Gly + Leu230→Ala caused an increase in k_{cat} of more than 100-fold to 8.5 s^{-1} (see Figure 4). More modest improvements have also been recorded with the Leu230→Ala and Ala198→Gly single mutants. The values of k_{cat} for all these mutants with L-lactate are lower than for the wild-type enzyme, but none yet show the degree of discrimination exhibited by the *Rhodotorula* enzyme.

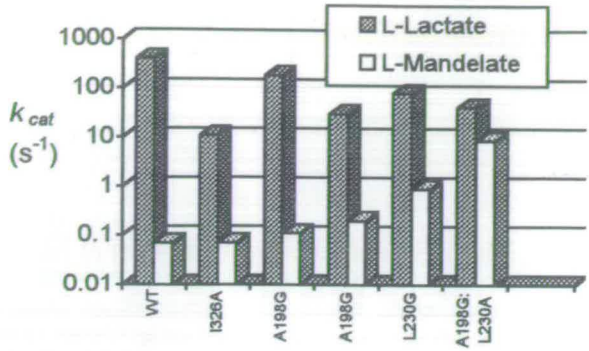

FIG. 4. A comparison of the activities of *S. cerevisiae* flavocytochrome b_2 mutant enzymes with L-lactate and L-mandelate (tabulated below).

TABLE I k_{cat} values, as plotted above (s^{-1}).

	Wild type	I326A	L230A	A198G	L230G	A198G:L230A
L-Lactate	400	11	185	30	82	41
L-Mandelate	0.07	0.07	0.11	0.2	0.89	8.5

In summary, it appears that the apparatus for substrate selection in both enzymes is built into a broadly consistent protein framework. This structural similarity is also a striking feature of the spinach glycolate oxidase structure when compared to that of *S. cerevisiae* flavocytochrome b_2 (2). Further mutations are planned to examine the limits of this hypothesis, with the aim of generating an efficient L-mandelate dehydrogenase from the framework of an almost incompatible enzyme.

REFERENCES

1. Xia, Z-X., Mathews, F.S. 1990. J. Mol. Biol. **212**, 837.
2. Lindqvist, Y. 1989. J. Mol. Biol. **209**, 151.
3. Ilias, R. (to be published)
4. Daff, S., Manson, F.D.C., Reid, G.A., Chapman, S.K. 1994. Biochem. J. **301**, 829.
5. Daff, S., Manson, F.D.C., Reid, G.A., Chapman, S.K., 1994. Biochem. Soc. Trans. **22**, 282.
6. Smékal, O., Yasin, M., Fewson, C.A., Reid, G.A., Chapman, S.K. 1993. Biochem. J. **290**, 103.